Quaternary Science Reviews 92 (2014) 40–67

Contents lists available at ScienceDirect

Quaternary Science Reviews

journal homepage: www.elsevier.com/locate/quascirev

Invited review

Arctic Ocean glacial history

Martin Jakobsson [a, i, *], Karin Andreassen [b], Lilja Rún Bjarnadóttir [c], Dayton Dove [d], Julian A. Dowdeswell [e], John H. England [f], Svend Funder [g], Kelly Hogan [e], Ólafur Ingólfsson [h, i], Anne Jennings [j], Nikolaj Krog Larsen [k], Nina Kirchner [l], Jon Y. Landvik [m], Larry Mayer [n], Naja Mikkelsen [o], Per Möller [p], Frank Niessen [q], Johan Nilsson [r], Matt O'Regan [a], Leonid Polyak [s], Niels Nørgaard-Pedersen [o], Ruediger Stein [q]

[a] Department of Geological Sciences, Stockholm University, 106 91 Stockholm, Sweden
[b] Department of Geology, University of Tromsø, Dramsveien 201, N-9037 Tromsø, Norway
[c] Geological Survey of Norway, P.O. Box 6315 Sluppen, N-7491 Trondheim, Norway
[d] British Geological Survey, Edinburgh, UK
[e] Scott Polar Research Institute, University of Cambridge, Cambridge CB2 1ER, UK
[f] Department of Earth and Atmospheric Sciences, University of Alberta, Canada
[g] Centre for GeoGenetics, Natural History Museum, University of Copenhagen, Øster Voldgade 5-7, DK-1350 Copenhagen, Denmark
[h] Faculty of Earth Sciences, University of Iceland, Sturlugata 7, Askja, Is-101 Reykjavik, Iceland
[i] The University Centre in Svalbard (UNIS), Norway
[j] Institute of Arctic and Alpine Research (INSTAAR), University of Boulder Colorado, USA
[k] Department of Geoscience, Aarhus University, 8000 Aarhus C, Denmark
[l] Department of Physical Geography and Quaternary Geology, Stockholm University, 106 91 Stockholm, Sweden
[m] Norwegian University of Life Sciences, Department of Plant and Environmental Sciences, P.O. Box 5003, N-1432 Ås, Norway
[n] Center for Coastal and Ocean Mapping, University of New Hampshire, USA
[o] Geological Survey of Denmark and Greenland (GEUS), Ø. Voldgade 10, DK-1350 Cph. K, Denmark
[p] Department of Geology, Lund University, Sölvegatan 12, SE-223 62 Lund, Sweden
[q] Alfred Wegener Institute for Polar and Marine Research, Am Handelshafen12, D-27570 Bremerhaven, Germany
[r] Department of Meteorology, Stockholm University, 106 91 Stockholm, Sweden
[s] Byrd Polar Research Center, Ohio State University, 1090 Carmack Rd., Columbus, OH 43210, USA

ARTICLE INFO

Article history:
Received 15 February 2013
Received in revised form
18 July 2013
Accepted 29 July 2013
Available online 15 November 2013

Keywords:
Quaternary
Arctic Ocean
Ice sheets
Ice shelves
Ice streams
Landforms
Glacial history
Last Glacial Maximum
Ice sheet modelling
Paleoceanography

ABSTRACT

While there are numerous hypotheses concerning glacial–interglacial environmental and climatic regime shifts in the Arctic Ocean, a holistic view on the Northern Hemisphere's late Quaternary ice-sheet extent and their impact on ocean and sea-ice dynamics remains to be established. Here we aim to provide a step in this direction by presenting an overview of Arctic Ocean glacial history, based on the present state-of-the-art knowledge gained from field work and chronological studies, and with a specific focus on ice-sheet extent and environmental conditions during the Last Glacial Maximum (LGM). The maximum Quaternary extension of ice sheets is discussed and compared to LGM. We bring together recent results from the circum-Arctic continental margins and the deep central basin; extent of ice sheets and ice streams bordering the Arctic Ocean as well as evidence for ice shelves extending into the central deep basin. Discrepancies between new results and published LGM ice-sheet reconstructions in the high Arctic are highlighted and outstanding questions are identified. Finally, we address the ability to simulate the Arctic Ocean ice sheet complexes and their dynamics, including ice streams and ice shelves, using presently available ice-sheet models. Our review shows that while we are able to firmly reject some of the earlier hypotheses formulated to describe Arctic Ocean glacial conditions, we still lack information from key areas to compile the holistic Arctic Ocean glacial history.

* Corresponding author. Department of Geological Sciences, Stockholm University, 106 91 Stockholm, Sweden.
E-mail address: martin.jakobsson@geo.su.se (M. Jakobsson).

http://dx.doi.org/10.1016/j.quascirev.2013.07.033
0277-3791/

1. Introduction

The glacial history of the Arctic Ocean involves the build-up and decay of marine-based ice sheets on the continental shelves, the development and disintegration of ice shelves, and significant changes in ocean-circulation regimes and sea-ice cover. None of the four other world ocean areas experienced such dramatic physiographic and environmental changes as the Arctic Ocean through the Quaternary glacial–interglacial cycles. This has been recognized for nearly a century, but a lack of direct field observations led to several postulated, rather contradictory, hypotheses concerning glacial–interglacial cycles in the Arctic Ocean (Donn and Ewing, 1966; Broecker, 1975; Hughes et al., 1977). When early hypotheses on the environmental setting of the glacial Arctic were developed, i.e. suggesting on one the hand an extensive ice shelf in the central Arctic Ocean during glacial periods (Mercer, 1970) and on the other hand sea-ice free conditions (Donn and Ewing, 1966), there were few field data available to test them. The modern perennial Arctic Ocean sea-ice cover has delayed data collection, but during the last decade, in particular during the last years with substantially reduced summer sea-ice extent, data collection has increased by an order of magnitude (Polyak and Jakobsson, 2011).

Since the Arctic Palaeoclimate and its Extremes (APEX) program started in 2007 as a continuation of two preceding programs PONAM (The Late Cenozoic Evolution of the Polar North Atlantic Margins, 1988–1994 (Elverhøi et al., 1998a)) and QUEEN (the Quaternary Environment of the Eurasian North, 1996–2002 (Thiede et al., 2004)) numerous field campaigns to the Arctic Ocean have been carried out (Jakobsson et al., 2010a). These have revealed new insights into the extent of ice sheets on the continental margins bordering the central Arctic Ocean, and how they fed into ice shelves that occupied regions of the central basin. Here we present an overview of present knowledge on the Arctic Ocean glacial history. It is divided into regions where the state-of-the art glacial history is presented based on mapped glaciogenic landforms, sediment stratigraphy and established chronologies (Fig. 1). We address the spatial extent of ice sheets that occupied the northernmost Arctic continental shelves and drained into the Arctic Ocean, including their possible extensions as ice shelves. The central Artic Ocean is treated as a separate region with a focus on how the marine sediment record has documented glacial–interglacial cycles. We also include recent developments concerning numerical simulations of Arctic ice sheets and glacial paleoceanographic conditions. We focus the overview on the Last Glacial Maximum (LGM) and the maximum extent of Quaternary ice sheets. The overarching question is what do we currently know about the past extent of ice sheets, ice streams and ice shelves, and related oceanographic changes, in the Arctic Ocean during the Quaternary? Which are the most important outstanding questions today? Finally, all data presented in our review allow us to revisit and shed new light on previous hypotheses regarding glacial conditions in the Arctic Ocean.

2. Background

2.1. The glacial Arctic Ocean: hypotheses and theories

In the 1950s and 1960s the driving mechanisms behind the glacial cycles were debated. Following two papers on the topic (Ewing and Donn, 1956, 1958), Donn and Ewing (1966) suggested that a sea-ice free Arctic Ocean was required as a moisture source to build up the northern components of the large Northern Hemisphere ice sheets. Furthermore, they suggested that sea-ice formation in the Arctic Ocean towards the end of glaciation led to ice sheet decay due to an efficient blockade of the moisture required to form precipitation. Their theory implied that changes in Arctic Ocean sea-ice extent were a dominant control on Northern Hemisphere glacial–interglacial dynamics. The Milankovitch theory advocating an orbital forcing behind glacial–interglacial cycles (Milankovitch, 1920) was at the time beginning to gain ground (Broecker, 1966), but was still being met by scepticism until the 1970s when more deep sea sediment cores became available and dating methods improved (Hays et al., 1976). Although the Arctic Ocean sea-ice extent still is considered a relevant factor for the moisture supply and mass balance of the large Quaternary ice sheets (Colleoni et al., 2009), the overall ice–age cycles are believed to be paced by orbital parameters (Imbrie et al., 1992). The first sediment cores from the central Arctic Ocean retrieved from drifting ice stations (Clark, 1971) did not contribute to this original debate due to the irregular preservation of calcium carbonate microfossils that prevented consistent application of key paleoceanographic proxies and hampered the establishment of reliable age models (Backman et al., 2004; Alexanderson et al., 2014).

Another hypothesis that was formulated before much field data were available from the central Arctic Ocean suggested that a vast floating ice shelf covered the deep waters around the North Pole during past glacial maxima. Although previously postulated by Sir William Thomson in 1888 as a likely consequence of a glacial climate, Mercer (1970) was the first to promote this hypothesis based mainly on physiographic analogies between the Arctic Ocean and West Antarctica. Several authors picked up on the ice shelf theory and developed it further (Broecker, 1975; Hughes et al., 1977; Grosswald, 1980; Denton and Hughes, 1981; Grosswald and Hughes, 1999, 2008) (Fig. 2). In its most extreme form, a 1000 m thick ice shelf was hypothesized to have covered the entire Arctic Ocean, even south of the Fram Strait. This massive ice shelf was argued to be a critical stabilizing element, by exerting backpressure, for marine ice sheets grounded on continental shelves and flowing into the Arctic Ocean (Grosswald and Hughes, 1999). The hypothesis of an Arctic Ocean ice shelf was considered extreme by much of the glaciological community, although by the mid-1990s evidence indicating deep grounding of ice, likely derived from ice shelves, began to be documented (Vogt et al., 1994; Jakobsson, 1999; Jakobsson et al., 2001, 2008b; Polyak et al., 2001). Subsequently, the mapping of widespread glaciogenic bedforms and the dating of sediment cores retrieved from areas of ice grounding on submarine ridges in the Arctic Ocean, now support the presence of an ice shelf in the Amerasian Basin of the central Arctic Ocean, in particular during Marine Isotope Stage (MIS) 6, ~135 ka BP (Jakobsson et al., 2010b). The development and stability of this ice shelf is supported by a conceptual oceanographic model indicating that the influx of Atlantic water occurred at a much greater depth during glacial periods than today, thus preventing this relatively warm water mass from reaching into the Amerasian Basin where it would cause basal melting of an ice shelf (Jakobsson et al., 2010b). This pattern of glacial paleo-circulation would in turn mean that ice shelves had a smaller likelihood of developing in the Eurasian Basin of the Arctic Ocean, where they would be exposed to warm inflowing Atlantic water.

Ice shelves may also form through a combination of seaward extension of glaciers and extensive multiyear thickening of landfast sea ice, i.e. *sikussak*, established along the coast and in fjords (Jeffries, 1992). Bradley and England (2008) postulated that this kind of extremely thick multi-year sea-ice cover developed towards the end of the Last Glacial period as a consequence of a more stagnant Arctic Ocean with a lower relative sea level and a diminished influx of warm Atlantic water. Such pervasive thick sea ice, termed *paleocrystic ice*, is suggested to have been massively

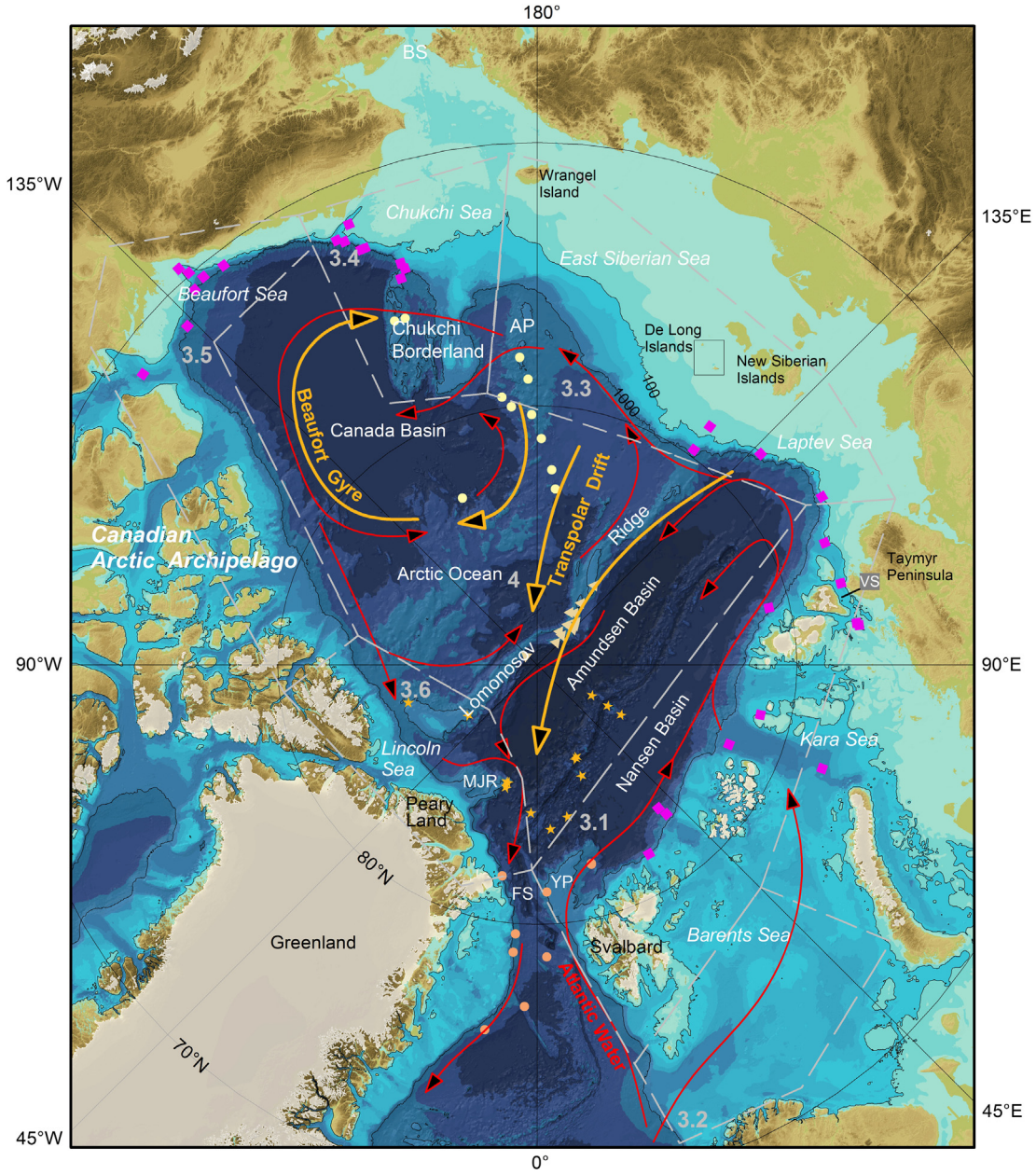

Fig. 1. Map of the Arctic Ocean showing the areas included in this overview of the Arctic Ocean glacial history. Each area has a number, displayed in grey, corresponding to a section in the text. The bathymetric portrayal in this figure, as well as in all other figures, is based on the International Bathymetric Chart of the Arctic Ocean (IBCAO) Version 3.0 (Jakobsson et al., 2012). The general circulation of Atlantic water in the present Arctic Ocean is shown with red arrows (modified from Rudels et al., 2012). Sediment cores discussed in Section 4 and shown in Fig. 11a–e are shown with coloured symbols. Yellow dots = Amerasian Basin cores; Fig. 11a, Yellow triangles = Lomonosov Ridge cores; Fig. 11b, Orange stars = Eurasian Basin/Southern Lomonosov/Morris Jesup Rise cores; Fig. 11c, Orange dots = Fram Strait/Yermak Plateau cores, Fig. 11d, Purple squares = Continental Slopes/Margin cores; Fig. 11e. AP = Arlis Plateau; BS = Bering Strait; FS = Fram Strait; MJR = Morris Jesup Rise; YP = Yermak Plateau; MJR.

discharged from the Arctic Ocean through the Fram Strait at ~11 ^{14}C ka BP (Bradley and England, 2008). The authors propose further that the export of paleocrystic ice at the end of the LGM may have disrupted North Atlantic deep water formation and thereby caused or contributed to the Younger Dryas cold snap. It should be noted that the hypothesis by Bradley and England (2008) is only one of a large number of theories suggested to have caused the Younger Dryas cold event.

2.2. Previously published reconstructions of ice-sheet extent

The most inclusive set of compilations of Quaternary ice-sheet extent is in Ehlers and Gibbard (2004), which includes papers dealing with the glacial history of the Arctic (Dyke, 2004; Funder et al., 2004; Hjort et al., 2004; Kauman and Manley, 2004; Zazula et al., 2004; Svendsen et al., 2004b) (Fig. 3). The Eurasian ice-sheet extent over several time slices was compiled by Svendsen et al. (2004a). They concluded that its maximum extent occurred during MIS 6 towards the end of the Saalian glaciation (~140 ka), and included a northward ice extension from Svalbard onto the Yermak Plateau (Fig. 2). The glaciogenic features behind this conclusion were later found to more likely originate from grounding of large ice shelf fragments exiting towards the Fram Strait (Dowdeswell et al., 2010b; Jakobsson et al., 2010b). Whether the Barents Sea Ice Sheet ever extended out from Svalbard onto the Yermak Plateau during the Quaternary remains unresolved. Several

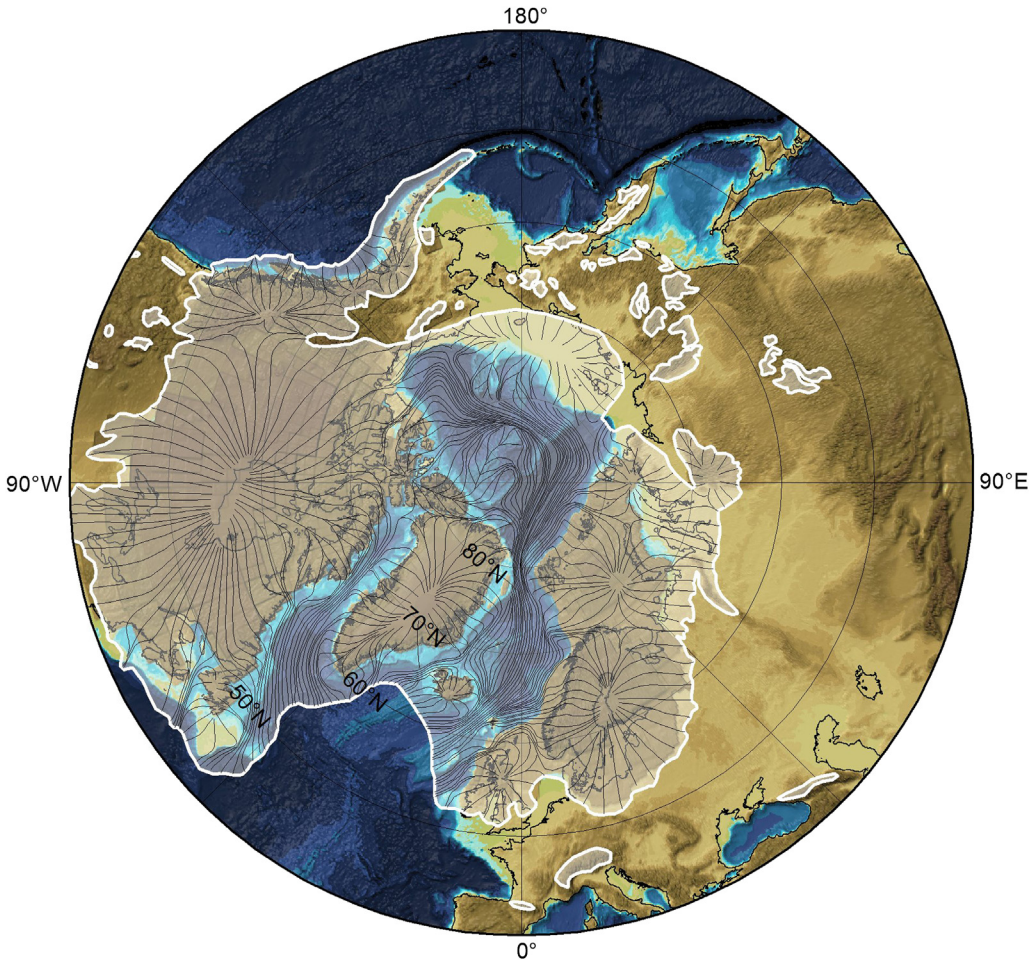

Fig. 2. The maximum version of the "late Würm Arctic Ice Sheet" (LGM) by Hughes et al. (1977), which includes a 1-km thick ice shelf in the Arctic Ocean. Note that all the Arctic Ocean continental shelves are glaciated including that of the East Siberian, and Chukchi seas. In the minimum version by Hughes et al. (1977), the shallow East Siberian Sea is ice free.

authors have pointed out striking differences between the Quaternary ice sheets, in particular between the Eurasian components of LGM (Late Weichselian) and MIS 6 (Late Saalian). While the LGM had a relatively small extension over West Siberia, landforms and glacial deposits suggest that the largest ice sheet during MIS 6 covered much more of this region (Svendsen et al., 2004a). The answer to why the MIS 6 ice sheet generally grew so large has been suggested to reside in the orbital configuration (Colleoni et al., 2011). The incoming solar radiation during MIS 6 springs is 20 W m^{-2} lower than during the LGM and the springs were also longer. This would allow snow cover to remain longer each season and lower the impact from summer melt.

A noticeable difference from the Dyke (2004) LGM limit of the north-western Laurentide ice sheet (LIS) was proposed by England et al. (2009) who inferred that the entire Banks Island was covered by a predominately cold-based ice sheet (Fig. 3). More recent fieldwork across western Banks Island provides further evidence for the advance of the NW Laurentide Ice Sheet onto the polar continental shelf (Lakeman and England, 2013). Furthermore, the Innuitian Ice Sheet (IIS) coalesced with the LIS to the south and also reached the polar continental shelf during the LGM (England et al., 2006). Although most of the islands were occupied by cold-based ice, at least half a dozen ice streams drained directly into the Arctic Ocean from the LIS and IIS via the deep marine channels of the CAA, supplying significant ice and sediment to the Arctic Ocean during the LGM (Stokes et al., 2005, 2006; England et al., 2006, 2009), discussed below.

There are not many LGM ice-sheet reconstructions published that include the entire circum-Arctic region and inferred ice extent into the Arctic Ocean. One such early reconstruction is that of Hughes et al. (1977), which contain the hypothesized 1-km thick ice shelf in the Arctic Ocean (Fig. 2). They suggest that all the Arctic Ocean continental shelves were glaciated at LGM including that of the East Siberian, and Chukchi seas (Fig. 2).

The global glacial isostasy model ICE-5G by Peltier (2004) includes ice-sheet extension, thickness, and land topography at time slices from the LGM to present. ICE-5G is based on a theoretical model of Earth's isostatic rebound following glacial unloading as well as input from regional ice margin mapping efforts, like the QUEEN program (Svendsen et al., 2004a) and by Dyke et al. (2002, 2004). ICE-5G has been used to define boundary conditions in many general circulation model (GCM) experiments addressing the LGM climatic and environmental conditions (Abe-Ouchi and Otto-Bliesner, 2009). This means that uncertainties in spatial reconstructions of LGM ice-sheets, as presented in this review, carry forward into the simulation results.

3. Continental shelves and adjacent bathymetric highs

In this section we describe glaciogenic landforms, stratigraphy and chronology for the regions shown in Fig. 1. We introduce the nomenclature of glaciogenic landforms and their interpretation used in this section in Appendix 1.

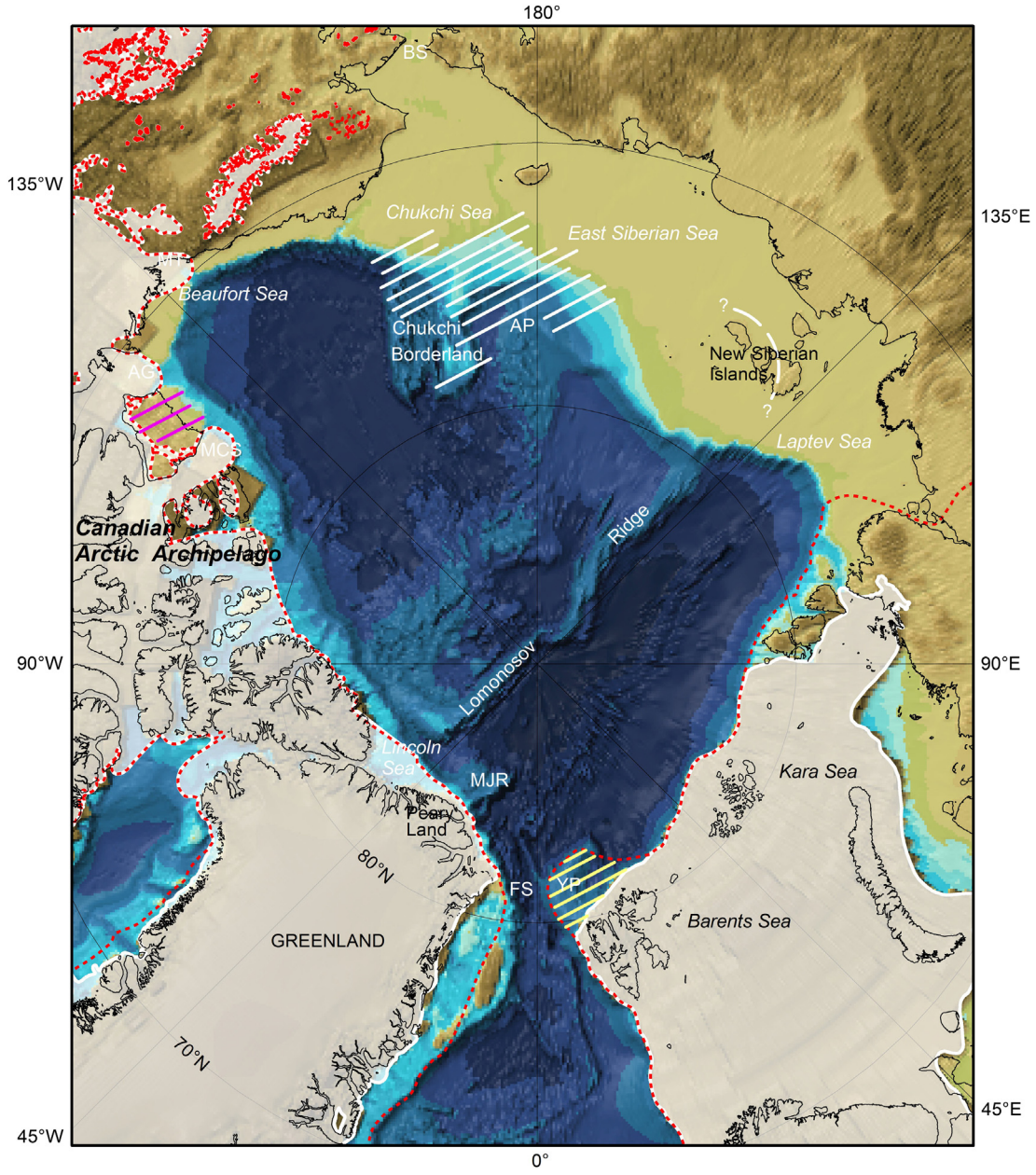

Fig. 3. Ice-sheet extension during the LGM (white semi-transparent) and Quaternary max (red dotted line). The Eurasian ice limit is from Svendsen et al. (2004a) and the Laurentide–Innuitian–Greenland is from the digital GIS files provided with the book *Quaternary Glaciations – Extent and Chronology* by Ehlers and Gibbard (2004). While several smaller revisions have been made to the shown ice limits, some of the more substantial revisions are indicated with cross hatching; purple (Banks Island) and yellow (Yermak Plateau). New results from the cross hatched area (white) of Chukchi Borderland – Arlis Plateau and East Siberian Sea will likely also lead to future major revisions of ice-sheet extent during the late Quaternary. The LGM topography is from ICE-5G (Peltier, 2004).

3.1. Northern Barents and Kara Sea

3.1.1. Landforms

The submarine glacial landforms west and north of Svalbard, on the Yermak Plateau, and along the Arctic Ocean margin of the Barents and Kara seas, mapped in Fig. 4, can be divided into those formed in subglacial, ice-contact and glaciomarine environments. The landforms, and landform assemblages, observed mainly from swath-bathymetric data and side-scan sonar imagery are used to make inferences about the extent, flow direction and dynamics of the ice sheet or glacier that produced them.

Streamlined sedimentary landforms occur in most major fjords and cross-shelf troughs west and north of Svalbard (Fig. 4) (Ottesen et al., 2005, 2007; Hogan et al., 2010a, 2010b). They indicate past ice-stream flow in the troughs, probably during the Late Weichselian glaciation. Fluting and larger streamlined features have also been observed or inferred from bathymetric data farther east in troughs on the Kara Sea margin (Polyak et al., 1997, 2008). Streamlined landforms are particularly well developed in Isfjorden and Kongsfjorden and their cross-shelf troughs (Howe et al., 2003; Ottesen et al., 2007). There is also evidence of their presence on the southern Yermak Plateau, northwest of Svalbard. On the Yermak Plateau, they are interpreted as relict Saalian (MIS 6) features, indicative of transient grounding across the plateau of an ice shelf remnant or an armada of megabergs from the Arctic Basin (c.f. section 2.1). An additional alternative could be the signature of the

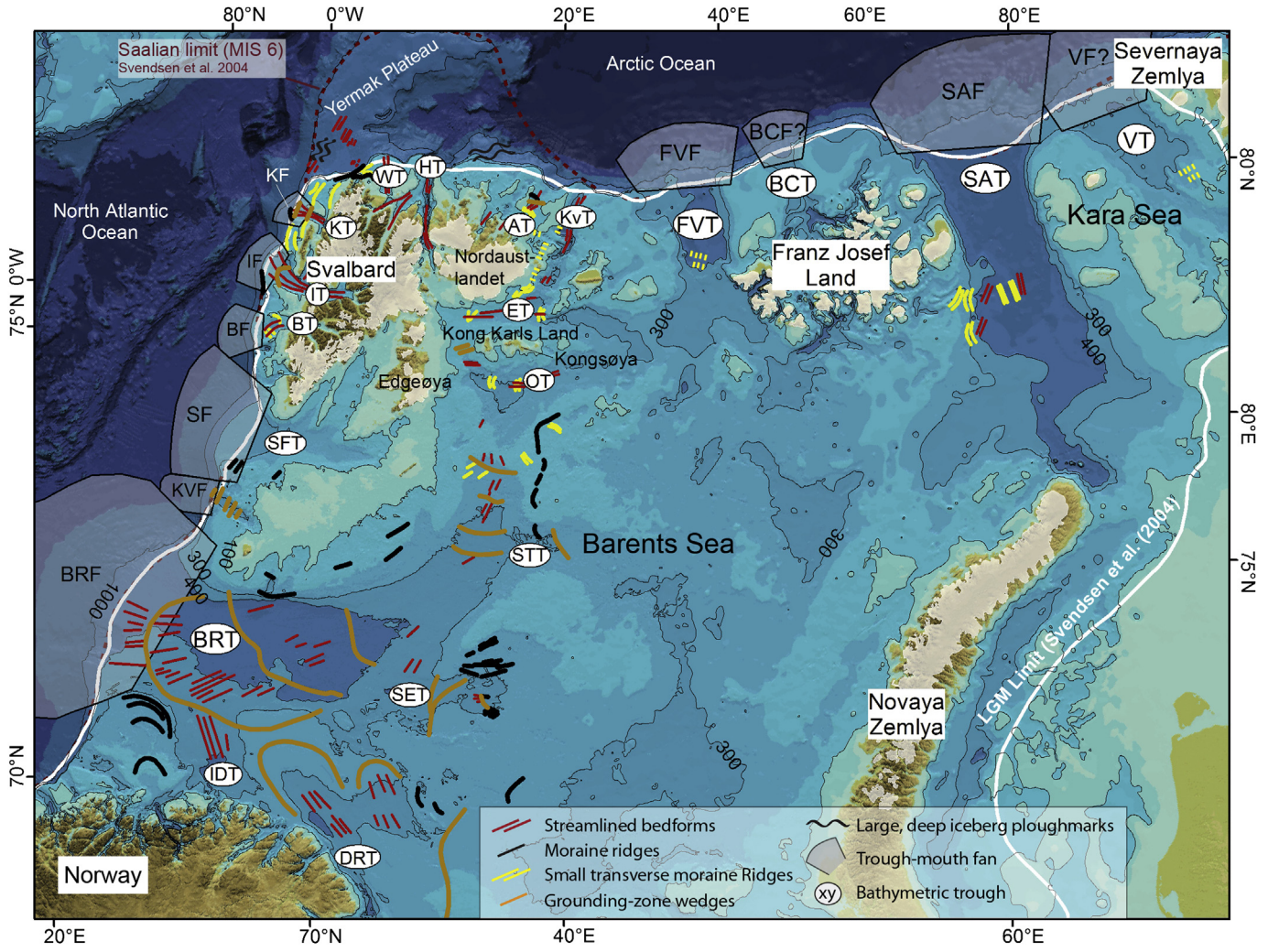

Fig. 4. Distribution of submarine glacial landforms in northern Barents and Kara seas (Section 3.1) and south-western and central Barents Sea (Section 3.2). The IBCAO Version 3.0 shows major cross-shelf troughs and trough-mouth fans (from bottom left and clockwise): DRT = Djuprenna; IDT = Ingøydjupet; SET = Sentralbankrenna; BRT/F = Bjørnøyrenna/Fan; KVT = Kveithola Trough/Fan; STT = Storbankrenna; SFT = Storfjordrenna/Fan; BT/F = Bellsund Trough/Fan; IT/F = Isfjorden Trough/Fan; KT/F = Kongfjorden Trough/Fan; WT = Woodfjorden Trough; HT = Hinlopen Trough; AT = Albertini Trough; KVT/F = Kvitøya Trough; FVT/F = Franz Victoria Trough/Fan; BCT = British Channel Trough; SAT/F = St. Anna Trough/Fan; VT = Voronin Trough; ET = Erik Eriksenstretet; OT = Olgastretet. Trough-mouth fans are drawn with a "?" seaward of the British Channel and Voronin troughs as they are based solely on the outward bulging of bathymetric contours and the presence of positive free-air gravity anomalies on the continental slope (Minakov et al., 2012); these features have not been confirmed by geophysical/geological surveying. Submarine landforms are mapped primarily from swath-bathymetric, side-scan sonar and acoustic/seismic data. In cases where only single acoustic profiles were used to map landforms, we have used a dashed line to indicate that the orientation of the features is not known. The submarine landform maps were compiled from: Solheim and Kristoffersen (1984); Vogt et al. (1994); Polyak et al. (1997); Vorren and Laberg (1997); Kleiber et al. (2000); Dowdeswell and Elverhøi (2002); Landvik et al. (2005); Ottesen et al. (2005); Ottesen et al. (2007); Andreassen et al. (2008); Polyak et al. (2008); Ottesen and Dowdeswell (2009); Dowdeswell et al. (2010b); Hogan et al. (2010a); Hogan et al. (2010b); Winsborrow et al. (2010); Batchelor et al. (2011); Noormets et al. (2012); Bjarnadóttir et al. (2013).

maximum Quaternary extent of relatively thin ice from Svalbard (Dowdeswell et al., 2010b). Grounding-zone sediments and sets of transverse-to-flow ridges on the north-west Svalbard shelf suggest that ice did not reach the Yermak Plateau during the Late Weichselian (Ottesen and Dowdeswell, 2009; Dowdeswell et al., 2010b). Streamlined landforms in troughs extending northwards from Nordaustlandet indicate that fast-ice flow drained the Austfonna ice cap, likely during the last glaciation (Noormets et al., 2012).

Mega-scale glacial lineations (MSGLs) and other streamlined sedimentary landforms have been mapped in the northern Barents sea, in Erik Eriksenstretet and Olgastretet, east of Nordaustlandet and around Kong Karls Land (Fig. 4) (Dowdeswell et al., 2010a; Hogan et al., 2010a), indicating ice flow into Franz Victoria Trough from eastern Svalbard. This flow direction is almost at right-angles to previously inferred ice flow from a major Late Weichselian ice dome in the central Barents Sea (Lambeck, 1995, 1996; Forman et al., 2004). More work is needed to resolve this apparent discrepancy and much may depend on the dating of the streamlined landforms in Olgastretet and Erik Eriksenstretet (Ingólfsson and Landvik, 2013). Landvik et al. (2013) propose a concept of a succession of ice flow styles (maximum, transitional and local flow) over a glacial cycle in western Svalbard, which might explain the seemingly incompatible ice flow directions observed from eastern Svalbard.

The presence of grounding-zone wedges (GZWs) in the western Svalbard cross-shelf troughs and in the Barents-Kara sector of the Arctic Ocean indicates that post-LGM retreat was episodic, with still-stands punctuating periods of more rapid cross-shelf deglaciation (Dowdeswell et al., 2008). GZWs are often subtle features in a bathymetric sense, and lack of detailed swath bathymetry and sub-

bottom profiles may contribute to their apparent absence in the major troughs of the Kara Sea.

Small transverse ridges occur, for example, in the Bellsund Trough and east of Nordaustlandet (Fig. 4). Morainic ridges also occur on shallow banks at the margins of several cross-shelf troughs in the Barents and Kara Seas, for example Kvitøya Trough in eastern Svalbard (Kleiber et al., 2000). At 250 m water depth in the St. Anna Trough, Polyak et al. (1997) describe ridges that are very similar to ridges in the Olgastretet (Hogan et al., 2010a). A series of ridges up to 30 m high and more than 5 km wide have been identified from acoustic profiles in the central part of St. Anna Trough between 79° and 81.5°N (Polyak et al., 1997). These ridges were interpreted as large moraines but have not been mapped in Fig. 4 because their orientations are unknown.

Seismic reflection profiles from the northern Barents and Kara Sea reveal a thin, relatively continuous cover of Quaternary sediments overlying a prominent erosional unconformity, the Upper Regional Unconformity (URU; Solheim and Kristoffersen, 1984; Vorren et al., 1986). Sediment-core and borehole data show that these units comprise a typical glacial–deglacial–post glacial sequence of basal diamicts overlain by glaciomarine and marine-hemipelagic sediments (Elverhøi and Solheim, 1983; Solheim and Kristoffersen, 1984; Polyak and Solheim, 1994; Polyak et al., 1997). The pebbly-mud lithofacies of the diamict units is usually less than 10 m thick, is stiff at its base, and varies in colour with changes in the underlying source bedrock. Glaciomarine muds can be massive or laminated, the latter being interpreted as resulting from changes in the melting regime of a nearby ice margin, as in parts of the Franz Victoria trough (Polyak and Solheim, 1994; Lubinski et al., 1996) and Erik Eriksenstretet (Hogan et al., 2010a). The transition to olive-grey marine-hemipelagic muds, which are regionally ubiquitous, is often gradual and occurs alongside a diversification in foraminifera assemblages indicating ameliorated environmental conditions and an advection of Atlantic water to the northern margin of the Barents and Kara seas (Polyak and Solheim, 1994; Lubinski et al., 1996). Shallow sub-bottom profiles show that the glacial landforms described above (streamlined landforms, moraines) were formed at or near the surface of the glaciogenic diamicts (Solheim et al., 1990; Polyak et al., 1997; Hogan et al., 2010a). Multiple radiocarbon ages from sediments just above the diamicts return ages around 13–14 cal ka BP, and ages of 10–12 cal ka BP for the glaciomarine–marine transition confirming that this stratigraphy relates to the Late Weichselian glaciation of the Barents-Kara Sea (Elverhøi and Solheim, 1983; Lubinski et al., 1996; Polyak et al., 1997).

Beyond the maximum extent of the full-glacial Eurasian Ice Sheet over Svalbard and the Barents Sea, trough-mouth fans (TMFs) are the largest landforms on the continental margin (Fig. 4). TMFs are identified off the major fjord-trough systems west of Svalbard (Vorren et al., 1998), larger TMFs also occur along the Arctic Ocean margin of the Kara Sea, offshore of the Franz Victoria and St. Anna troughs (Fig. 4) (Polyak et al., 1997; Kleiber et al., 2000). Additional TMFs may be present offshore of the British Channel, north of Franz Josef Land, and the Voronin Trough to the west of Severnaya Zemlya, on the basis of convex upper-slope bathymetry and free-air gravity anomalies (Jakobsson et al., 2012; Minakov et al., 2012). A TMF off Hinlopen Trough appears to have been largely removed by the Hinlopen Slide (Vanneste et al., 2006; Winkelmann and Stein, 2007; Batchelor et al., 2011). Glaciogenic debris flows observed on acoustic profiles of some TMFs are often stacked to form major building blocks of the fans (e.g. Laberg and Vorren, 1995; Dowdeswell et al., 1996; King et al., 1998).

Between full-glacial ice streams, the submarine landform assemblage of inter-trough areas is different from that of cross-shelf troughs (Ottesen and Dowdeswell, 2009). Whereas the troughs are dominated by flow-parallel streamlined sedimentary landforms, the inter-ice stream landform assemblage is more typically defined by transverse-to-flow ridges (Ottesen and Dowdeswell, 2009). Such a landform assemblage is present in the fjords of north-westernmost Svalbard (Smeerenbergfjorden, Raudfjorden).

Large areas of the northern Barents Sea floor are marked by iceberg keels that form a palimpsest of cross-cutting furrows. On the Yermak Plateau and the shelf north of Svalbard, there are distinctive zones where very deep iceberg keels have ploughed the sea floor to depths of up to about 800 m (Vogt et al., 1994, 1995; Dowdeswell et al., 2010b); some plough marks indicate multiple keels on a coherent iceberg up to 7 km wide. These very deep and wide plough marks have been interpreted to be produced by either very large free-drifting icebergs, probably from the first stages of deglaciation of the large Franz Victoria and St. Anna trough ice streams, or from groups of large icebergs frozen into huge multi-year sea-ice floes that may have been present in the Arctic Ocean under Quaternary full-glacial conditions (Vogt et al., 1994; Dowdeswell et al., 2010b; Jakobsson et al., 2010b).

3.1.2. Stratigraphy and chronology

3.1.2.1. Svalbard and the northern Barents Sea margin.

Volume estimates of sediments offshore indicate that a 2–3 km thickness of rock has been removed from central Spitsbergen since the Eocene (Eiken and Austergard, 1987; Vorren et al., 1991), and at least half of this volume was removed during the Quaternary glaciations (Svendsen et al., 1989; Dimakis et al., 1998; Elverhøi et al., 1998b). Glaciations of limited extent over the Svalbard–Barents Sea region probably began in the Pliocene–Pleistocene, 3.5–2.4 Ma ago (Knies et al., 2009). Glaciations intensified in the Early Pleistocene 2.6–1.0 Ma and glaciers were initially land-based, with evidence of Early Pleistocene glaciofluvial melt-water transport to the surrounding oceans (Laberg et al., 2010), before the ice sheets reached the shelf break at around 1.6 Ma and ice-rafted debris (IRD) delivery to the adjacent ocean increased (Knies et al., 2009). Based on isostatic modelling, Butt et al. (2002) suggested that the Barents Sea continental shelf region was subaerially exposed at 2.3 Ma, i.e. at the time when glaciers began to spread over larger areas. Sejrup et al. (2005) suggested that extensive shelf glaciations were taking place in the Svalbard region at 1.6–1.3 Ma, and a large scale intensification of Barents Sea glaciations started about 1 Ma with grounded ice reaching the Yermak Plateau (Knies et al., 2009). The erosional surface from this first ice grounding is located well below the MIS 6 streamlined glacial features mapped on the Yermak Plateau (Dowdeswell et al., 2010b; O'Regan et al., 2010). At Kongsfjordhallet, northern Kongsfjorden, western Spitsbergen, there is also evidence for a Spitsbergen glaciation that dates back to the Early Pleistocene (2–1 Ma) (Houmark-Nielsen and Funder, 1999). Miller (1982) likewise found indications of Early-middle Pleistocene (1–0.3 Ma) glaciations along the southern shore of Kongsfjorden, with at least three emergence cycles and two distinct glacial events. After 0.78 Ma, at least eight full-scale glaciations occurred over Svalbard and the Barents Sea, evidenced by trough-mouth fan deposition along the western Barents margin where cross-shelf ice streams reached the shelf edge (Vorren et al., 2011).

The Svalbard terrestrial record of full-scale glaciations is fragmentary and biased towards Late Quaternary glacial events because of the prevailing erosion at times of major ice-sheet expansion. The Late Quaternary glacial record of western Svalbard (Fig. 5) comprises an extensive Saalian (>130 ka BP) and three Weichselian major glaciations (Landvik et al., 1998; Mangerud et al., 1998). These are fingerprinted by tills in the stratigraphy, overlain by coarsening upwards sequences signifying isostatic rebound and marine regressions. The glaciation curve of Mangerud et al. (1998)

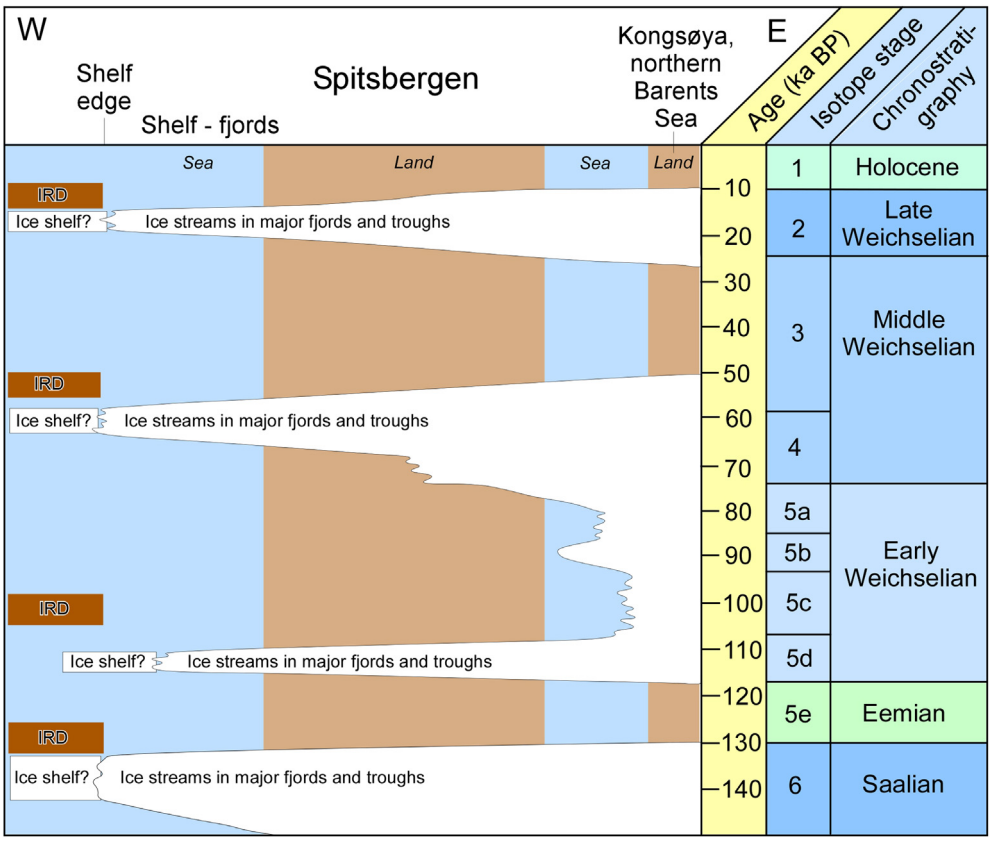

Fig. 5. Conceptual Late Quaternary Svalbard–Barents Sea ice sheet glaciations curve, based on Mangerud et al. (1998) correlations along a transect from northern Barents Sea in the east to the shelf edge west of Svalbard.

is still the best approximation for the glacial events also along the margin to the Arctic Ocean (Fig. 5). However, it probably represents the ice-stream systems of the fjords and cross-shelf troughs along western Svalbard, rather than simultaneous oscillations along the entire margin of the Svalbard–Barents Sea ice sheet (Ingólfsson and Landvik, 2013; Landvik et al., 2013).

Three major ice-stream pulses are suggested for the Last Interglacial/Glacial cycle, at approximately 110 ka, 60 ka and 20 ka ago, interacting with the ocean through delivery of sediments to the shelf break and release of icebergs. The 60 ka and 20 ka pulses do both correspond to input of terrigenous material in sediment cores north of Svalbard, whereas no input from the 110 ka pulse has been found (Winkelmann et al., 2008). These periods of high zonal ice flux could have led to repeatedly extensive ice-shelf formation (Fig. 5). The raised beach record of postglacial emergence on Franz Josef Land (Forman et al., 2004) confirms, together with marine geological evidence (Polyak and Solheim, 1994; Lubinski et al., 1996), that the archipelago and fringing shelf areas and cross-shelf troughs were covered by the Svalbard–Barents Sea ice sheet during the LGM (Landvik et al., 1998). Svendsen et al. (2004a) imply that ice-sheet oscillations over the Last Interglacial–Glacial cycle along the northern margin of the Svalbard–Barents Sea ice sheet largely mirror its western margin oscillations, but stratigraphical data substantiating this are largely lacking. It has been pointed out that there is still insufficient chronological data to evaluate regional variability in the timing of ice-sheet maxima for different sectors of the Svalbard–Barents Sea ice sheet (Clark et al., 2009; Ingólfsson and Landvik, 2013).

3.1.2.2. Kara Sea and north-western Siberia. Major glaciations in western Siberia and over the Kara Sea shelf started in Middle Pleistocene, during MIS 16 (the Mansi glaciation), and maximum ice-sheet extension at the south-eastern fringe of Eurasian Ice Sheets occurred during the Samarovo glaciation (MIS 8) (Astakhov, 2004, 2013). These very extensive Middle Pleistocene ice sheets could have covered the eastern Barents Sea and the Kara Sea margins, west and east of Novaya Zemlya, respectively, and across the continental break into the Arctic Ocean. The most complete Middle Pleistocene terrestrial stratigraphy is on October Revolution Island in the Severnaya Zemlya archipelago (Fig. 1). Möller et al. (2006) report five marine units intercalated with tills, all in superposition, and all of Middle Pleistocene age except for the uppermost till/marine cycle. Till bed II is firmly age-constrained into MIS 6 (Saalian/Taz) whereas the two lowermost till beds are suggested to be from MIS 8 and MIS 10 (or possibly MIS 12), respectively. The highest located marine sediments and beach–ridge complexes, tied to the Saalian/Taz deglaciation at the MIS 6/5e transition on Severnaya Zemlya and at Cape Chelyuskin on Taymyr Peninsula, reach ~140 m a.s.l. (Möller et al., 2006, 2008), only some 200 km from the shelf break to the north. This implies a Saalian/Taz ice-sheet thickness over the Kara Sea shelf in excess of 3000 m, as suggested from earth rheological modelling (Lambeck et al., 2006). The timing concurs with possible ice-shelf grounding at 1000 m water depths on the Lomonosov Ridge in the central Arctic Ocean (Jakobsson et al., 2001; Polyak et al., 2001).

Late Pleistocene glacial events over north Siberia and the Kara Sea are reasonably well constrained. Svendsen et al. (2004a) suggest that there were three major ice-advance/-retreat phases during the

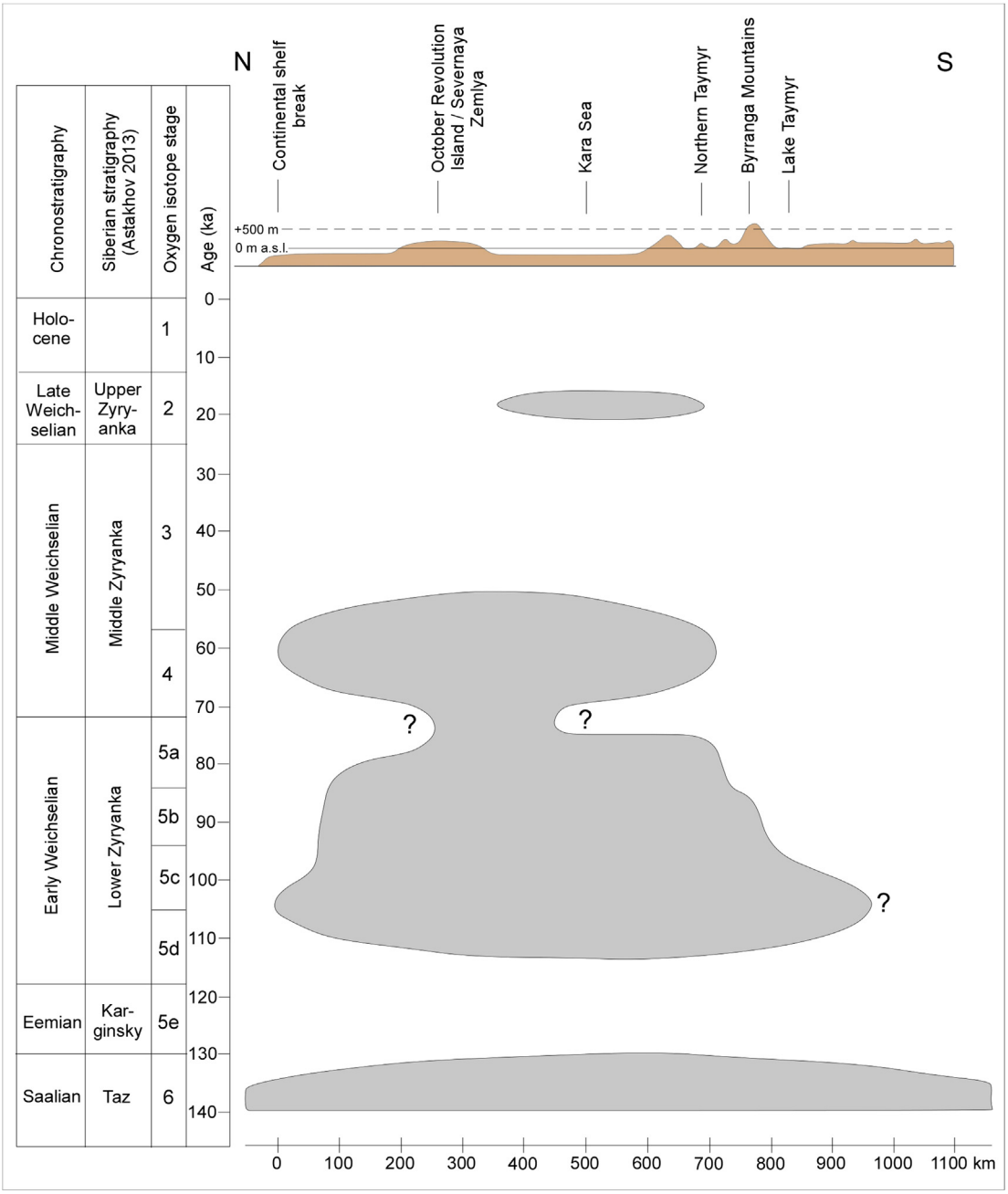

Fig. 6. Glaciation curve for the Taymyr Peninsula, October Revolution Island/Severnaya Zemlya archipelago and the Kara Sea shelf. The ice sheets advanced onto the Taymyr Peninsula from the north to north-west. During the Saalian, the entire Taymyr was been ice covered. The three Weichselian glaciations were of progressively decreasing amplitude. Modified from Möller et al. (2011). Siberian stratigraphic division from Astakhov (2013).

Weichselian (Fig. 6), but with successively smaller ice volumes (Möller et al., 2011). The maximum expansion of a Kara Sea ice sheet was in the Early Weichselian (MIS 5d-5b), reaching well south of the Byrranga Mountains on the Taymyr Peninsula, merging with the Putorana Plateau ice cap in the SE and advancing onto the northwest-Siberian lowlands, and reaching the northern shelf edge. The Early Weichselian ice retreat was followed by a limited Middle Weichselian (MIS 4) advance to the south. However, in the north ice reached the shelf edge and merged with the Svalbard–Barents Sea ice sheet to the west. The uppermost till/marine cycle on Severnaya Zemlya suggests that this archipelago was ice-covered through MIS 5d to MIS 4 (Möller et al., 2006). Cape Chelyuskin in the east was not ice covered (Möller et al., 2008), but the northern Siberian coast was impinged by MIS 4 ice on the Taymyr Peninsula (Alexanderson et al., 2001) that extended well into to the northwest-Siberian lowlands (Astakhov and Nazarov, 2010; Astakhov, 2013). The LGM extent of Kara Sea ice sheet is problematic (Svendsen et al., 2004a). Terrestrial evidence of its advance is only at hand on the northernmost coast of Taymyr Peninsula (Alexanderson et al., 2001), while Severnaya Zemlya was largely ice free during LGM (Raab et al., 2003; Möller et al., 2006). However, based on marine sub-bottom profiling over the Kara Sea shelf, Polyak et al. (2008) argue for the presence of a LGM till over parts of it. LGM ice is suggested to have reached the Vilkitsky Strait in the east and flowed across the shelf towards the Voronin Trough

that drains into the Arctic Ocean (Fig. 3). Detailed echo-sounding east of Novaya Zemlya, show no indication for a LGM ice sheet immediately west and north-west of Taymyr Peninsula (Stein et al., 2002; Dittmers et al., 2008). This speaks against a southern connection between the LGM Barents–Kara Sea ice sheet and a local ice sheet on Taymyr Peninsula (Stein et al., 2002; Dittmers et al., 2008).

Although most stratigraphic and glacio-isostatic data suggest repeated build-up of centres of ice mass in the Kara Sea, ice-flow directional data, as interpreted from till fabrics and glaciotectonics in key sections from Severnaya Zemlya (Möller et al., 2006), Cape Chelyuskin (Möller et al., 2008), Yamal Peninsula (Forman et al., 2002) and Yugorski Peninsula (Lokrantz et al., 2003), suggest ice flow from other dispersal centres. A possible solution to this enigma is suggested by Möller et al. (2006) and Ingólfsson et al. (2008). In their model of ice sheet build-up and decay they argue that islands and highlands in the periphery of the Kara Sea were critical as nucleation areas for the formation of local ice caps that later merged on the shallow shelf area and here grew into full Kara Sea ice-sheet domes.

3.2. South-western and central Barents Sea

3.2.1. Landforms

The south-western and central Barents Sea is characterized by shallow banks between deeper troughs, of which Bjørnøyrenna is the largest (Fig. 1). The geomorphic imprints of the Barents Sea ice sheet occurring on the banks are very different from those in the troughs. Banks are characterized by the occurrence of large and small morainic ridges formed in relation to the last deglaciation of the Barents Sea (Elverhøi and Solheim, 1983; Andreassen et al., 2013; Bjarnadóttir et al., 2013) and considered to be diagnostic of slow ice retreat (Ottesen and Dowdeswell, 2009). MSGLs and trough-mouth-fans indicate that the troughs have been occupied by fast-flowing ice streams which during glacial maxima reached the western Barents Sea–Svalbard continental shelf break, whereas grounding-zone sediment accumulations indicate that ice-stream retreat occurred in an episodic manner (Solheim et al., 1990; Faleide et al., 1996; Vorren and Laberg, 1997; Ottesen et al., 2005; Andreassen et al., 2008; Dowdeswell et al., 2008; Winsborrow et al., 2010; Bjarnadóttir et al., 2013, 2014). MSGLs have also been identified on several buried surfaces identified in 3-D seismic data, indicating that ice streams were a common feature during earlier glaciations as well (Andreassen et al., 2004, 2007).

The distribution of geomorphic features shows that the ice streams experienced large spatial and temporal variations in extent, flow velocity, and basal conditions. 3-D seismic data from south-western Barents Sea reveal repeated sequences of glacial rafts and mega-blocks overlain by MSGLs, inferred to be the result of basal freeze-on during periods of ice stream slowdown/quiescence followed by reactivation and resumed fast ice-flow (Andreassen et al., 2004; Andreassen and Winsborrow, 2009). Furthermore, sets of landforms ascribed to the last deglaciation of the upper regions of Bjørnøyrenna indicate that the Bjørnøyrenna Ice Stream repeatedly experienced rapid shifts from fast ice flow to stagnation as inferred from the distribution of MSGLs and crevasse-squeeze ridges respectively (Andreassen et al., 2013; Bjarnadóttir et al., 2014) (Fig. 4). However, the upstream extent and duration of these events of ice stream stagnation are unknown. Finally, glacial lineations and recessional features grouped into juxtaposed ice stream flow-sets indicate the occurrence of ice-stream flow switching (Winsborrow et al., 2010, 2012), which also suggests local changes in subglacial thermal regime and ice-flow velocities (Fig. 4).

In the upper parts of Bjørnøyrenna, large plough marks of highly uniform orientation occur immediately downstream of selected trough-transverse grounding-zone sediment accumulations. These are interpreted to indicate events of high iceberg discharge, with mega-iceberg release and ice stream break-up, probably associated with ice-shelf disintegration and/or extremely high ice-flow velocities (Andreassen et al., 2013; Bjarnadóttir et al., 2014). The plough marks and mapped corrugation ridges in this part of the Barents Sea are similar to those in Pine Island Bay, Western Antarctica (Jakobsson et al., 2011). This landform assemblage is interpreted to represent ice shelf break up, and release of mega-icebergs from the grounding zone that move along in an armada and under the influence of tidal motion that squeeze out small ridges in their trails; the corrugation ridges (Jakobsson et al., 2011).

3.2.2. Stratigraphy and chronology

The southwestern and southern Barents Sea has been subject to repeated shelf-wide glaciations through several glacial cycles during the late Pliocene–Pleistocene, with glacial erosion on the continental shelf and deposition and subsidence at the continental margins. This is recorded in thick sediment records on the outer south-western continental shelf (Faleide et al., 1996; Solheim et al., 1996; Vorren and Laberg, 1997; Butt et al., 2000). The glacial sediments are separated from older sedimentary bedrock by the erosional Upper Regional Unconformity (URU) (Solheim and Kristoffersen, 1984; Vorren et al., 1986). At the south-western Barents Sea margin the glaciogenic sediments above URU are up to 3–4 km thick while their thickness is significantly less (typically up to a few hundred metres) and more poorly constrained in the central part of the Barents Sea (Vorren et al., 1984; Elverhøi et al., 1989, 1989). Based on a combination of seismic stratigraphy and well information the sedimentary column in the south-western part of the Barents Sea has been divided into three main seismic sequences representing different depositional conditions (GI, GII and GIII) (Faleide et al., 1996; Butt et al., 2000). Knies et al. (2009) suggested that three main phases of glacial development took place in the Barents Sea. During an initial ice sheet build-up phase (3.5–2.4 Ma) ice growth was restricted to the northern Barents Sea and Novaya Zemlya. A phase of continued ice-sheet growth and southwards expansion occurred 2.4–1.0 Ma, followed by a final phase (<1 Ma) during which Barents Sea glaciations were repeatedly characterised by shelf-wide expansion (Knies et al., 2009).

The last time a Barents Sea ice sheet reached the western shelf edge was around 20 cal ka BP (Vorren and Laberg, 1996; Jessen et al., 2010). Due to limited datable material it is hard to constrain the timing of deglaciation stages on the Barents Shelf. However, the distribution of available ages provides a rough estimate. These indicate that initial deglaciation of the Barents Sea coincided with, and was likely triggered by rising global eustatic sea levels (Landvik et al., 1998; Winsborrow et al., 2010). The outer shelf was deglaciated between 18 and 16 cal ka ago (Rokoengen et al., 1977; Vorren et al., 1978; Bischof, 1994; Polyak et al., 1995; Rasmussen et al., 2007; Aagaard-Sørensen et al., 2010; Junttila et al., 2010; Rüther et al., 2012). At roughly the same time (18–16 cal ka) the Barents Sea/Scandinavian ice sheets are inferred to have reached their maximum extent in north-western Russia (Larsen et al., 1999; Demidov et al., 2006). Recent geomorphic studies of the sea floor support the idea of a delayed maximum in the south-eastern sector of the Barents Sea and further suggest there was a shift in the focus of maximum ice volume and dynamics to the eastern sector of the ice sheet (Winsborrow et al., 2010). The ice-free conditions in the west allowed moisture to penetrate farther east, leading to further ice sheet build-up and advance of this sector. For the central Barents Sea less is known about the timing of ice-sheet retreat, although it may be inferred that the shores of Kong Karls Land and Edgeøya were ice-free at ~11.2 cal ka (Salvigsen, 1981; Bondevik et al., 1995), by which time the ice had probably retreated from Bjørnøyrenna and Olga Stret.

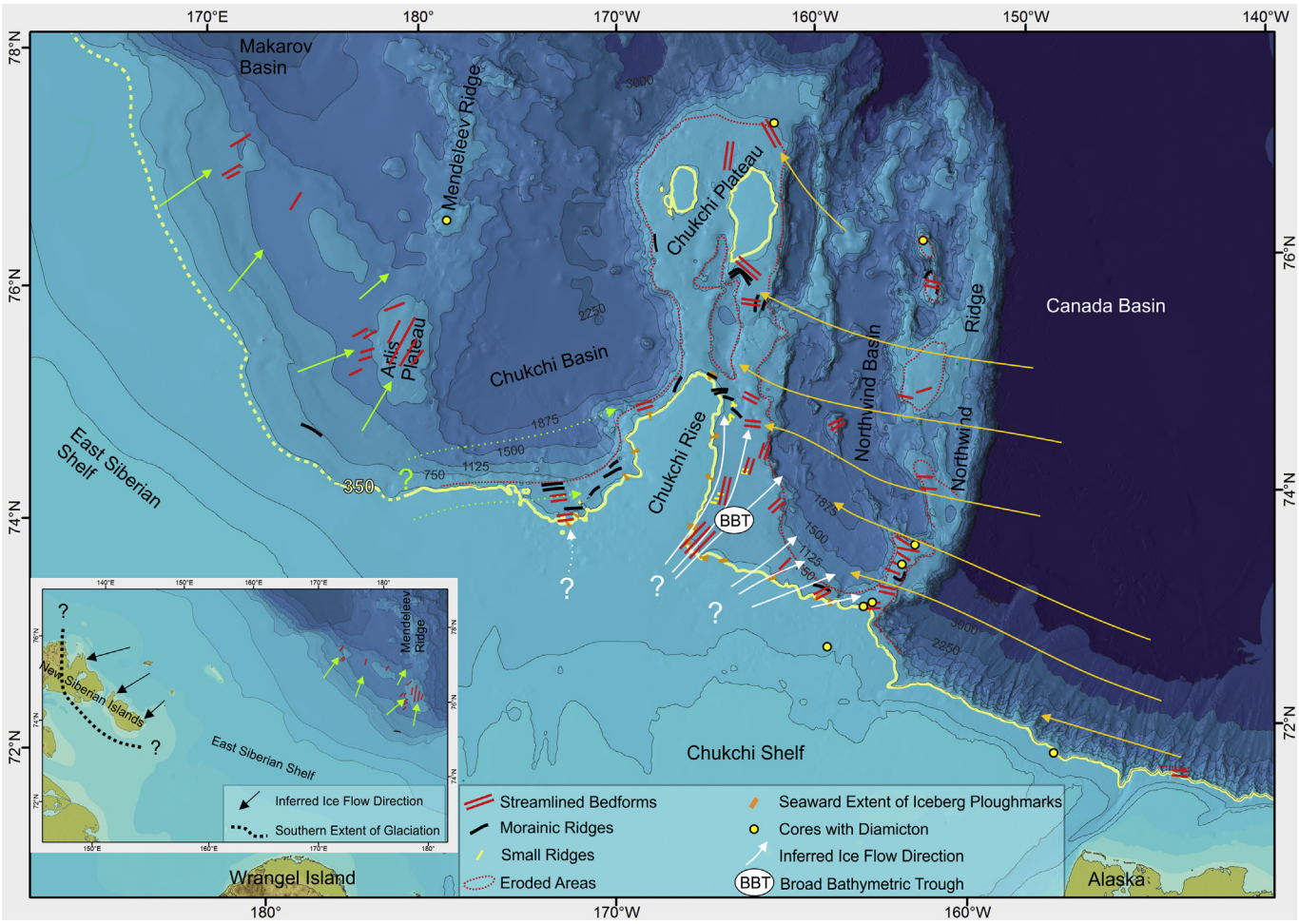

Fig. 7. Distribution of observed glaciogenic features in the Chukchi and East Siberian seas (Jakobsson et al., 2008b; Niessen et al., 2013; Dove et al., 2014). Inset shows south-western limit of glaciation mapped on the New Siberian islands (Basilyan et al., 2010). Yellow line is the 350 m isobath which correlates well with observed seaward limits (orange) of iceberg-scoured seabed. Colour-coded arrows show inferred ice flows of different provenance: Orange = Laurentide source; White = Chukchi Shelf; Green = East Siberian Shelf; Black = New Siberian Islands/East Siberian Shelf. Dotted arrows are most hypothetical. Cores shown recovered glacial and iceberg-turbated diamictons on the borderland and shelf, respectively (unpublished data; Polyak et al., 2007; Stein et al., 2010).

3.3. Laptev Sea, East Siberian Sea and the Arlis Plateau

The glacial history of the East Siberian Sea and adjacent bathymetric highs in the Arctic Ocean is poorly investigated. The international marine research community only has permit-free access to a relatively small sector of the outer continental shelf between Wrangel Island and De Long islands, i.e. between about 170°E and 175°E, north of 74°40′N. In addition, before 2007 persistent sea-ice cover during the summer months made geophysical seafloor mapping difficult in the area.

3.3.1. Landforms

The *RV Polarstern* expedition ARK-XXIII/3 in 2008 carried out seismic investigations and sediment coring between the Chukchi Plateau and the East Siberian Shelf (Fig. 7) (Jokat, 2009; Stein et al., 2010). The data reveal clear evidence that the outermost edge of the East Siberian Sea towards the central Arctic Ocean has characteristics of a formerly glaciated continental margin (Niessen et al., 2013). Glacial lineations found on the flank and top of the Arlis Plateau, located on the southern Mendeleev Ridge, are interpreted as MSGL and/or iceberg plough marks, which have NNE–SSW and NW–SE directions, respectively (Fig. 7). Here the ice-grounding events are possibly related to floating ice masses from the Chukchi Borderland (Stein et al., 2010; Jakobsson et al., 2010b) and/or from the East Siberian Shelf (Niessen et al., 2013).

In seismic profiles across the shelf edge of the East Siberian and Chukchi seas, the top of Neogene sedimentary sequences is truncated. This truncation, accompanied by correlative sedimentary wedges on the upper slope, has tentatively been attributed to ice erosion (Hegewald and Jokat, 2013). In several locations along the East Siberian continental margin, this erosion is associated with MSGL mapped by swath bathymetry or wedges of debris-flow deposits visible in high resolution sub-bottom profiles (Niessen et al., 2013). Debris-flow deposits adjacent to eroded areas on the slope are interpreted as being formed by gravitational redeposition of eroded sediments near former ice-grounding lines. In all locations the MSGL and glaciogenic wedges are covered by hemipelagic sediments, which drape several generations of grounding events. The thickness of well-stratified sediments overlying proglacial and subglacial diamicton ranges from 3 m on top of the Arlis Plateau to 20 m on the East Siberian continental slope. Older glacial streamlined lineations are found in deeper water where they survived subsequent grounding events in shallower water, for example, at about 900 m below present sea level on the Arlis Plateau (Fig. 7). In summary, the mapped landforms on the Arlis Plateau and along the East Siberian Sea margin may stem

from thick coherent ice shelves or local ice sheets covering the Chukchi and East Siberian shelves during several glacial cycles in the past.

Iceberg plough marks from the final glacial event are mapped at present water depths between 350 m and 100 m in the entire area between the Chukchi Borderland and the East Siberian slope to 170°E (Fig. 7). The pattern is irregular with crosscutting plough marks. These glaciogenic features are similar to the iceberg scouring described from the Chukchi Sea margin and overlain by deglacial–Holocene marine deposits (Polyak et al., 2007; Hill and Driscoll, 2010). More mapping in this part of the Arctic Ocean is required in order to unravel the glacial history of the outer East Siberian Sea margin and adjacent bathymetric highs.

3.3.2. Stratigraphy and chronology

Terrestrial investigations carried out on Wrangel Island include studies of elevated shorelines, glaciogenic landforms and radiometric exposure dating (Gualtieri et al., 2003, 2005). Dated raised shorelines, ranging in age between 459 to 780 ka and 64 to 73 ka, are interpreted as eustatic in origin rather than being indicative of former isostatic uplift following ice unloading. Ice-marginal features, such as end moraines, or other glacial landforms are absent in the higher mountains of the island. Exposure dating excludes extensive glaciation during the last c. 84.4 ka (Stauch and Gualtieri, 2008). Permafrost records from the southernmost of the New Siberian Islands contain pollen that suggest a cold tundra-steppe vegetation in the area during LGM (Wetterich et al., 2011). Furthermore, permafrost has been preserved at Bol'shoy Lyakhovsky Island for at least 200 ka suggesting an absence of ice sheets over this entire period (Schirrmeister et al., 2002). In the Laptev Sea region, permafrost records also suggest ice-free conditions during the LGM (Boucsein et al., 2002; Hubberten et al., 2004). Taken together, a large ice-free cold tundra-steppe appears to have stretched from the easternmost Taymyr Peninsula in the west to east of Wrangel Island in the east during LGM. These results contradict the hypothesis of a 2 km thick East Siberian Sea ice sheet centred between Wrangel Island and the East Siberian Islands during the LGM (Hughes et al., 1977; Grosswald and Hughes, 2002) (Fig. 2). However, data from the northern part of the East Siberian Islands provide evidence of glacial impact including large bodies of relict glacier ice, deformed and eroded bedrock and Quaternary deposits, and till units with far-travelled erratics (Grosswald, 1989; Basilyan et al., 2010). This data indicates an ice sheet impinging on the north-eastern part of the archipelago from the East Siberian shelf. The age of this event (or the last ice cover) is estimated as late MIS 6 from thorium/uranium dating of mollusc shells (Basilyan et al., 2010).

Sediment cores were recovered along a transect from the Chukchi Abyssal Plain across the southern Mendeleev Ridge (Stein et al., 2010). These cores are characterized by prominent changes in sediment colour, grain-size, sediment composition, and degree of bioturbation (Stein et al., 2010). In all cores, prominent dark brown intervals were found, which together with the pink–white layers and microfossil abundance are used for core correlation and age control (Stein et al., 2010). A preliminary age model of the upper part of these cores is based on correlation to cores NP-26 and HLY0503-8JPC (Polyak et al., 2004; Darby et al., 2006; Adler et al., 2009; Backman et al., 2009; Polyak et al., 2009). This age model suggests that one core likely encompass MIS 1 to MIS 8, whereas two of them did not reach MIS 6. Furthermore, the age model inferred in the cores located in water depths between 800 and 900 m at southern Mendeleev Ridge implies that an identified diamicton with erosional structures is related to ice-grounding events that occurred before MIS 5a.

3.4. Chukchi margin

The first report of glacial impact on the sea-floor in the Chukchi region dates back 50 years ago (Hunkins et al., 1962). A focused investigation of seafloor morphology and related stratigraphy began, however, first with the 1998–1999 SCICEX swath and sub-bottom survey (Polyak et al., 2001; Edwards and Coakley, 2003). Data collected since indicate a widespread impact of deep-keeled ice from past ice sheets/shelves – especially on the Chukchi Borderland (Chukchi Plateau and Northwind Ridge), and more sparsely at the Chukchi–Beaufort shelf margin (Fig. 7) (Jakobsson et al., 2005, 2008b; Polyak et al., 2007; Engels et al., 2008). Based on the initial mapping of glacial lineations, Polyak et al. (2001) inferred two major sources of eroding ice – from the Laurentide ice sheet to the east and from the Chukchi shelf to the south. However, a lack of evidence for large ice sheets on the Chukchi Sea coast and Wrangel Island, at least in the Late Pleistocene (e.g. Brigham-Grette et al., 2001; Gualtieri et al., 2005) casts doubt on the southern ice source. Accordingly, in later studies mapped glaciogenic landforms on the sea floor in this area have been related to ice originating from the Laurentide ice sheet only, with possibly local ice cap(s) on the Chukchi Plateau (Jakobsson et al., 2005, 2008b, 2010b; Polyak et al., 2007). Exact pathways, provenance, and ages of these glacial advances remained poorly constrained. An improved understanding emerges from data collected in recent years from the northern part of the Chukchi shelf (Chukchi Rise), which characterizes both sea-floor morphology with underlying shallow stratigraphy (Dove et al., 2014) and deeper strata (Coakley et al., 2011; Hegewald and Jokat, 2013). This new data reveals a widespread grounded-ice presence on the Chukchi Rise with ice source located farther south or southwest indicating ice-sheet centres on the Chukchi and/or East Siberian shelf.

3.4.1. Landforms

The most common features of the shallower part of the Chukchi margin are iceberg plough marks. The cut-off depth of scouring is consistently found at water depth of ~350 m (Fig. 7). Isolated or sparsely aggregated plough marks may occur at greater depths; they have curved paths and do not form parallel clusters typical for MSGL. At depths above ~130 m scours fade away due to sediment infill, because the inner shelf is swept by currents that remove all pre-existing bedforms. Such plough marks were described earlier from the Chukchi Borderland (Hill and Driscoll, 2010) and are also evident in sub-bottom data from about 167°E, 76°40′, at 180 m water depth in the East Siberian Sea (Gusev et al., 2012). Thus, it seems reasonable to assume that the intensively ploughed zone in the depth range between 130 and 350 m extends farther west to an unknown extent along the margin of the East Siberian Sea (Fig. 7).

As iceberg scouring eliminates evidence of previous sea-floor processes, glaciogenic landforms such as lineations and morainic ridges are primarily found at depths >350 m. The lower limit of their distribution varies and often coincides with the inflection point in the slope profile. Around the Chukchi Rise and Plateau this limit commonly occurs at depths between 550 and 900 m, whereas at other sites on the Northwind Ridge it can exceed 1000 m below present sea level (Jakobsson et al., 2008b). In comparison to the Chukchi Plateau and Rise, the distribution of glaciogenic landforms on the Northwind Ridge is fragmentary as the ridge consists of isolated, limited highs, often with steep slopes.

Clusters of parallel, linear to slightly curved grooves and ridges are common for the edge of the Chukchi Rise and Plateau and the highs of the Northwind Ridge. Their pattern and dimensions are characteristic of MSGL identified elsewhere on glaciated shelves. In addition to the shelf edge, MSGL occur in a broad bathymetric

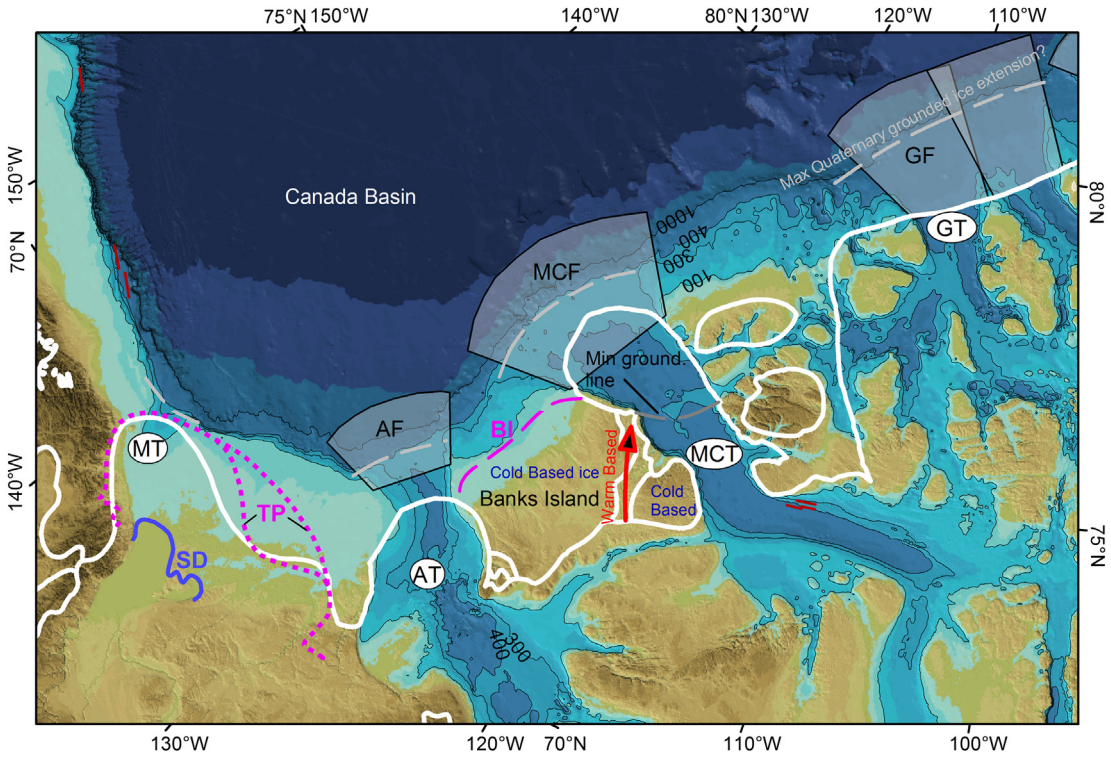

Fig. 8. Ice-sheet extension in the Beaufort Sea area during LGM inferred from Dyke (2004) (white line). The Toker Point Stade (TP) from Murton et al. (2010), recently suggested to represent LGM, is shown with a purple medium dashed line. The LGM ice extension on Banks Island (purple, medium dashed line), including distribution of cold respective warm based ice, is from England et al. (2009). The Sitidgi Stade (SD) is suggested to represent a re-advance during the deglaciation (see Section 3.5). Red lines indicated mapped streamlined glaciogenic bedforms as in Figs. 4 and 7. MT = Mackenzie Trough; AT/F = Amundsen Trough/Fan; MCT/F = McClure Trough/Fan; GT/F = Gustav Adolf Trough/Fan.

trough on the eastern side of the Chukchi Rise (Dove et al., 2014), similar to cross-shelf troughs in the Barents and Kara seas (c.f. Sections 3.1 and 3.2). Several sites such as on the northern Northwind Ridge (Jakobsson et al., 2008b), Chukchi Plateau (Mayer et al., 2010), and in the trough on the Chukchi Rise (Dove et al., 2014) feature drumlinized seabed, which is especially helpful for identifying the direction of ice flow.

Streamlined bedforms east and north of the Chukchi Rise, including its north-eastern edge, are predominantly E–W to SE–NW trending (Fig. 7), consistent with the inferred arrival of eroding ice from the north-western sector of the Laurentide ice sheet (Fig. 7) (Jakobsson et al., 2001, 2005, 2008b; Polyak et al., 2007; Engels et al., 2008). The curved path of this ice flow along the Alaskan margin and then NW-wards across the Northwind Ridge is not well understood, but has been proposed to possibly indicate the presence of very thick shelf ice over the Canada Basin (Jakobsson et al., 2010b).

On the Chukchi Rise, MSGL mostly occur in the bathymetric trough and on the western edge and appear to have SW–NE orientation, same as at some highs on and near the Northwind Ridge (Fig. 7). The provenance of ice that has formed these features is not yet understood. Possible sources are the Chukchi shelf farther south and/or the East Siberian margin (Fig. 7).

Curvilinear to sinuous, symmetric or asymmetric ridges composed of diamict material are common for the shelf edge, especially between 350 and 550 m water depth around the Chukchi Rise (Dove et al., 2014). Similar ridges occur on the Chukchi Plateau, but their distribution is more sparsely constrained by existing data. Ridges are between 100 and 800 m wide and can grade into depositional wedges up to 50 m thick. Multiple ridges can form long bands running along the shelf edge, where sub-parallel ridges are interspaced with hummocky seabed. Broadly grouped, the ridges are interpreted as moraines and/or GZW. At several locations distribution of ridges indicates up-slope retreat(s) of the grounded-ice mass after the advance phase(s).

Smaller ridges oblique or transverse to MSGL have been mapped at the north-eastern part of the Chukchi Rise at the flanks of the bathymetric trough (Dove et al., 2014). They may have a diverse origin: two sets of linear to sinuous, sub-parallel ridges may be recessional moraines or basal crevasse-fill, whereas a set of multiple, closely and regularly spaced ridges is similar to ribbed moraines. The adherence of these features to the trough, along with MSGL and a thick package of till, provides further evidence of extensive, possibly pulsed ice streaming from the Chukchi Rise eastwards.

Tills are persistent at the shelf edge around the Chukchi Rise, commonly infilling underlying depressions or channels or forming large cross-sectional wedges, sometimes with multiple till units (Dove et al., 2014). Downslope from the till wedges till-like packages occur with characteristic asymmetric cross-section, probably re-deposited from the eroded sites. The slope and adjacent basins also feature multiple debris lobes up to 50 m thick, interstratified with layered hemipelagic sediments. Altogether, a combination of till wedges, redeposited packages, and debris lobes indicates large amounts of sediment delivered by glaciers to the slope throughout the Chukchi margin.

3.4.2. *Stratigraphy and chronology*

Based on the position of regional erosional unconformity within Plio-Pleistocene deposits on the Chukchi margin (Hegewald and Jokat, 2013), glacial impact on the seabed in this region has a long history. Direct age assessment of its initiation is not yet possible, but sediment-core data throughout the western Arctic Ocean indicate a sharp increase in iceberg-rafted material at the

beginning of Middle Pleistocene, around MIS 16 (ca 0.7 Ma) (Polyak et al., 2009; Stein et al., 2010; Polyak and Jakobsson, 2011).

Cores from the Northwind Ridge (Fig. 7) constrain the age of the last erosional event associated with the Laurentide-sourced ice to the penultimate glaciation, estimated MIS 4 (Polyak et al., 2007). A younger erosional age of the Last Glacial Maximum (MIS 2) has been obtained only for the shelf-proximal area of the Ridge with water depths <450 m. Data on bedforms from the Chukchi Rise indicate that it was the source of this younger ice, consistent with the Holocene age of sediments overlying iceberg-scoured surface on the Rise and adjacent shelf (Polyak et al., 2007; Hill and Driscoll, 2010). We note that these ages constrain only the last ice impact at a given sea floor site. They do not preclude older grounding events, obliterated by later impacts, neither the occurrence of younger ice shelves that were too thin to reach the sea floor.

3.5. Beaufort Sea and the northern Canadian Arctic Archipelago

At least seven primary ice streams discharged directly into the Arctic Ocean from the Laurentide and Innuitian ice sheets during the LGM, some reaching or exceeding 1 km in thickness. The LIS advanced northwestward from the Canadian mainland inundating both the Beaufort Sea and adjoining marine channels and islands of the western Canadian Arctic Archipelago (CAA). There, the LIS coalesced with the southern margin of the Innuitian Ice Sheet (IIS) that inundated the Queen Elizabeth Islands (QEI) to the north. The Canadian Shelf of the Beaufort Sea marks the northwestern limit of the LIS, which during maximal phases of late Quaternary ice-sheet growth extended west along the Yukon Coastal Plain, possibly overriding parts of the Alaskan coast farther west.

3.5.1. Landforms

Three large glacial troughs extend across the Beaufort Sea Shelf and southwest CAA; the Mackenzie Trough, Amundsen Gulf and M'Clure Strait (Fig. 8). Furthermore, eastward (up-ice) from these three prominent troughs, satellite and bathymetric data reveal large MSGLs converging into them from many of the islands and intervening channels of the western CAA (Stokes et al., 2005, 2006, 2009; MacLean et al., 2010).

Where M'Clure Strait and Amundsen Gulf intersect the continental shelf break, a pronounced "duck-foot" pattern in the bathymetry is consistent with the presence of classic TMFs (Stokes et al., 2005, 2006) (Fig. 8). Sub-bottom profiles crossing the shelf break at the mouth of M'Clure Strait reveals a series of stacked glacial debris flows supporting this interpretation (Niessen et al., 2010). In Amundsen Gulf, high-resolution multichannel seismic data also indicate a substantial TMF that purportedly records up to nine Pleistocene advances of the LIS to the shelf break (Batchelor et al., 2013). In contrast, Mackenzie Trough lacks a well-defined large TMF. However, west of this trough, lineations are mapped on the sea floor along the Beaufort outer margin in 400–700 m water depths (Fig. 8). These lineations are interpreted to be of glaciogenic origin and to originate from an ice-shelf that flowed along the Alaska-Beaufort margin and possibly extended to and across the Chukchi Borderland (Engels et al., 2008).

3.5.2. Stratigraphy and chronology

Based on the abundance of terrestrially dated sites and documented glacial landforms in northwestern Canada and the western CAA, the advance of the northwest LIS is now recognized to be pervasive, extending to the polar continental shelf during the LGM (England et al., 2006, 2009; Lakeman and England, 2013). As a result of the LGM ice cover, information on pre-MIS 2 glacial activity for much of the northwest LIS remains undocumented (Kleman et al., 2010). Furthermore, there are still no direct chronological constraints on the limit of the LIS offshore on the polar continental shelf (Dyke and Prest, 1987).

The existence of active ice streams in M'Clure Strait and Amundsen Gulf during the LGM presents a significant update on previous glacial reconstructions that portrayed ice shelves occupying these channels north and south of Banks Island (Dyke and Prest, 1987; Dyke et al., 2002; Dyke, 2004) (Fig. 8). Furthermore, earlier interpretations also showed multiple till sheets on Melville and Banks islands, most of which were interpreted to record undisturbed pre-Late Wisconsinan glaciations (Vincent, 1982, 1983). However, recent field mapping and widespread dating of ice-transported shells on both islands indicate that these till sheets all date to the LGM (England et al., 2009). Indeed, most of the previously mapped multiple till sheets on Banks Island (Vincent, 1982, 1983) are in fact weathered bedrock with only scattered, far-travelled Laurentide erratics deposited during MIS 2 (England et al., 2009). Most recently, the Laurentide ice retreat has been mapped from the polar continental shelf successively eastward across Banks Island to Prince of Wales Strait, during the Late Wisconsinan (Lakeman and England, 2012, 2013). Farther north, on southern Melville island, AMS radiocarbon dates on individual shell fragments were obtained from the Dundas and Bolduc tills (Hodgson and Vincent, 1984; Hodgson et al., 1984) and range from 24 to 49 ka BP (England et al., 2009). Although these till sheets were originally assigned to two separate Laurentide glaciations, they are now assigned to the LGM. Important implications of these findings are that the northwest LIS had to have advanced across Viscount Melville Sound onto Melville Island after ~24 ka BP requiring at least partially ice-free conditions in the Sound during MIS 3 (England et al., 2009). Granite glacial erratics deposited by the LIS on southern Melville Island occur up at least 235 m above present sea level, recording a minimum thickness of 635 m for the LGM M'Clure Strait ice stream (England et al., 2009). Furthermore U/Pb zircon dating of some far-travelled erratics collected across the western CAA demonstrate for the first time that their provenance can be assigned to orogenic belts with unique radiometric ages located within the mainland Canadian Shield up to 1000 km to the southeast (Doornbos et al., 2009). These recently identified Shield erratics also would have been en route to the Arctic Ocean via M'Clure Strait and adjoining channels within the central CAA during the LGM (MacLean et al., 2010; Pieńkowski et al., 2012, 2013).

The LIS appears to have reached the Mackenzie delta region on at least two occasions during the Last Glacial cycle. On the mainland, these events are delineated by the Toker Point Stade, and the younger Sitidgi Lake Stade (Fig. 8). Early work based on radiocarbon dates obtained from wood fragments from within the Toker Point till and marine shells from overlying sediments, suggested that this advance was Early Wisconsinan (MIS 5–4) (Murton et al., 2007). As a result, there was a long-standing view that a limited northwesterly advance of the LIS during the LGM (Sitidgi Stade) followed a more extensive early Wisconsinan glaciation (Toker Point Stade/Buckland Glaciation) (MIS 5–4) (Rampton, 1982; Beget, 1987; Vincent and Prest, 1987; Dyke et al., 2002) (Fig. 8). However, more recent luminescence dating of aeolian dune sand on the Tuktoyaktuk Penninsula, now constrain the age of the Toker Point Stade to a short advance between ~22 and 16 ka BP, requiring that the Sitidgi Stade represents a deglacial re-advance of the Mackenzie ice stream (Murton et al., 2007). Offshore work on the Canadian Beaufort shelf, provides evidence that the fluvial and aeolian sands underlying the Toker Point till extend out towards the shelf break. This implies a period of prolonged subaerial exposure during the Last Glacial cycle, and possibly, for much of the eastern Canadian Beaufort shelf, throughout the LGM. During this time, thick permafrost developed on the exposed shelf (Mackay, 1959; Murton et al., 2010).

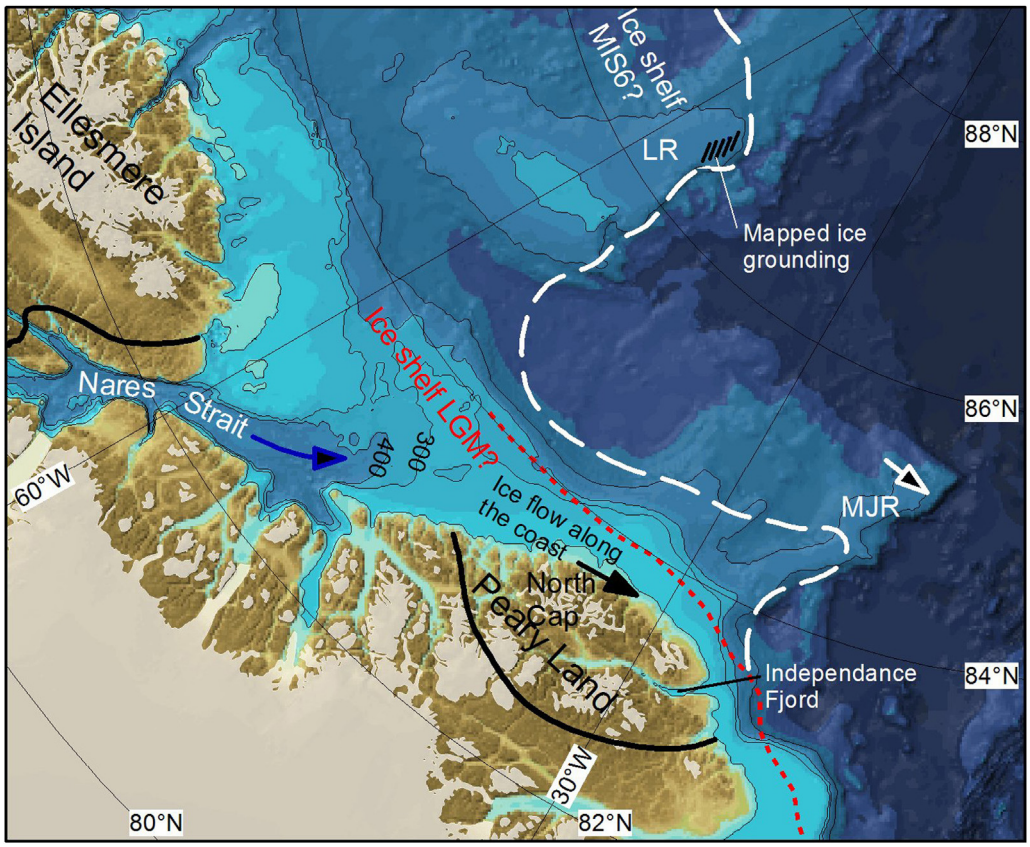

Fig. 9. Map of northern Greenland and the adjacent part of the Arctic Ocean. The red dotted line shows a conceptual limit for LGM ice extension by Funder et al. (2011b), with the outermost part represented by an ice shelf. The hypothesized MIS 6 ice-shelf extension by Jakobsson et al. (2010b) is shown with a white stippled line. Deep iceberg plough marks on the Morris Jesup Rise (MJR) are indicated with a white arrow pointing along in their mapped drift direction. Black lines on the southern Lomonosov Ridge show an area where a distinctive ice erosional surface is mapped. Both the iceberg plough marks and erosional surface is dated to MIS 6 (Jakobsson et al., 2010b).

Seismic reflection profiles from the Mackenzie Trough were first used to suggest that the basal unconformity was formed in the Early Wisonsinan (60–120 ka), with evidence of a second ice advance in the Late Wisconsin (Blasco et al., 1990). A recent study based on an extensive set of industry seismic data has largely confirmed these findings (Batchelor et al., 2013). The presence of a buried GZW and two buried lateral moraines indicate a second ice advance out to the shelf edge that followed the initial excavation of the Mackenzie Trough (Batchelor et al., 2013). However, the absence of a distinct TMF in front of the Mackenzie Trough, despite the large available sediment supply, likely indicates that it was only in the late Quaternary that the LIS started to reach this sector of northwestern Canada.

There is evidence that the Mackenzie ice stream may have travelled west along the Yukon and even along the Alaskan coastal plan during pre-LGM glaciations. Herschel Island, immediately west of the Mackenzie Trough, is an ice-thrust moraine resulting from the advance of the LIS. The position of the island coincides with the westernmost moraines on the adjacent Yukon Coastal Plan, both marking the limit of LIS (Mackay, 1959; Rampton, 1982.). Massive ice exposed on Herschel Island shows signs of glaciotectonic deformation and an isotopic signature that resembles buried glacier ice (Fritz et al., 2012). Furthermore, they report radiocarbon-dated plant detritus as young as 16.2 cal ka BP within the glaciotectonized sediments of Herschel Island. If correct, this date would require that the maximum limit of the LIS along the Yukon Coastal Plain and southern Beaufort Sea occurred during late MIS 2. This LGM age is also coeval with the maximum advance of the LIS from the Mackenzie Valley westward into the Richardson Mountains and onto the Peel Plateau to the south. It also corresponds to a much more expansive advance of the LIS across the western CAA during the LGM (England et al., 2009; Lakeman and England, 2013).

England et al. (2006) provide a summary of three decades of glacial geology conducted across the Queen Elizabeth Islands (QEI) that constitute the northern half of the CAA. This synthesis reconstructs the configuration, primary divides and ice streams comprising the IIS. The last full development of IIS during MIS 2 is reconstructed, when it advanced from margins similar to present after 19 ka BP, inundating all of the marine channels of the QEI and flowing offshore to an unmapped margin on or beyond the polar continental shelf. The IIS coalesced with the Greenland Ice Sheet throughout Nares Strait and with the LIS throughout Parry Channel. Several prominent marine gateways occupied by these coalescent ice sheets fed ice streams with significant thicknesses towards the Arctic Ocean during MIS 2 documented by the uppermost moraines and erratics left by ice margins that subsequently thinned to widespread deglacial deltas dating to the early Holocene. In northern Nares Strait, Greenland erratics and lateral meltwater channels on Ellesmere Island document an upper ice surface at least 800 m asl, and together with water depths of >600 m in adjacent Hall Basin, require an ice thickness of at least 1400 m locally. How much of this thickness was maintained farther north, where the Nares Strait trunk glacier (likely an ice stream) would have thinned as it crossed the continental shelf of the Lincoln Sea, is currently undetermined. However, at least one deep trough

(>600 m) runs northward from northern Ellesmere Island crossing the shelf. Immediately inland, erratics deposited by northward flowing Innuitian ice reach ~900 m asl, again recording potential ice delivery (>1 km thick) from this locality to the Arctic Ocean during the LGM (Lemmen and England, 1992).

Other regional ice streams from the IIS flowed northward to the Arctic Ocean through Nansen Sound (>500 m deep), that was occupied by coalescent ice from adjacent Axel Heiberg and Ellesmere islands during the LGM (Bednarski, 1998). A third prominent ice stream flowed northwestward from southern Ellesmere Island via Eureka Sound and Massey Channel, transporting granite erratics >600 km to the Arctic Ocean (Lamoureux and England, 2000; Ó Cofaigh et al., 2000; Atkinson and England, 2004; England et al., 2004). A fourth ice stream from the IIS likely advanced westward through the Prince Gustolf Adolf Sea, possibly buttressed by the northwest LIS that coalesced with the IIS along the eastern coast of Melville Island (England et al., 2009).

3.6. Lincoln Sea: Northern Greenland Margin and southern Lomonosov Ridge

3.6.1. Landforms

The Northern Greenland continental margin bordering the Arctic Ocean is sparsely investigated due to its remoteness and hard sea-ice conditions. There are yet no marine geophysical surveys of the shelf carried out that reveal whether or not informative glaciogenic landforms exist. Instead, investigations of the northernmost coastal region are the main source of information concerning how far ice extended from Greenland towards the Arctic Ocean during glacial maxima. Along the Peary Land coast, between the ocean and the North Greenland mountain range, there is a 10–15 km wide coastal plain with landforms and sediments recording glacial and marine events back to LGM. For two summers the "LongTerm Project" studied the Quaternary geology here with the main aim to investigate the relation between glaciation and Arctic Ocean sea ice. The results from this work have provided a substantial database on glacial and environmental events since LGM (Nørgaard-Pedersen et al., 2008; Larsen et al., 2010; Möller et al., 2010; Funder et al., 2011b; Olsen et al., 2012).

Geological mapping of glacial erratics on the coastal plain initially led Koch (1923) to suggest that a local ice cap, the *North Cap*, developed over the mountain range during LGM, which to the south and southeast merged with the Greenland inland ice sheet. Later fieldworks confirmed this view (Dawes, 1986; Funder, 1989). Intriguingly, both erratics and striations showed that instead of heading directly towards the ocean, the outlet glaciers on the plain were deflected and moved south-eastwards along the coast, and some erratics had travelled long distances from the west. Recent field work added extensive new evidence such as damming of valleys, till fabric, and observations on "epishelf" lakes, dammed between the deflected glaciers and the mountains. The deflection of the glaciers was explained as a result of buttressing by massive and more or less stagnant "palaeocrystic" sea ice in this part of the Arctic Ocean (Bradley and England, 2008), which forced the glaciers to run alongside the coast (Larsen et al., 2010; Möller et al., 2010; Funder et al., 2011b) (Fig. 9). In this scenario the outlet glaciers on the coastal plain would be minor contributors to an ice shelf fed by ice streams in Nares Strait and the Greenland fjords to the west of the plain (Kelly and Bennike, 1992; England et al., 2006) (Fig. 9). These new results indicate more vigorous LGM glacier dynamics especially in the Nares Strait region and the Greenland fjords to the west while a more passive regime prevailed over northernmost Greenland, probably because of precipitation–starvation, as at present where this area contains some of the largest contiguous ice-free areas in Greenland. Recently, in support of this, IBCAO Version 3.0 with a relatively dense amount of spot soundings, shows a glacial trough-like bottom morphology at the northern entrance to Nares Strait that extends directly to the inferred LGM ice limit. These data have been contributed by the Canadian Hydrographic Service (Jakobsson et al., 2012), and it seems reasonable that this ice stream could feed an ice shelf. Similarly, at the eastern side of the North Cap, at the Fram Strait coast, an outlet from the Greenland ice sheet carved troughs during LGM outside the mouth of Independence Fjord, and fed shelf-ice that extended to the mid-outer shelf (Nørgaard-Pedersen et al., 2008; Funder et al., 2011b) (Fig. 9).

About 80 km northeast of Kap Morris Jesup (Peary Land) is the submarine Morris Jesup Rise that begins its northward extension from the Greenland shelf towards the Arctic Ocean (Fig. 9). The northernmost tip of this bathymetric high was mapped with a sub-bottom profiler (Fütterer, 1992) revealing a glacially scoured seabed extending to approximately 1000 m present water depth (Spielhagen et al., 2004). This area of Morris Jesup Rise was later mapped by a multibeam and chirp sub-bottom profiler (Jakobsson et al., 2008a). Large iceberg scours were found crossing the crest from approximately west to east at a present water depth of 1045 m (Jakobsson et al., 2010b) (Fig. 9). The part of Morris Jesup Rise surveyed by *Oden* extends at the shallower end to a water depth of 940 m and contains no signs of grounding by a coherent ice shelf (Jakobsson et al., 2010b).

During LOMROG 2007 some parts of the flat topped south-eastern Lomonosov Ridge was mapped. Sea-ice conditions hampered the geophysical mapping severely, but the few acquired chirp sonar profiles did show that the ridge crest had been subjected to extensive ice grounding at depths shallower than 785 m present water depth. The character of the mapped ice grounding led Jakobsson et al. (2010b) to propose that a large coherent ice shelf extended out to this location from the nearby Ellesmere Island–Greenland continental shelf (Fig. 9). Prior to LOMROG 2007, Kristoffersen and Mikkelsen (2006) and Nørgaard-Pedersen et al. (2007) found, from seismic and sediment-core data retrieved from the GreenIce drift station over the south-westernmost part of the Lomonosov Ridge, evidence of ridge top erosion at a depth of about 500–600 m. They suggested that erosion might have been caused by deep draft icebergs or an ice shelf tongue extending at least 100 km north from the shelf edge north of Ellesmere Island.

3.6.2. Stratigraphy and chronology

Combining the evidence from land with IRD, detrital Fe, and sediment-accumulation rates in nearby ocean cores Larsen et al., (2010) suggest that the proposed ice shelf adjacent to the coastal plain began to build up as early as 30 cal ka BP. Furthermore, they suggest that both here and farther south at the Fram Strait the ice extent on the shelf culminated at 25–20 cal ka BP. After this, retreat began, and shortly before 10 cal ka BP the presently ice free land on the plain had been exposed and glacier margins had reached their present location (Larsen et al., 2010; Möller et al., 2010; Olsen et al., 2012). However, up until c. 8.5 cal ka BP abundant icebergs floated along the coast and deposited large boulders. This shows both that glaciers were calving in the fjords, and that the sea ice was allowed to float freely at least for some time of the year and not locked in palaeocrystic ice or fast ice as at present (Funder et al., 2011a). To the south-east, at the mouth of Nares Strait, deglaciation followed the same pattern, and when the Nares Strait ice stream finally disappeared, an important connection between the Arctic and the North Atlantic Oceans was established allowing the development of modern ocean circulation in Baffin Bay and the Labrador Sea (England 1999; England et al., 2006; Jennings et al., 2011). Larsen et al. (2010) suggested that the final disintegration of the marine ice sheet component was caused by higher summer temperatures

and eustatic sea-level rise, but also by inflow of warm Atlantic water through Fram Strait, providing a shallower halocline, and a switch of glacial–interglacial paleoceanographic circulation regimes. This is in agreement with results from other parts of the Arctic Ocean and its borderland (Bradley and England, 2008; Jakobsson et al., 2010b; Jennings et al., 2011). The possibility that the Arctic Ocean operates with different glacial–interglacial circulation regimes is further discussed below. The deep ice scouring on the Morris Jesup Rise and the ice grounding on southern Lomonosov Ridge is dated to MIS 6 (Jakobsson et al., 2010b). This point to that ice shelves most likely were reoccurring phenomena at the Quaternary glacial maxima.

4. Marine records from the central Arctic Ocean

4.1. Landforms

The first discoveries of ice groundings in the deep (>800 m below present sea level) Arctic Ocean were made by Vogt et al. (1994) who mapped both lineations and individual plough marks on the Yermak Plateau. This was followed by the discovery of extensive ice grounding on the central Lomonosov Ridge down to 1000 m present water depth (Jakobsson, 1999; Polyak et al., 2001) (Figs. 1 and 10). Later, the bathymetric highs adjacent to the Arctic Ocean continental margins have been partly mapped during several different icebreaker expeditions. Few mapped areas shallower than 900–1000 m are without plough marks from deep drafting icebergs or more coherent ice masses. More detailed mapping of this part of the ridge crest is needed to further interpret the glaciogenic landforms in the context of the glacial history of the Arctic Ocean.

4.2. Stratigraphy and chronology

Modern and Holocene sedimentation rates in the Arctic decrease significantly with distance from the continental margins and oceanic gateways. This largely reflects shelf-to-basin transport processes, inputs from major rivers, and commonly much higher sedimentation rates in the marginal ice zone. In the central Arctic, the two major transport processes for sediments include melt-out from sea ice, and the lateral transport of fine-grained material in ocean currents. As a result, while sedimentation rates of 10's to 100's cm/ka are found along the continental slopes, radiocarbon dating of central Arctic sediments reveal rates of rarely not more than a few cm/ka (Backman et al., 2004). The lowest sedimentation rates occur in regions with the most persistent sea-ice conditions, including the central Amerasian Basin (Levitan and Stein, 2008; Polyak et al., 2009; Stein et al., 2010). This precludes studies of millennial-scale climate variations with a few exceptions where sediment focussing has taken place (Hanslik et al., 2010).

During MIS 2 (14–29 ka; Lisiecki and Raymo, 2005) sedimentation rates in the central Arctic were significantly reduced compared to the Holocene. This reduction has been interpreted largely as a sign of more severe ice conditions and reduced bioproductivity (Darby et al., 1997; Nørgaard-Pedersen et al., 1998; Poore et al., 1999). One of the most striking observations from the Western Arctic is the apparent cessation in LGM sedimentation on the Mendeleev Ridge, where a hiatus between 13.7 and 19.7 ^{14}C yr BP occurs in 8 radiocarbon dated sediment cores (Fig. 11). This break in sedimentation has been previously associated with the development of coherent and thick perennial sea ice in the region during full-glacial conditions, or the development of paleocrystic sea ice, and/or an ice shelf (Polyak et al., 2009).

In the Eurasian sector of the central Arctic, there is a less distinct break in LGM sedimentation (Fig. 11). For example, on the circumpolar regions of the Lomonosov Ridge, high resolution ^{14}C dating of *Neogloboquadrina pachyderma* from some cores reveal continued but diminished sedimentation rates during the LGM, while in other records there is evidence for a correlative LGM hiatus (Hanslik et al., 2010) (Fig. 11). On the Morris Jessup Rise, Lomonosov Ridge, North of Greenland and across the central Eurasian Basin, sedimentation also appears to have continued during the LGM at a reduced rate (Fig. 11). These patterns contrast with sedimentation rates in Fram Strait, Yermak Plateau and at sites close to glaciated continental margins, like north-eastern Greenland and the Barents–Kara shelf, where relatively high sedimentation rates persisted (Nørgaard-Pedersen et al., 2003).

Overall, in the Eurasian Basin, clear gradients towards higher sedimentation rates, fluxes of planktic foraminfera and surface water δ^{18}O, are interpreted as evidence for a less extensive LGM sea-ice cover and the presence of Atlantic water masses (Nørgaard-Pedersen et al., 2003). Relatively high biologic productivity is also reported for LGM sediments along the Northern Barents Sea margin, where upwelling of Atlantic water from katabatic winds coming off the Svalbard/Barents ice sheet may have generated a persistent coastal polyna along the Barents margin to at least the position of the Saint Anna Trough (Knies et al., 1999) (for location see Fig. 1). More recent reconstructions of LGM sea ice, based on phytoplankton derived biomarkers, indicate that perennial sea ice extended south of 81°N in the Fram Strait and over the Yermak Plateau between 29–27.5 ka, and 23.5–17 ka (Müller et al., 2009), and also across the Southern Lomonosov Ridge near the Laptev shelf between 30 and ~15 ka (Stein and Fahl, 2013).

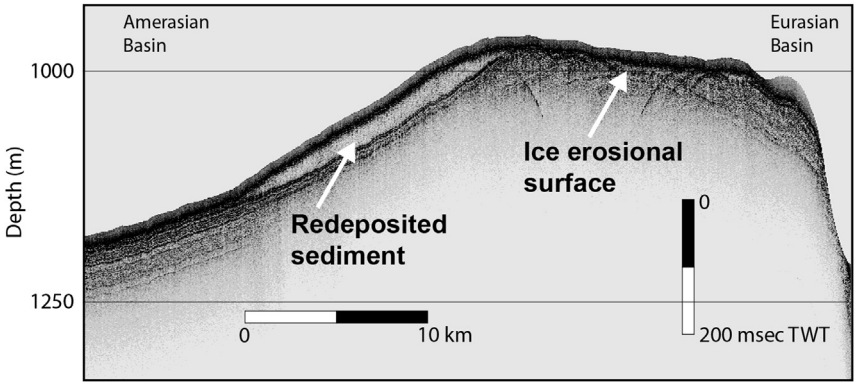

Fig. 10. Sub-bottom profile across the shallow crest of the Lomonosov Ridge acquired from USS Hawkbill 1999 (Edwards and Coakley, 2003). The ridge crest has been extensively eroded by deep drafting ice.

The development of less severe sea-ice in Fram Strait began ~17 cal ka BP, a transition attributed to enhanced inflow of Atlantic water to the Arctic, and the subsequent or coincident retreat of the Svalbard/Barents Sea Ice sheet (Müller et al., 2009). However, perennial sea ice over southern Yermak Plateau between 23.5 and 17 cal ka BP, also corresponds to peak abundances of benthic foraminifera associated with Atlantic water inflow (Wollenburg et al., 2004), suggesting a subsurface inflow of Atlantic water to the glacial Arctic; something that will be further addressed below in Section 5.

The low sedimentation rates that dominate much of the central Arctic during the LGM do not characterize the entire glacial period. Although the temporal resolution of most central Arctic cores remains either too low or too poorly resolved to capture millennial scale changes, evidence for abrupt environmental changes during the Last Glacial cycle (MIS 4–1) are captured by recently published stacked records of ostracode abundance and species composition (Poirier et al., 2012), bottom water temperature reconstructions (Cronin et al., 2012), and preliminary studies on sea ice biomarkers from Southern Lomonosov Ridge/Laptev shelf (Stein and Fahl, 2013). Similarly, sudden inputs of iceberg-derived IRD to the western Fram Strait during MIS 3 and 2, are linked through the provenance of Fe-oxide grains to calving events of the Laurentide ice sheet (Darby et al., 2002). Similar events are recorded in cores with lower temporal resolution from western and central Arctic (Darby and Zimmerman, 2008). Improved constraints on the timing of these events requires dedicated drilling in more marginal settings of the Arctic where high sedimentation rates have so far prevented the acquisition of sedimentary records capturing the entire Last Glacial cycle.

Beyond the range of ^{14}C dating, age models for central Arctic sediments become difficult to establish (Backman et al., 2004; Alexanderson et al., 2014). However, across much of the central Arctic, cyclic patterns in sediment composition indicate distinct modes of glacial/stadial and interglacial/interstadial sedimentation (O'Regan et al., 2008; Sellén et al., 2010). Interglacial/interstadial sediments are largely bioturbated fine-grained muds (i.e. dominated by silt and clay), with moderate to low amounts of sea-ice transported coarse-grained material (<10% wt). They generally contain benthic and planktic foraminifer, ostracods and calcareous nannofossils that are indications of moderate productivity under seasonally variable sea-ice. These sediments are often dark brown in colour, owing to an enrichment of manganese hydroxides, derived from riverine and shelf sediments delivered to the Arctic (März et al., 2011; Löwemark et al., 2012). By contrast, glacial and stadial sediments are often beige to grey in colour, are largely devoid of microfossils and signs of bioturbation, and contain higher amounts of coarse-grained material (e.g. Jakobsson et al., 2000; O'Regan et al., 2008; Polyak et al., 2009).

Even in the central Arctic, elevated amounts of coarse-grained material can occur in thick diamictons (decimetres to >1 m thick), as found on the Lomonosov Ridge (Svindland and Vorren, 2002) during MIS 6, 5b, 5/4 and 4/3 (Jakobsson et al., 2001; Spielhagen et al., 2004). These diamictons are related through timing and mineral composition to the extension of the Barents–Kara ice sheet to the shelf edge, where presumably armadas of large tabular icebergs were shed during the Last 2 Glacial cycles (Jakobsson et al., 2001; Kristoffersen et al., 2004; Spielhagen et al., 2004). However, there is no indication that such facies were deposited on the Lomonosov Ridge prior to MIS 6, even when looking at the longer 20–30 m Pliocene through Quaternary section recovered during the Arctic Coring Expedition (ACEX) (O'Regan et al., 2010). The oldest recognized diamicton on the central Lomonosov Ridge occurs during MIS 6, and corresponds to the earliest dated period of glacial erosion on the ridge crest, likely caused by the scouring of deep drafted and coherent masses of ice (Jakobsson, 1999; Jakobsson et al., 2010b; O'Regan et al., 2010).

Based on current studies, correlative thick late Quaternary diamictons are not clearly recognized in sediments from the Amerasian Basin. While coarser-grained beige and laminated grey coloured sediments still dominate glacial sediments, in the Amerasian Basin there appears to be an overall increase in the coarse fraction content in the middle part of the Pleistocene. These coarse grained units are often elevated in dolomites, which point towards a provenance in the Canadian Arctic Archipelago (Phillips and Grantz, 2001; Darby et al., 2006; Polyak et al., 2009; Stein et al., 2010). For most of the Quaternary, direct correlations between these events and the growth and decay of the LIS remain difficult because of the poor age control in the marine sediment records, the generally low sedimentation rates in these distal settings, and in contrast to the Eurasian ice sheets, a lack of calibrated ages for the timing of Laurentide ice sheet advances to the shelf edge. On top of this, there remains considerable uncertainty about the timing, nature and extent of Quaternary glaciations in the Bering and East Siberian seas.

5. Simulation of glacial–interglacial ocean circulation

During full-glacial conditions with >100 m lower sea level (Lambeck et al., 2002), the Arctic Ocean, including Greenland, Iceland and Norwegian seas, differed significantly from its present day configuration. The closing of the Barents Sea, the Bering Strait and the channels through the Canadian Archipelago, together with the subareal exposure of the shallow Chukchi–East Siberian–Laptev Sea region, represents the most dramatic physiographic reorganization. During peak glacial times, Fram Strait was the single oceanic gateway to the Arctic Ocean (Figs. 1 and 3). Furthermore, freshwater input to the glacial Arctic Ocean was reduced during glacial conditions, due the termination of low salinity Pacific waters entering through the Bering Strait and an overall reduction of the hydrological cycle (Lohmann and Lorenz, 2000). Different surface wind conditions in the glacial world (Shin et al., 2003; Stärz et al., 2012) may also yield altered circulation in the Arctic Ocean (Stigebrandt, 1985) and deep water formation in the North Atlantic appears to have been reduced (Broecker, 1997; Shin et al., 2003).

Given these pronounced changes, it likely that the Arctic Ocean circulation has a glacial mode, distinctly different from present-day. Based on theoretical considerations and paleoceanographic data, a number of circulation schemes have been proposed. These range from an essentially ice-free Arctic Ocean (Donn and Ewing, 1966; Olausson and Jonasson, 1969) to one that is completely covered by thick sea ice (Weyl, 1968; Bradley and England, 2008). On the basis of the reduced freshwater input, Olausson and Jonasson (1969) hypothesized that the low salinity surface layer was absent in the glacial Arctic Ocean. They envisioned a weakly stratified Arctic Ocean, which was kept ice free through heat transport associated with Atlantic water circulation. A rough estimate, using an annual-mean heat loss of 100 W m^{-2} from an open-water area of approximately $7 \cdot 10^{12}$ m^2, suggests that an oceanic heat transport of about 0.7 PW across the Greenland–Scotland Ridge is required to keep the glacial Arctic sea-ice free. This is about three times greater than the present-day northward oceanic heat flux (Hansen and Østerhus, 2000), indicating that the completely ice-free scenario of Olausson and Jonasson (1969) is less plausible. Indeed, there are paleoceanographic data indicating that the low-salinity surface water, which is presently confined to the Arctic Ocean and along the east coast of Greenland, frequently extended south eastward over the Greenland and Norwegian seas (Dokken and Jansen, 1999; Bauch et al., 2001). The low-salinity surface layer stabilized the water column in the Nordic Seas, allowing an expansion of the sea-

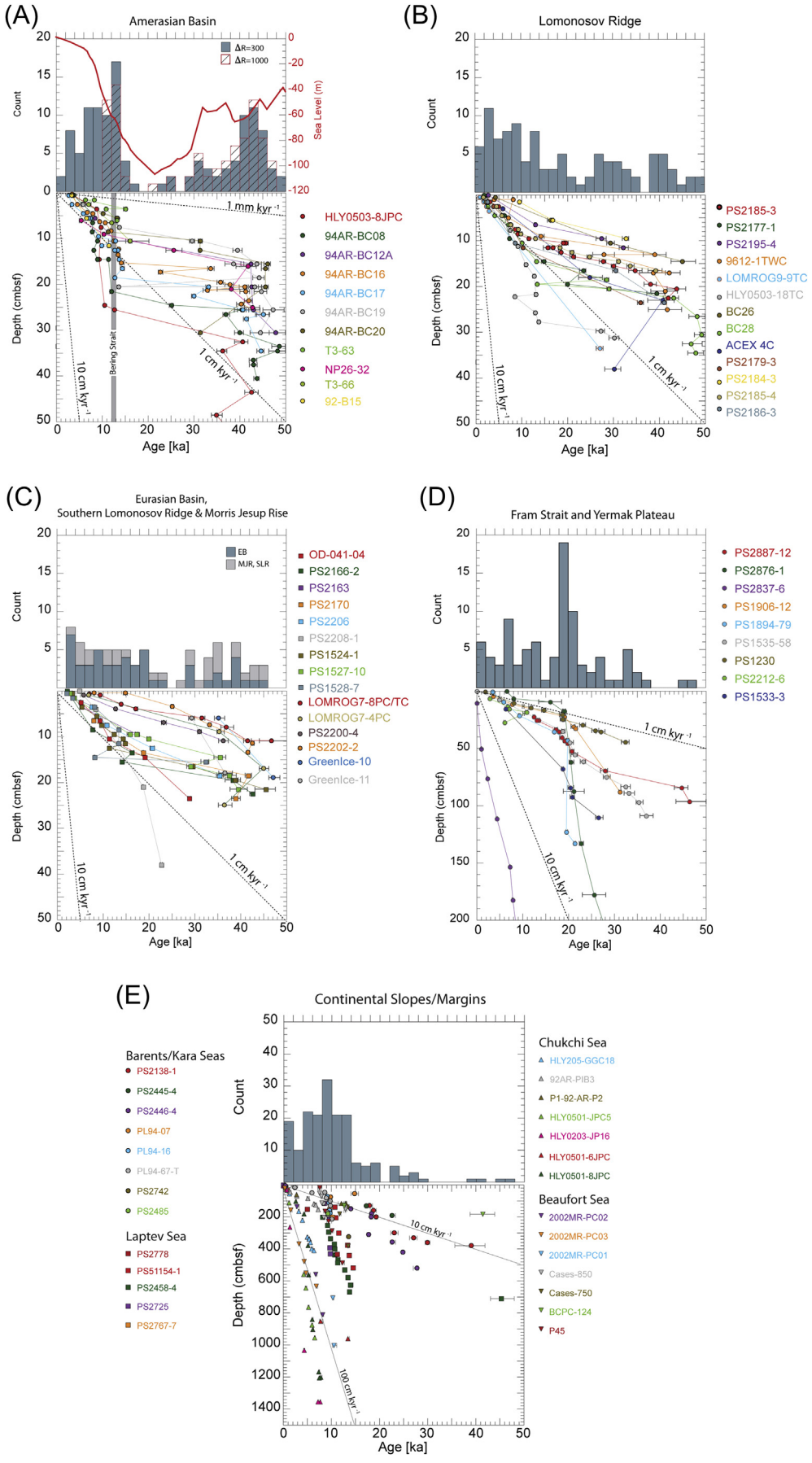
(A)
Amerasian Basin
ΔR=300
ΔR=1000
Count
Sea Level (m)
Depth (cmbsf)
Age [ka]
1 mm kyr⁻¹
1 cm kyr⁻¹
10 cm kyr⁻¹
Bering Strait
HLY0503-8JPC
94AR-BC08
94AR-BC12A
94AR-BC16
94AR-BC17
94AR-BC19
94AR-BC20
T3-63
NP26-32
T3-66
92-B15
(B)
Lomonosov Ridge
PS2185-3
PS2177-1
PS2195-4
9612-1TWC
LOMROG9-9TC
HLY0503-18TC
BC26
BC28
ACEX 4C
PS2179-3
PS2184-3
PS2185-4
PS2186-3
(C)
Eurasian Basin,
Southern Lomonosov Ridge & Morris Jesup Rise
EB
MJR, SLR
OD-041-04
PS2166-2
PS2163
PS2170
PS2206
PS2208-1
PS1524-1
PS1527-10
PS1528-7
LOMROG7-8PC/TC
LOMROG7-4PC
PS2200-4
PS2202-2
GreenIce-10
GreenIce-11
(D)
Fram Strait and Yermak Plateau
PS2887-12
PS2876-1
PS2837-6
PS1906-12
PS1894-79
PS1535-58
PS1230
PS2212-6
PS1533-3
(E)
Continental Slopes/Margins
Barents/Kara Seas
PS2138-1
PS2445-4
PS2446-4
PL94-07
PL94-16
PL94-67-T
PS2742
PS2485
Laptev Sea
PS2778
PS51154-1
PS2458-4
PS2725
PS2767-7
Chukchi Sea
HLY205-GGC18
92AR-PIB3
P1-92-AR-P2
HLY0501-JPC5
HLY0203-JP16
HLY0501-6JPC
HLY0501-8JPC
Beaufort Sea
2002MR-PC02
2002MR-PC03
2002MR-PC01
Cases-850
Cases-750
BCPC-124
P45
100 cm kyr⁻¹

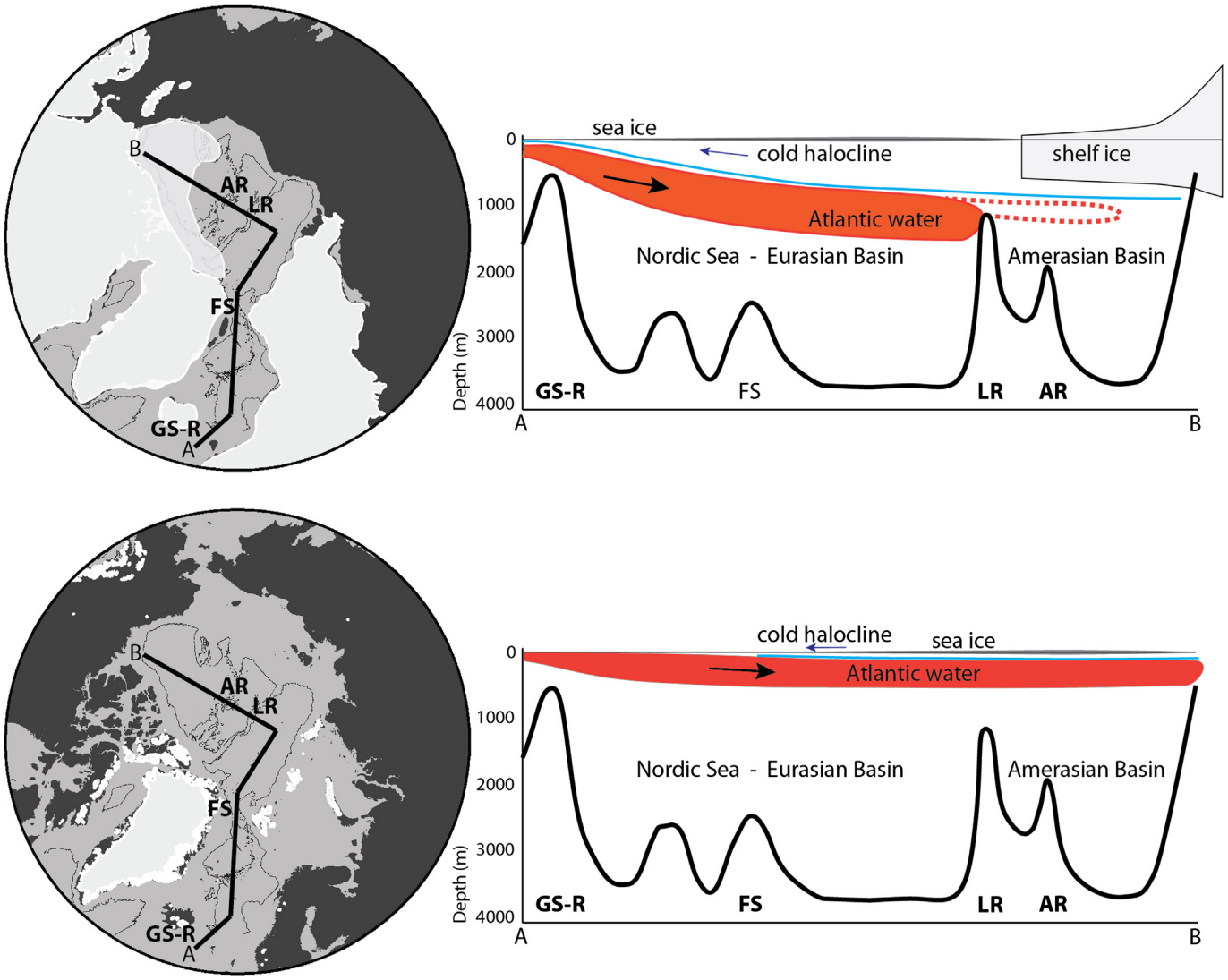

Fig. 12. Conceptual oceanographic model for the glacial (A) and interglacial (B) Arctic Ocean. AR = Alpha Ridge; LR = Lomonosov Ridge; GS-R = Greenland Scotland Ridge; FS = Fram Strait.

ice cover. As a result the deep water sources north of the Greenland–Scotland Ridge shifted from predominantly open-ocean convection in the central Nordic Seas to brine-related dense water formation in the near-coast shelf areas (Dokken and Jansen, 1999; Bauch et al., 2001; Haley et al., 2008). However, the oceanographic conditions in the northern North Atlantic and the Arctic Ocean appears to have varied significantly within a glacial period, exhibiting pronounced shifts between warmer interstadials and colder stadials (Stigebrandt, 1985; Ganopolski et al., 1998; Dokken and Jansen, 1999).

During glacial times, warmer Atlantic water masses appears to have penetrated northward over the Greenland–Scotland Ridge and into the Norwegian–Greenland seas and Arctic Ocean (e.g. Hebbeln et al., 1994; Bauch et al., 2001; Cronin et al., 2012). The subsurface warming was particularly pronounced during MIS 3, when the central Arctic Basin from 1000 to 2500 m was occupied by water masses that could have been as much as 2–4 °C warmer than today (Cronin et al., 2012). Simultaneously, it appears that temperatures between the surface and 500 m water depth were close to the freezing point, a depth interval occupied today by warm Atlantic Waters. Though the vertical resolution of existing data is limited, this seems to suggest that the cold halocline deepened, resulting in a downward displacement of the glacial intermediate layer of warm Arctic Atlantic Water. A downward displacement of

Fig. 11. ^{14}C based sedimentation rates and histograms displaying the number of calibrated ages from cores in different sectors of the Arctic Ocean. Location of cores in each sector are shown in Fig. 1 (see Supplementary information Table 1). Calibrated ages are presented with ±2 standard deviations, and were calculated using the CALIB 6.0 program with the Marine09 reservoir correction curve. For consistency, an additional regional Δ*R* of 300 years was applied to all samples. Figures highlight the generally low sedimentation rates in the central Arctic (A–C) when compared to marginal sites (D, F). A reduction in sedimentation rates is seen across the central Arctic Ocean during MIS 2 (A–C), but it is only in the Amerasian Basin that an apparent widespread hiatus exists. Increasing the Δ*R* to 1000 years for samples with uncalibrated ages >10 ka (Hanslik et al., 2010), does not significantly affect the distribution of ages, or the duration of the inferred hiatus (A; hatched bars in histogram). This period of reduced sedimentation appears to correspond to the sea-level lowstand beginning 28–30 ka and lasting until ~12–14 ka when Pacific inflow through the Bering Strait resumed (CALIB 6.0.1 Reservoir Correction program. Available online at: http://calib.qub.ac.uk/calib/).

the warm Arctic Atlantic Water is also suggested to be the premise for the development of extensive marine shelf-ice complexes in the Arctic Ocean during MIS 6 and presumably also during the LGM (Fig. 12).

To what extent does climate and ocean-circulation modelling provide additional information and constraints on the glacial Arctic Ocean circulation? Most climate-model based efforts have targeted the LGM and model-data comparisons have mainly concerned the Atlantic Ocean and the Southern Ocean (Otto-Bliesner et al., 2007). Moreover, even high-resolution regional ocean-circulation models have difficulties in reproducing the present-day circulation of Arctic and Atlantic waters (Holloway et al., 2007). Recently Stärz et al. (2012) adopted a regional (~30 × 30 km resolution) North Atlantic–Arctic Ocean circulation model to study LGM conditions. Results from a global climate model simulation by Shin et al. (2003) provide boundary conditions at the southern model boundary as well as initial conditions. Under their standard LGM forcing, the Atlantic water entering the Arctic Ocean via Fram Strait has temperatures close to the freezing point. Furthermore, the main halocline shoals to about 100 m in the LGM experiment, compared to 200 m in the present-day control experiment. At first sight this result appears to contradict evidence for the presence of a deep glacial halocline, which Jakobsson et al. (2010b) and Cronin et al. (2012) proposed based on conceptual modelling and paleoceanographic data (Fig. 12). However, the LGM simulation of Stärz et al. (2012) shows that, in the Fram Strait, the outflowing layer from the Arctic extends down to about 1500 m and that the Atlantic inflow has its centre displaced towards the bottom. This is in broad agreement with the glacial Arctic Ocean stratification suggested by Jakobsson et al. (2010b) and Cronin et al. (2012), although the Arctic Atlantic Water temperature in the LGM simulation of Stärz et al. (2012) appears to be somewhat too cold to match the available Mg/Ca temperature proxies from Arctic Ocean ostracodes.

There are also theoretical ideas that can illuminate the glacial circulation of the Arctic Ocean. A more estuarine circulation in the glacial Arctic Ocean, characterized by an extensive low salinity surface layer, could emerge if the northward heat flux across the Greenland–Scotland Ridge was reduced sufficiently (Stigebrandt, 1985; Spall, 2012). If an estuarine circulation mode prevailed, then the generally decreased freshwater input to the Arctic Ocean is expected to cause the upper-ocean low-salinity layer to extend deeper; i.e. a deeper cold halocline (Nilsson and Walin, 2010; Jakobsson et al., 2010b).

The closing of the Bering Strait and the Barents Sea would have impacted ocean circulation patterns both regionally and globally (Hu et al., 2010, 2012). Stigebrandt (1984) proposed that the salinity difference between the North Atlantic and the North Pacific is presently regulated by the Bering Strait flow. This idea has inspired further speculations on how a closing of the Bering Strait gateway could affect the Atlantic thermohaline circulation (De Boer and Nof, 2004). Circulation modelling suggests that a closing of the Barents Sea may reduce the flow of Atlantic water through the Arctic (Aksenov et al., 2011). Another key factor is the winds over the Arctic Ocean that generate a current flow, which is important for transporting the Atlantic water through the Arctic Ocean (Nøst and Isachsen, 2003). In the glacial state, both the wind forcing and the geometry of the closed depth contours change. Evidently, this would change Atlantic water circulation in the Arctic Ocean.

In summary, our understanding of the glacial Arctic Ocean circulation has been significantly advanced by data-based analyses during the last decade. However, the data also pose some theoretical challenges, including the possibility of a very deep cold halocline and ocean–ice-sheet interactions in the glacial Arctic Ocean. It is foreseen, however, that the picture emerging from recent reconstructions together with theoretical and numerical modelling will help to further improve our knowledge of the glacial Arctic Ocean circulation.

6. Simulation of ice sheets and ice shelf complexes

Prior to the 1970s, only few numerical models simulating ice sheets and ice shelf shelves were available. Stability of ice shelf complexes was mainly discussed for the West Antarctic Ice Sheet in the context of the sparse database of field observations available and/or mathematical analyses of the first theoretical descriptions of ice shelf and ice sheet dynamics (Weertman, 1974; Hughes, 1975; Thomas, 1979). Both Mercer (1970) and Hughes et al. (1977) transferred ideas and concepts developed for Antarctic configurations to the Arctic when they proposed extensive Arctic Ocean ice shelves. Numerical simulations of hypothesized Arctic Ocean ice shelves were, however, impossible at this time. Early numerical ice shelf models, e.g. by Thomas and Bentley (1978), were not treating ice dynamics in the transition zone between an ice shelf and an ice sheet correctly. At present, ice shelf dynamics are being incorporate into advanced ice sheet models, although it still presents a great challenge. To be able to outline how this is done, a brief summary of numerical ice sheet models is provided here.

Based on numerical glaciological concepts from the pioneering work by Weertman (1974); Hughes et al. (1977) reconstructed a huge “late-Würm Arctic Ice Sheet”. However, until roughly a decade ago, numerical ice models only captured the behaviour of the slowly moving (tens of meters/year) homogeneous interior parts of land-based ice sheets. These “zero order Shallow Ice Approximation (SIA)" models regard ice sheets as essentially flat in order to simplify the equations governing their dynamics (Hutter, 1983; Kirchner et al., 2011). Due to the shallowness-assumption, SIA models work well in the interior of an ice sheet, but fail in regions with highly variable ice dynamics, e.g. fast-flowing ice streams and outlet glaciers (velocities of up to 1000 m/yr) and when approaching the grounding-line zone. Furthermore, ungrounded floating ice including ice shelves and glacier tongues cannot be treated with SIA models.

Although SIA models have limitations, they have added valuable insights on the glacial history of ice sheets in the circumpolar Arctic (e.g. Siegert et al., 1999; Siegert and Dowdeswell, 2004; Tarasov and Peltier, 2004; Stokes and Tarasov, 2010). Comparison of simulated ice sheets using SIA models with landforms, such as MSGL, GZW, and moraine ridges, is difficult because SIA models fail where these landforms typically are produced, i.e. at the marine ice margins where ice shelves and floating glacier tongues interlink the terrestrial and ocean glacial system (Joughin and Alley, 2011).

During the last decade, the ice-sheet modelling community has developed improved ice-sheet models, so-called “higher order” and “full Stokes” models. These account for the slow flow dominating the grounded inland ice motion, the rapid ice flow in ice streams, ice flow across the grounding line, and ice-shelf flow (Pattyn, 2003; Schoof, 2007; Pollard and Deconto, 2012; Seddik et al., 2012; Larour et al., 2012). Full Stokes models are the most accurate ones from a physical point of view, but they are the most costly to run. Furthermore, Simulation results from SIA models, higher order, and full Stokes models have been compared with respect to simplified model problems (Pattyn et al., 2008, 2012; Calov et al., 2010).

Simulation of ice dynamics of the Quaternary Arctic Ocean marine glaciers calls for the use of full Stokes models. However, their spatial dimensions and longevity do not yet allow for it, because full Stokes models are still restricted to centennial timescales and smaller spatial domains. Alternatively, full Stokes models and SIA models could be coupled adaptively, i.e. switching to SIA mode where permitted and to full Stokes mode where required. This coupling is technically complicated and requires re-

investigation of typically applied scaling relations (Ahlkrona et al., 2013). Of the existing higher order models only two have so far been applied to simulate past glacial conditions in the circum-Arctic (DeConto et al., 2008; Alvarez-Solas and Ramstein, 2011; Koenig et al., 2011). However, even in these applications, coupled ice-sheet/ice-shelf dynamics have either been switched off or could not be resolved by the experimental setup, implying that the higher order ice-sheet model component was run in SIA mode only.

Until ice sheet models of higher-order and full Stokes models are adapted to become more easily applicable, simulations of Arctic Ocean palaeo–ice complexes including ice streams and ice shelves have to rely on SIA models, or employ entirely different modelling strategies. Kirchner et al. (2013) proposed a statistical model to investigate likely spatial dimensions of the hypothesized Arctic Ocean MIS 6 ice-shelf complex of Jakobsson et al. (2010b). The statistical model by Kirchner et al. (2013) is designed to specifically assess whether the extensive MIS 6 ice shelf complex could have been a likely source of deep draft icebergs since this has been proposed (e.g. Dowdeswell et al., 2010b; Jakobsson et al., 2010b; O'Regan et al., 2010). The statistical concept is based on establishing relations between contemporary Antarctic ice shelves and their local physical environment, and the assumption that Arctic Ocean MIS 6 ice shelves scaled similarly. Data of contemporary Antarctic ice shelf areas, calving front length, and ice thickness along the calving front are combined with methods from extreme values statistics to derive a probabilistic description of the maximum draft (depth below sea level) along the calving fronts of various hypothesized MIS 6 ice shelf configurations in the Amerasian sector of the Arctic Ocean. The assumption that mapped ice groundings at exceptionally deep water depths should have been generated during extreme events when unusually deep-drafting icebergs were produced is reflected in the specific choice of statistical methodology: concepts from extreme value statistics provide a firm-based statistical framework that is designed to deal with extreme, rather than common events. The results obtained proved robust, and likely sources for icebergs large enough to scour the seafloor at ~1000 m depth below present sea level were identified. Furthermore, results from the statistical model also indicate the range of the possible extent of the Amerasian Arctic Ocean ice shelf complex, of which one configuration is suggested in Jakobsson et al. (2010b).

7. Discussion and conclusions

Advances made since Mercer (1970) presented the hypothesis of a former ice sheet in the Arctic Ocean are numerous, yet we still lack information from key areas required to compile the holistic Arctic Ocean glacial history. This present circumpolar overview of glacial landforms, stratigraphies, and chronologies summarizes the current state of knowledge and identifies a set of outstanding questions arising from this synthesis. It should be noted that several of the questions we identify are easier to answer today than a few decades ago due to the recent development of techniques including new dating methods and much improved high-resolution sea-floor mapping capabilities. This implies that some previously investigated areas of the Arctic Ocean may benefit from being revisited for new surveys. There is also a need for an improved integration of the different datasets, e.g. marine and terrestrial as well as ice-sheet modelling results.

The question of huge ice shelves in the central Arctic Ocean and how these were fed from circumpolar margins is far from resolved. Although the ice-grounding events reaching >1000 m below present sea level are currently dated to MIS 6 (e.g. Jakobsson et al., 2010b), other expansive but thinner ice shelves likely formed throughout the Quaternary (Polyak et al., 2007). In fact, given evidence for dynamic growth and collapse of Arctic ice shelves through the Holocene (Antoniades et al., 2011), and considering the Antarctic as an analogue to the glacial Arctic, it seems plausible that ice shelves would have developed in several parts of the Arctic Ocean. However, these enigmatic features of the glacial Arctic, including their extent and links to terrestrial ice sheets, are difficult to establish. Identification of subice-shelf sedimentary facies in the Arctic could provide a critical way to constrain their past distribution, but few 10–20 m long sediment cores collected from the marginal sites of the Arctic extend back to the LGM, where these subice-shelf sediments would be most obviously preserved. Whether the lack of LGM sedimentation in numerous Arctic Ocean cores from the Western Arctic is attributable to the existence of large ice shelves remains an open question. Similarly, assertions that these ice shelves may have extended over the central Lomonosov Ridge are not conclusive (Jakobsson, 1999; Polyak et al., 2001). This area is one that should be revisited and fully mapped with modern high-resolution swath bathymetry. Furthermore, the southern Lomonosov Ridge off Greenland is another hot spot for the central Arctic Ocean glacial history as evident from seismic lines collected in this region showing extensive ice erosion (Kristoffersen and Mikkelsen, 2006) and terrestrial landforms that suggest the passage of large ice shelves during the LGM and possibly earlier glaciations.

The Barents Sea is likely the best known area in the high Arctic regarding the glacial history, although large gaps in data coverage still remain. Outstanding questions are therefore on a more detailed level. One such question is how the Svalbard–Barents Sea ice sheet behaved dynamically, from the LGM to the time of its retreat (e.g. Ingólfsson and Landvik, 2013). Did ice domes undertake major reorganizations during the rapid retreat phase, which likely was strongly coupled to oceanographic and sea-level changes? This could explain why marine and terrestrial data from the eastern Svalbard region are still from many points of view contradictory. The new discoveries of landforms suggesting a highly dynamic post-LGM retreat of the Svalbard–Barents Sea ice sheet, with the ice leapfrogging back, is of particular interest considering the present day concerns regarding instabilities of marine ice sheets, in particular the Pine Island Bay area of West Antarctica (e.g. Katz and Worster, 2010).

Ice-stream dynamics in the Beaufort Sea are a key to unravelling the glacial history in the western Arctic Ocean. The advances of the north-western LIS appear to be linked to glaciogenic features on the sea floor along the Alaskan shelf and Chukchi Borderland (Northwind Ridge and Chukchi Plateau). Recent research indicates that only two ice-advances reached the Mackenzie Trough in the late Quaternary, and one of these took place during LGM (Murton et al., 2010; Batchelor et al., 2013). This raises the question whether there have been additional large ice advances onto the Canadian Beaufort Sea shelf that are not yet mapped, and if so, did they contribute to the growth of ice shelves in the western Arctic Ocean? The stratigraphic record from the Chukchi supports this possibility, as an ice erosional event there is associated with Laurentide-sourced ice in MIS 4 (Polyak et al., 2007). Alternatively, was the growth of huge ice shelves limited to MIS 6, as the central Arctic Ocean records seems to imply, with erosional events in the Chukchi Sea area linked to independent glacial activity in Beringia? One key area that may be worth revisiting to further investigate links between the LIS and Chukchi is the Alaskan Beaufort where Engels et al. (2008) suggested the presence of glacial lineations from side-scan imagery. New high-resolution swath-bathymetric mapping and coring in this area may provide important pieces of information. Finally the widespread evidence for IRD events in central Arctic sediments, and as far away as the Fram Strait, suggest multiple and large ice-surging events of the CAA ice streams, from which at least seven ice streams discharged from the IIS and northwest LIS during MIS 2

(Blasco et al., 1990; Stokes et al., 2005; England et al., 2006; Stokes et al., 2009; MacLean et al., 2010; Fritz et al., 2012). Earlier glaciations from the CAA will require higher-resolution and deeper penetrating offshore records proximal to the ice sources.

The recent mapping of the Chukchi Borderland and easternmost East Siberian Sea margin raises several outstanding questions regarding the glacial history in this part of the Arctic Ocean (Dove et al., 2014). Previous assumptions of an ice free cold tundra-steppe stretching from the easternmost Taymyr Peninsula in the west to east of Wrangel Island during LGM will have to be revisited. New data seems to suggest that ice-sheet centres indeed existed on the Chukchi and/or outer East Siberian shelf (Dove et al., 2014); even on the northern part of the East Siberian Islands glacial impacts seems to be preserved (Basilyan et al., 2010). Much more field work will be required in these areas before a holistic view of the Quaternary glacial components in this area can be established.

Acknowledgements

Financial support to M. Jakobsson and M. O'Regan was received from the Knut and Alice Wallenberg Foundation (KAW) and the Swedish Research Council (VR). Stockholm University scientists are affiliated with the Bolin Centre for Climate Research, supported through a grant from FORMAS. The Research Council of Norway grant 20067 provided funding for K. Andreassen. For four decades J. England's research group in the Canadian Arctic Archipelago has been supported by an NSERC Discovery Grant, an NSERRC Northern Research Chair (2002–2012), and additional grants from the Canadian Circumpolar Institute, University of Alberta. Full logistical support to stage field camps throughout this remote region was provided during this same interval by the Polar Continental Shelf Program, NRCan. Funding for marine research north and east of Svalbard (J.A. Dowdeswell, K. Hogan) was provided by UK Natural Environment Research Council Grant NER/T/S/2003/00318 to Dowdeswell. Dayton Dove publishes with the permission of the Executive Director of the British Geological Survey. We are grateful for the comprehensive and insightful comments provided by two anonymous reviewers.

Appendix A. Supplementary data

Supplementary data related to this article can be found at http://dx.doi.org/10.1016/j.quascirev.2013.07.033.

References

Aagaard-Sørensen, S., Husum, K., Hald, M., Knies, J., 2010. Paleoceanographic development in the SW Barents Sea during the Late Weichselian – Early Holocene transition. Quat. Sci. Rev. 29, 3442–3456.
Abe-Ouchi, A., Otto-Bliesner, B., 2009. Ice sheet-climate interactions during the ice age cycle. PAGES News 17, 73–74.
Adler, R.E., Polyak, L., Ortiz, J.D., Kaufman, D.S., Channell, J.E.T., Xuan, C., Grottoli, A.G., Sellén, E., Crawford, K.A., 2009. Sediment record from the western Arctic Ocean with an improved Late Quaternary age resolution: HOTRAX core HLY0503-8JPC, Mendeleev Ridge. Global Planet. Change 68, 18–29.
Ahlkrona, J., Kirchner, N., Lötstedt, P., 2013. A numerical study of scaling relations for non-Newtonian thin film flows with applications in ice sheet modeling. Q. J. Mech. Appl. Math. (in press). http://dx.doi.org/10.1093/qjmam/hbt009.
Aksenov, Y., Ivanov, V.V., Nurser, A.J.G., Bacon, S., Polyakov, I.V., Coward, A.C., Naveira-Garabato, A.C., Beszczynska-Moeller, A., 2011. The arctic circumpolar boundary current. J. Geophys. Res. 116, C09017.
Alexanderson, H., Backman, J., Cronin, T.M., Funder, S., Jakobsson, M., Löwemark, L., Mangerud, J., März, C., Möller, P., O'Regan, M., Spielhagen, R., 2014. An Arctic perspective on dating late Pleistocene environmental history. Quat. Sci. Rev. 92, 9–31.
Alexanderson, H., Hjort, C., Möller, P., Antonov, O., Pavlov, M., 2001. The North Taymyr ice-marginal zone, Arctic Siberia – a preliminary overview and dating. Global Planet. Change 31, 427–445.
Alvarez-Solas, J., Ramstein, G., 2011. On the triggering mechanism of Heinrich events. Proc. Natl. Acad. Sci. U. S. A. 108, E1359–E1360.
Andreassen, K., Laberg, J.S., Vorren, T.O., 2008. Seafloor geomorphology of the SW Barents Sea and its glaci-dynamic implications. Geomorphology 97, 157–177.
Andreassen, K., Nilssen, L.C., Rafaelsen, B., Kuilman, L., 2004. Three-dimensional seismic data from the Barents Sea margin reveal evidence of past ice streams and their dynamics. Geology 32, 729–732.
Andreassen, K., Ødegaard, C.M., Rafaelsen, B., 2007. Imprints of Former Ice Streams, Imaged and Interpreted Using Industry Three-dimensional Seismic Data from the South-western Barents Sea, pp. 151–169.
Andreassen, K., Winsborrow, M., 2009. Signature of ice streaming in Bjørnøyrenna, Polar North Atlantic, through the pleistocene and implications for ice-stream dynamics. Ann. Glaciol. 50, 17–26.
Andreassen, K., Winsborrow, M.C.M., Bjarnadottir, L.R., Rüther, D.C., 2013. Landform assemblage from the collapse of the Bjørnøyrenna palaeo-ice stream, northern Barents Sea. Quat. Sci. Rev. (in this volume).
Antoniades, D., Francus, P., Pienitz, R., St-Onge, G., Vincent, W.F., 2011. Holocene dynamics of the Arctic's largest ice shelf. Proc. Natl. Acad. Sci. U. S. A. 108, 18899–18904.
Astakhov, V., 2004. Pleistocene Ice Limits in the Russian Northern Lowlands, pp. 309–319.
Astakhov, V., Nazarov, D., 2010. Correlation of Upper Pleistocene sediments in northern West Siberia. Quat. Sci. Rev. 29, 3615–3629.
Astakhov, V.I., 2013. Pleistocene glaciations of northern Russia – a modern view. Boreas 42, 1–24.
Atkinson, N., England, J., 2004. Postglacial emergence of Amund and Ellef Rignes islands, Nunavut: implications for the northwest sector of the Innuitian Ice Sheet. Can. J. Earth Sci. 41, 271–283.
Backman, J., Fornaciari, E., Rio, D., 2009. Biochronology and paleoceanography of late Pleistocene and Holocene calcareous nannofossils across the Arctic Basin. Mar. Micropaleontol. 72, 86–98.
Backman, J., Jakobsson, M., Løvlie, R., Polyak, L., Febo, L.A., 2004. Is the central Arctic Ocean a sediment starved basin? Quat. Sci. Rev. 23, 1435–1454.
Basilyan, A.E., Nikol'skyi, P.A., Maksimov, F.E., Kuznetsov, V.Y., 2010. Age of Cover Glaciation of the New Siberian Islands Based on 230Th/U-dating of Mollusk Shells, Structure and Development of the Lithosphere. Paulsen, Moscow, pp. 506–514.
Batchelor, C.L., Dowdeswell, J.A., Hogan, K.A., 2011. Late Quaternary ice flow and sediment delivery through Hinlopen Trough, Northern Svalbard margin: submarine landforms and depositional fan. Mar. Geol. 284, 13–27.
Batchelor, C.L., Dowdeswell, J.A., Pietras, J.T., 2013. Variable history of Quaternary ice-sheet advance across the Beaufort Sea margin, Arctic Ocean. Geology 41, 131–134.
Bauch, H.A., Erlenkeuser, H., Spielhagen, R.F., Struck, U., Matthiessen, J., Thiede, J., Heinemeier, J., 2001. A multiproxy reconstruction of the evolution of deep and surface waters in the subarctic Nordic seas over the last 30,000 yr. Quat. Sci. Rev. 20, 659–678.
Bednarski, J.M., 1998. Quaternary history of Axel Heiberg Island bordering Nansen Sound, Northwest Territories, emphasizing the last glacial maximum. Can. J. Earth Sci. 35, 520–533.
Beget, J., 1987. Low profile of the Northwest Laurentide Ice Sheet. Arct. Alp. Res. 19, 81–88.
Bischof, J.F., 1994. The decay of the Barents ice sheet as documented in nordic seas ice-rafted debris. Mar. Geol. 117, 35–55.
Bjarnadóttir, L.R., Rüther, D.C., Winsborrow, M.C.M., Andreassen, K., 2013. Grounding-line dynamics during the last deglaciation of Kveithola, W Barents Sea, as revealed by seabed geomorphology and shallow seismic stratigraphy. Boreas 42, 84–107.
Bjarnadóttir, L.R., Winsborrow, M.C.M., Andreassen, K., 2014. Deglaciation of the central Barents Sea. Quat. Sci. Rev. 92, 208–226.
Blasco, S.M., Fortin, G., Hill, P.R., O'Connor, M.J., Brigham-Grette, J., 1990. The geology of north America, V.L., the Arctic Ocean Region: Geological Society of America. In: Grantz, A., Johnson, L., Sweeney, J.F. (Eds.), The Late Neogene and Quaternary Stratigraphy of the Canadian Beaufort Continental Shelf, The Geology of North America. Geological Society of America, pp. 491–501.
Bondevik, S., Mangerud, J., Ronnert, L., Salvigsen, O., 1995. Postglacial sea-level history of Edgeoya and Barentsoya, eastern Svalbard. Polar Res. 14, 153–180.
Boucsein, B., Knies, J., Stein, R., 2002. Organic matter deposition along the Kara and Laptev Seas continental margin (eastern Arctic Ocean) during last deglaciation and Holocene: evidence from organic-geochemical and petrographical data. Mar. Geol. 183, 67–87.
Bradley, R.S., England, J.H., 2008. The Younger Dryas and the Sea of Ancient Ice. Quat. Res. 70, 1–10.
Brigham-Grette, J., Hopkins, D.M., Ivanov, V.F., Basilyan, A.E., Benson, S.L., Heiser, P.A., Pushkar, V.S., 2001. Last Interglacial (isotope stage 5) glacial and sea-level history of coastal Chukotka Peninsula and St. Lawrence Island, Western Beringia. Quat. Sci. Rev. 20, 419–436.
Broecker, W.S., 1966. Absolute dating and the astronomical theory of glaciation. Science 151, 299–304.
Broecker, W.S., 1975. Floating Glacial Ice Caps in Arctic Ocean. Science 188, 1116–1118.
Broecker, W.S., 1997. Thermohaline circulation, the Achilles heel of our climate system: will man-made CO_2 upset the current balance? Science 278, 1582–1588.
Butt, F.A., Drange, H., Elverhøi, A., Otter, O.H., Solheim, A., 2002. Modelling Late Cenozoic isostatic elevation changes in the Barents Sea and their implications for oceanic and climatic regimes: preliminary results. Quat. Sci. Rev. 21, 1643–1660.

Butt, F.A., Elverhøi, A., Solheim, A., Forsberg, C.F., 2000. Deciphering late cenozoic development of the western Svalbard Margin from ODP Site 986 results. Mar. Geol. 169, 373–390.
Calov, R., Greve, R., Abe-Ouchi, A., Bueler, E., Huybrechts, P., Johnson, J.V., Pattyn, F., Pollard, D., Ritz, C., Saito, F., Tarasov, L., 2010. Results from the Ice-Sheet Model Intercomparison Project-Heinrich Event INtercOmparison (ISMIP HEINO). J. Glaciol. 56, 371–383.
Clark, D.L., 1971. Arctic Ocean ice cover and its Late Cenozoic history. Geol. Soc. Am. Bull. 82, 3313–3324.
Clark, P.U., Dyke, A.S., Shakun, J.D., Carlson, A.E., Clark, J., Wohlfarth, B., Mitrovica, J.X., Hostetler, S.W., McCabe, A.M., 2009. The Last Glacial Maximum. Science 325, 710–714.
Coakley, B., Ilhan, I., Chukchi Edges Science Party, 2011. Chukchi Edges Project – Geophysical Constraints on the History of the Amerasia Basin, American Geophysical Union Fall Meeting 2011. American Geophysical Union, San Fransisco, USA pp. Abstract T33A-2365.
Colleoni, F., Krinner, G., Jakobsson, M., Peyaud, V., Ritz, C., 2009. Influence of regional parameters on the surface mass balance of the Eurasian ice sheet during the peak Saalian (140 kya). Global Planet. Change 68, 132–148.
Colleoni, F., Liakka, J., Krinner, G., Jakobsson, M., Masina, S., Peyaud, V., 2011. The sensitivity of the Late Saalian (140 ka) and LGM (21 ka) Eurasian ice sheets to sea surface conditions. Clim. Dyn. 37, 531–553.
Cronin, T.M., Dwyer, G.S., Farmer, J., Bauch, H.A., Spielhagen, R.F., Jakobsson, M., Nilsson, J., Briggs, W.M., Stepanova, A., 2012. Deep Arctic Ocean warming during the last glacial cycle. Nat. Geosci. 5, 631–634.
Darby, D.A., Bischof, J.F., Jones, G.A., 1997. Radiocarbon chronology of depositional regimes in the western Arctic Ocean. Deep-Sea Res. Part II Top. Stud. Oceanogr. 44, 1745–1757.
Darby, D.A., Bischof, J.F., Spielhagen, R.F., Marshall, S.A., Herman, S.W., 2002. Arctic ice export events and their potential impact on global climate during the late Pleistocene. Paleoceanography 17, 15-1–15-17.
Darby, D.A., Polyak, L., Bauch, H.A., Martinez, N., 2006. Past glacial and interglacial conditions in the Arctic Ocean and marginal seas – a review. Prog. Oceanogr. 71, 129–144.
Darby, D.A., Zimmerman, P., 2008. Ice-rafted detritus events in the arctic during the last glacial interval and the timing of the Innuitian and laurentide ice sheet calving events. Polar Res. 27, 114–127.
Dawes, P.R., 1986. Glacial erratics on the Arctic margin of North Greenland: implications for an extensive ice shelf. Bull. Geol. Soc. Den. 35, 59–69.
De Boer, A.M., Nof, D., 2004. The exhaust valve of the North Atlantic. J. Clim. 17, 417–422.
DeConto, R.M., Pollard, D., Wilson, P.A., Pälike, H., Lear, C.H., Pagani, M., 2008. Thresholds for Cenozoic bipolar glaciation. Nature 455, 652–656.
Demidov, I., Houmark-Nielsen, M., Kjær, K., Larsen, E., 2006. The last Scandinavian Ice Sheet in northwestern Russia: ice flow patterns and decay dynamics. Boreas 35, 425–443.
Denton, G.H., Hughes, T.J., 1981. The arctic ice sheet: an outrageous hypothesis. In: Denton, G.H., Hughes, T.J. (Eds.), The Last Great Ice Sheets. Wiley Interscience, New York, pp. 437–467.
Dimakis, P., Braathen, B.I., Faleide, J.I., Elverhøi, A., Gudlaugsson, S.T., 1998. Cenozoic erosion and the preglacial uplift of the Svalbard-Barents Sea region. Tectonophysics 300, 311–327.
Dittmers, K., Niessen, F., Stein, R., 2008. Acoustic facies on the inner Kara Sea Shelf: implications for Late Weichselian to Holocene sediment dynamics. Mar. Geol. 254, 197–215.
Dokken, T.M., Jansen, E., 1999. Rapid changes in the mechanism of ocean convection during the last glacial period. Nature 401, 458–461.
Donn, W.L., Ewing, M., 1966. A theory of ice ages III. Science 152, 1706–1712.
Doornbos, C., Heaman, L., Doupe′, J.P., England, J.H., Simonetti, A., Lajeunesse, P., 2009. The first integrated use of in situ U–Pb geochronology and geochemical analyses to determine long-distance transport of erratics, from mainland Canada to the western Canadian Arctic Archipelago. Can. J. Earth. Sci. 46, 101–122.
Dove, D., Polyak, L., Coakley, B., 2014. Widespread, multi-source glacial erosion on the Chukchi margin, Arctic Ocean. Quat. Sci. Rev. 92, 112–122.
Dowdeswell, J.A., Elverhøi, A., 2002. The timing of initiation of fast-flowing ice streams during a glacial cycle inferred from glacimarine sedimentation. Mar. Geol. 188, 3–14.
Dowdeswell, J.A., Hogan, K.A., Evans, J., Noormets, R., Ó Cofaigh, C., Ottesen, D., 2010a. Past ice-sheet flow east of Svalbard inferred from streamlined subglacial landforms. Geology 38, 163–166.
Dowdeswell, J.A., Jakobsson, M., Hogan, K.A., O'Regan, M., Antony, D., Backman, J., Darby, D., Eriksson, B., Evans, D.J.A., Hell, B., Janzen, T., Löwemark, L., Marcussen, C., Noormets, R., Ó Cofaigh, C., Polyak, L., Sellén, E., Sölvsten, M., 2010b. High-resolution geophysical observations from the Yermak Plateau and northern Svalbard margin: implications for ice-sheet grounding and deep-keeled icebergs. Quat. Sci. Rev. 29, 3518–3531.
Dowdeswell, J.A., Kenyon, N.H., Elverhøi, A., Laberg, J.S., Hollender, F.J., Mienert, J., Siegert, M.J., 1996. Large-scale sedimentation on the glacier-influenced Polar North Atlantic margins: long-range side-scan sonar evidence. Geophys. Res. Lett. 23, 3535–3538.
Dowdeswell, J.A., Ottesen, D., Evans, J., Ó Cofaigh, C., Anderson, J.B., 2008. Submarine glacial landforms and rates of ice-stream collapse. Geology 36, 819–822.
Dyke, A.S., 2004. An outline of North American deglaciation with emphasis on central and northern Canada. In: Ehlers, J., Gibbard, P.L. (Eds.), Developments in Quaternary Sciences. Elsevier, pp. 373–424.
Dyke, A.S., Andrews, J.T., Clark, P.U., England, J.H., Miller, G.H., Shaw, J., Veillette, J.J., 2002. The Laurentide and Innuitian ice sheets during the last glacial maximum. Quat. Sci. Rev. 21, 9–31.
Dyke, A.S., Prest, V.K., 1987. The Laurentide Ice Sheet. Géogr. Phys. Quat. 41, 237–263.
Edwards, M.H., Coakley, B.J., 2003. SCICEX investigations of the Arctic Ocean System. Chem. Erde 63, 281–328.
Ehlers, J., Gibbard, P.L., 2004. Preface. In: Ehlers, J., Gibbard, P.L. (Eds.), Developments in Quaternary Sciences. Elsevier, pp. VII–VIII.
Eiken, O., Austergard, A., 1987. The tertiary belt of west-Spitsbergen: seismic expressions of the offshore sedimentary basins. Nor. Geol. Tidsskr. 67, 383–394.
Elverhøi, A., Dowdeswell, J.A., Funder, S., Mangerud, J., Stein, R., 1998a. Glacial and oceanic history of the Polar North Atlantic Margins: an overview. Quat. Sci. Rev. 17, 1–10.
Elverhøi, A., Hooke, R.L., Solheim, A., 1998b. Late cenozoic erosion and sediment yield from the Svalbard-Barents sea region: implications for understanding erosion of glacierized basins. Quat. Sci. Rev. 17, 209–241.
Elverhøi, A., Pfirman, S.L., Solheim, A., Larssen, B.B., 1989. Glaciomarine sedimentation in epicontinental seas exemplified by the northern Barents Sea. Mar. Geol. 85, 225–250.
Elverhøi, A., Solheim, A., 1983. The Barents Sea ice sheet – a sedimentological discussion. Polar Res. 1.
Engels, J.L., Edwards, M.H., Polyak, L., Johnson, P.D., 2008. Seafloor evidence for ice shelf flow across the Alaska–Beaufort margin of the Arctic Ocean. Earth Surf. Process. Landf. 32, 1–17.
England, J., 1999. Coalescent Greenland and Innuitian ice during the Last Glacial Maximum: revising the Quaternary of the Canadian High Arctic. Quat. Sci. Rev. 18, 421–456.
England, J., Atkinson, N., Bednarski, J., Dyke, A.S., Hodgson, D.A., Ó Cofaigh, C., 2006. The Innuitian Ice Sheet: configuration, dynamics and chronology. Quat. Sci. Rev. 25, 689–703.
England, J., Atkinson, N., Dyke, A.S., Evans, D.J.A., Zreda, M., 2004. Late Wisconsinan buildup and wastage of the Innuitian Ice Sheet across southern Ellesmere Island, Nunavut: dominance of the Greenland Ice Sheet. Can. J. Earth Sci. 41, 39–61.
England, J.H., Furze, M.F.A., Doupe′, J.P., 2009. Revision of the NW Laurentide Ice Sheet: implications for paleoclimate, the northeast extremity of Beringia, and Arctic Ocean sedimentation. Quat. Sci. Rev. 28, 1573–1596.
Ewing, M., Donn, W.L., 1956. A theory of Ice Ages. Science 123, 1061–1066.
Ewing, M., Donn, W.L., 1958. A theory of Ice Ages II. Science 127, 1159–1162.
Faleide, J.I., Solheim, A., Fiedler, A., Hjelstuen, B.O., Andersen, E.S., Vanneste, K., 1996. Late Cenozoic evolution of the western Barents Sea–Svalbard continental margin. Global Planet. Change 12, 53–74.
Forman, S.L., Ingólfsson, Ó., Gataullin, V., Manley, W., Lokrantz, H., 2002. Late Quaternary stratigraphy, glacial limits, and paleoenvironments of the Marresale area, western Yamal Peninsula, Russia. Quat. Res. 57, 355–370.
Forman, S.L., Lubinski, D.J., Ingólfsson, Ó., Zeeberg, J.J., Snyder, J.A., Siegert, M.J., Matishov, G.G., 2004. A review of postglacial emergence on Svalbard, Franz Josef Land and Novaya Zemlya, northern Eurasia. Quat. Sci. Rev. 23, 1391–1434.
Fritz, M., Wetterich, S., Schirrmeister, L., Meyer, H., Lantuit, H., Preusser, F., Pollard, W.H., 2012. Eastern Beringia and beyond: Late Wisconsinan and Holocene landscape dynamics along the Yukon Coastal Plain, Canada. Palaeogeogr. Palaeoclimatol. Palaeoecol. 319–320, 28–45.
Funder, S., 1989. Quaternary geology of the ice-free areas and adjacent shelves of Greenland. In: Fulton, R.J. (Ed.), Quaternary Geology of Canada and Greenland. Geological Survey of Canada, pp. 743–792.
Funder, S., Goosse, H., Jepsen, H., Kaas, E., Kjær, K.H., Korsgaard, N.J., Larsen, N.K., Linderson, H., Lyså, A., Möller, P., Olsen, J., Willerslev, E., 2011a. A 10,000-year record of Arctic Ocean Sea-ice variability—view from the Beach. Science 333, 747–750.
Funder, S., Jennings, A., Kelly, M., 2004. Middle and late quaternary glacial limits in Greenland. In: Ehlers, J., Gibbard, P.L. (Eds.), Developments in Quaternary Sciences. Elsevier, pp. 425–430.
Funder, S., Kjeldsen, K.K., Kjær, K.H., O Cofaigh, C., 2011b. The Greenland Ice Sheet during the past 300,000 years: a review. In: Ehlers, J., Gibbard, P., Hughes, P. (Eds.), Quaternary Glaciations – Extent and Chronology, Part IV: a Closer Look, pp. 699–713.
Fütterer, D.K., 1992. ARCTIC '91: the Expedition ARK-VIIII3 of RV "Polarstern" in 1991, Berichte zur Polarforchung. Alfred Wegener Institute for Polar and Marine Research (AWI), Bremerhaven, p. 268.
Ganopolski, A., Rahmstorf, S., Petoukhov, V., Claussen, M., 1998. Simulation of modern and glacial climates with a coupled global model of intermediate complexity. Nature 391, 351–356.
Grosswald, M.G., 1980. Late Weichselian ice sheets of northern Eurasia. Quat. Res. 13, 1–32.
Grosswald, M.G., 1989. Submerged shorelines on glaciated continental shelves – solving the puzzle. J. Coast. Res. 5, 113–121.
Grosswald, M.G., Hughes, T.J., 1999. The case for an ice shelf in the Pleistocene Arctic Ocean. Polar Geogr. 23, 23–54.
Grosswald, M.G., Hughes, T.J., 2002. The Russian component of an Arctic Ice Sheet during the Last Glacial Maximum. Quat. Sci. Rev. 21, 121–146.
Grosswald, M.G., Hughes, T.J., 2008. The case for an ice shelf in the Pleistocene Arctic Ocean. Polar Geogr. 31, 69–98.
Gualtieri, L., Vartanyan, S., Brigham-Grette, J., Anderson, P.M., 2003. Pleistocene raised marine deposits on Wrangel Island, northeast Siberia and implications for the presence of an East Siberian Ice Sheet. Quat. Res. 59, 399–410.

Gualtieri, L., Vartanyan, S.L., Brigham-Grette, J., Anderson, P.M., 2005. Evidence for an ice-free Wrangel Island, northeast Siberia during the Last Glacial Maximum. Boreas 34, 264–273.
Gusev, E.A., Zinchenko, A.G., Bondarenko, C.A., Anikin, N.Y., Derevjanko, L.G., Maksimov, F.E., Kuznetsov, V.Y., Levchenko, S.B., Zherebtsov, I.E., Popov, V.V., 2012. New Data on the Topography and Quaternary Deposits of the Outer Shelf, East Siberian Sea, Geology and Geoecology of the Eurazian Continental Margin. GEOS, Moscow.
Haley, B.A., Frank, M., Spielhagen, R.F., Eisenhauer, A., 2008. Influence of brine formation on Arctic Ocean circulation over the past 15 million years. Nat. Geosci. 1, 68–72.
Hansen, B., Østerhus, S., 2000. North Atlantic–Nordic Seas exchanges. Prog. Oceanogr. 45, 109–208.
Hanslik, D., Jakobsson, M., Backman, J., Björck, S., Sellén, E., O'Regan, M., Fornaciari, E., Skog, G., 2010. Quaternary Arctic Ocean sea ice variations and radiocarbon reservoir age corrections. Quat. Sci. Rev. 29, 3430–3441.
Hays, J.D., Imbrie, J., Shackleton, N.J., 1976. Variations in the earth's orbit: pacemaker of the Ice Ages. Science 194, 1121–1132.
Hebbeln, D., Dokken, T., Andersen, E.S., Hald, M., Elverhøi, A., 1994. Moisture supply for northern ice-sheet growth during the last glacial maximum. Nature 370, 357–360.
Hegewald, A., Jokat, W., 2013. Relative sea level variations in the Chukchi region – Arctic Ocean – since the late Eocene. Geophys. Res. Lett. (n/a–n/a).
Hill, J.C., Driscoll, N.W., 2010. Iceberg discharge to the Chukchi shelf during the Younger Dryas. Quat. Res. 74, 57–62.
Hjort, C., Möller, P., Alexanderson, H., 2004. Weichselian glaciation of the Taymyr Peninsula, Siberia. In: Ehlers, J., Gibbard, P.L. (Eds.), Developments in Quaternary Sciences. Elsevier, pp. 359–367.
Hodgson, D.A., Vincent, J.-S., 1984. A 10,000 yr. BP extensive ice shelf over Viscount Melville Sound, Arctic Canada. Quat. Res. 22, 18–30.
Hodgson, D.A., Vincent, J-S., Fyles, J.G., 1984. Quaternary Geology of Central Melville Island, Northwest Territories. Geological Survey of Canada. Paper 83-16, 25 pp.
Hogan, K.A., Dowdeswell, J.A., Noormets, R., Evans, J., Cofaigh, C.Ó., 2010a. Evidence for full-glacial flow and retreat of the Late Weichselian Ice Sheet from the waters around Kong Karls Land, eastern Svalbard. Quat. Sci. Rev. 29, 3563–3582.
Hogan, K.A., Dowdeswell, J.A., Noormets, R., Evans, J., Ó Cofaigh, C., Jakobsson, M., 2010b. Submarine landforms and ice-sheet flow in the Kvitøya Trough, northwestern Barents Sea. Quat. Sci. Rev. 29, 3545–3562.
Holloway, G., Dupont, F., Golubeva, E., Häkkinen, S., Hunke, E., Jin, M., Karcher, M., Kauker, F., Maltrud, M., Morales Maqueda, M.A., Maslowski, W., Platov, G., Stark, D., Steele, M., Suzuki, T., Wang, J., Zhang, J., 2007. Water properties and circulation in Arctic Ocean models. J. Geophys. Res. Oceans 112 (n/a–n/a).
Houmark-Nielsen, M., Funder, S., 1999. Pleistocene stratigraphy of kngsfjordhallet, Spitsbergen, Svalbard. Polar Res. 18, 39–49.
Howe, J.A., Moreton, S.G., Morri, C., Morris, P., 2003. Multibeam bathymetry and the depositional environments of Kongsfjorden and Krossfjorden, western Spitsbergen, Svalbard. Polar Res. 22, 301–316.
Hu, A., Meehl, G.A., Han, W., Timmermann, A., Otto-Bliesner, B., Liu, Z., Washington, W.M., Large, W., Abe-Ouchi, A., Kimoto, M., Lambeck, K., Wu, B., 2012. Role of the Bering Strait on the hysteresis of the ocean conveyor belt circulation and glacial climate stability. Proc. Natl. Acad. Sci. U. S. A. 109, 6417–6422.
Hu, A., Meehl, G.A., Otto-Bliesner, B.L., Waelbroeck, C., Han, W., Loutre, M.-F., Lambeck, K., Mitrovica, J.X., Rosenbloom, N., 2010. Influence of Bering Strait flow and North Atlantic circulation on glacial sea-level changes. Nat. Geosci. 3, 118–121.
Hubberten, H.W., Andreev, A., V.I., A., Demidov, I., Dowdeswell, J.A., Henriksen, M., Hjort, C., Houmark-Nielsen, M., Jakobsson, M., Kuzmina, S., Larsen, E., Lunkka, J.P., Lyså, A., Mangerud, J., Möller, P., Saarnisto, M., Schirrmeister, L., Sher, A.V., Siegert, C., Siegert, M.J., Svendsen, J.-I., 2004. The periglacial environment and climate in Northern Eurasia during the last glaciation. Quat. Sci. Rev. 23, 1333–1357.
Hughes, T., 1975. West Antarctic Ice Sheet: instability, disintegration, and initiation of ice ages. Rev. Geophys. Space Phys. 13, 502–526.
Hughes, T.J., Denton, G.H., Grosswald, M.G., 1977. Was there a late-Würm Arctic ice sheet? Nature 266, 596–602.
Hunkins, K., Herron, T., Kutschale, H., Peter, G., 1962. Geophysical studies of the Chukchi Cap, Arctic Ocean. J. Geophys. Res. 67, 235–247.
Hutter, K., 1983. Theroretical Glaciology: Material Science of Ice and the Mechanics of Glaciers and Ice Sheets. Dordrecht Reidel Publishing Company, Dordrecht.
Imbrie, J., Boyle, E.A., Clemens, S.C., Duffy, A., Howard, W.R., Kukla, G., Kutzbach, J., Martinson, D.G., McIntyre, A., Mix, A.C., Molfino, B., Morley, J.J., Peterson, L.C., Pisias, N.G., Prell, W.L., Raymo, M.E., Shackleton, N.J., Toggweiler, J.R., 1992. On the structure and origin of major glaciation cycles: 1. Linear responses to Milankovitch forcing. Paleoceanography 7, 701–738.
Ingólfsson, Ó., Landvik, J.Y., 2013. The Svalbard–Barents Sea ice-sheet – historical, current and future perspectives. Quat. Sci. Rev. 64, 33–60.
Ingólfsson, Ó., Möller, P., Lokrantz, H., 2008. Late Quaternary marine-based Kara Sea ice sheets: a review of terrestrial stratigraphic data highlighting their formation. Polar Res. 27, 152–161.
Jakobsson, M., 1999. First high-resolution chirp sonar profiles from the central Arctic Ocean reveal erosion of Lomonsov Ridge sediments. Mar. Geol. 158, 111–123.
Jakobsson, M., Anderson, J.B., Nitsche, F.O., Dowdeswell, J.A., Gyllencreutz, R., Kirchner, N., O'Regan, M.A., Alley, R.B., Anandakrishnan, S., Mohammad, R., Eriksson, B., Fernandez, R., Kirshner, A., Minzoni, R., Stolldorf, T., Majewski, W., 2011. Geological record of Ice Shelf Breakup and Grounding Line Retreat, Pine Island Bay, West Antarctica. Geology 39, 691–694.
Jakobsson, M., Gardner, J.V., Vogt, P., Mayer, L.A., Armstrong, A., Backman, J., Brennan, R., Calder, B., Hall, J.K., Kraft, B., 2005. Multibeam bathymetric and sediment profiler evidence for ice grounding on the Chukchi Borderland, Arctic Ocean, Arctic Ocean. Quat. Res. 63, 150–160.
Jakobsson, M., Long, A., Ingólfsson, Ó., Kjær, K.H., Spielhagen, R.F., 2010a. New insights on Arctic Quaternary climate variability from palaeo-records and numerical modelling. Quat. Sci. Rev. 29, 3349–3358.
Jakobsson, M., Løvlie, R., Al-Hanbali, H., Arnold, E., Backman, J., Mörth, M., 2000. Manganese and color cycles in Arctic Ocean sediments constrain Pleistocene chronology. Geology 28, 23–26.
Jakobsson, M., Løvlie, R., Arnold, E.M., Backman, J., Polyak, L., Knutsen, J.-O., Musatov, E., 2001. Pleistocene stratigraphy and paleoenvironmental variation from Lomonosov Ridge sediments, central Arctic Ocean. Global Planet. Change 31, 1–22.
Jakobsson, M., Marcussen, C., LOMROG, S.P., 2008a. Lomonosov Ridge Off Greenland 2007 (LOMROG) – Cruise Report. Special Publication Geological Survey of Denmark and Greenland. Geological Survey of Denmark and Greenland, Copenhagen, p. 122.
Jakobsson, M., Mayer, L., Coakley, B., Dowdeswell, J.A., Forbes, S., Fridman, B., Hodnesdal, H., Noormets, R., Pedersen, R., Rebesco, M., Schenke, H.W., Zarayskaya, Y., Accettella, D., Armstrong, A., Anderson, R.M., Bienhoff, P., Camerlenghi, A., Church, I., Edwards, M., Gardner, J.V., Hall, J.K., Hell, B., Hestvik, O., Kristoffersen, Y., Marcussen, C., Mohammad, R., Mosher, D., Nghiem, S.V., Pedrosa, M.T., Travaglini, P.G., Weatherall, P., 2012. The international bathymetric Chart of the Arctic Ocean (IBCAO) Version 3.0. Geophys. Res. Lett. 39, L12609.
Jakobsson, M., Nilsson, J., O'Regan, M., Backman, J., Löwemark, L., Dowdeswell, J.A., Mayer, L., Polyak, L., Colleoni, F., Anderson, L., Björk, G., Darby, D., Eriksson, B., Hanslik, D., Hell, B., Marcussen, C., Sellén, E., Wallin, Å., 2010b. An Arctic Ocean ice shelf during MIS 6 constrained by new geophysical and geological data. Quat. Sci. Rev. 29, 3505–3517.
Jakobsson, M., Polyak, L., Edwards, M., Kleman, J., Coakley, B., 2008b. Glacial geomorphology of the Central Arctic Ocean: the Chukchi Borderland and the Lomonosov Ridge. Earth Surf. Process. Landf. 33, 526–545.
Jeffries, M.O., 1992. Arctic ice shelves and ice islands: origin, growth and disintegration, physical characteristics, structural–stratigraphic variability, and dynamics. Rev. Geophys. 30, 245–267.
Jennings, A.E., Sheldon, C., Cronin, T.M., Francus, P., Stoner, J., Andrews, J., 2011. The Holocene history of Nares Strait: transition from glacial bay to Arctic–Atlantic throughflow. Oceanography 24, 26–41.
Jessen, S.P., Rasmussen, T.L., Nielsen, T., Solheim, A., 2010. A new Late Weichselian and Holocene marine chronology for the western Svalbard slope 30,000–0 cal years BP. Quat. Sci. Rev. 29, 1301–1312.
Jokat, W., 2009. The Expedition of the Research Vessel "Polarstern" to the Arctic in 2008 (ARK-XXIII/3). In: Berichte zur Polar und Meeresforschung. Alfred Wegener Institute for Polar and Marine Research, Bremerhaven.
Joughin, I., Alley, R.B., 2011. Stability of the West Antarctic ice sheet in a warming world. Nat. Geosci. 4, 506–513.
Junttila, J., Aagaard-Sørensen, S., Husum, K., Hald, M., 2010. Late Glacial–Holocene clay minerals elucidating glacial history in the SW Barents Sea. Mar. Geol. 276, 71–85.
Katz, R.F., Worster, M.G., 2010. Stability of ice-sheet grounding lines. Proc. R. Soc. A Math. Phys. Eng. Sci. 466, 1597–1620.
Kauman, D.S., Manley, W.F., 2004. Pleistocene Maximum and Late Wisconsinan glacier extents across Alaska, U.S.A. In: Ehlers, J., Gibbard, P.L. (Eds.), Developments in Quaternary Sciences. Elsevier, pp. 9–27.
Kelly, M., Bennike, O., 1992. Quaternary Geology of Western and Central North Greenland. Rapport Grønlands Geologiske Undersøgelse. GGU, Copenhagen, p. 34.
King, E.L., Haflidason, H., Sejrup, H.P., Løvlie, R., 1998. Glacigenic debris flows on the North Sea Trough Mouth Fan during ice stream maxima. Mar. Geol. 152, 217–246.
Kirchner, N., Furrer, R., Jakobsson, M., Zwally, H.J., Robbins, J.W., 2013. Statistical modeling of a former Arctic Ocean ice shelf complex using Antarctic analogies. J. Geophys. Res. Earth Surf. 118, 1–13.
Kirchner, N., Hutter, K., Jakobsson, M., Gyllencreutz, R., 2011. Capabilities and limitations of numerical ice sheet models: a discussion for Earth-scientists and modelers. Quat. Sci. Rev. 30, 3691–3704.
Kleiber, H.P., Knies, J., Niessen, F., 2000. The Late Weichselian glaciation of the Franz Victoria Trough, northern Barents Sea: ice sheet extent and timing. Mar. Geol. 168, 25–44.
Kleman, J., Jansson, K., De Angelis, H., Stroeven, A.P., Hättestrand, C., Alm, G., Glasser, N., 2010. North American Ice Sheet build-up during the last glacial cycle, 115–21 kyr. Quat. Sci. Rev. 29, 2036–2051.
Knies, J., Matthiessen, J., Vogt, C., Laberg, J.S., Hjelstuen, B.O., Smelror, M., Larsen, E., Andreassen, K., Eidvin, T., Vorren, T.O., 2009. The Plio-Pleistocene glaciation of the Barents Sea–Svalbard region: a new model based on revised chronostratigraphy. Quat. Sci. Rev. 28, 812–829.
Knies, J., Vogt, C., Stein, R., 1999. Late Quaternary growth and decay of the Svalbard/Barents Sea ice sheet and paleoceanographic evolution in the adjacent Arctic Ocean. Geo-Mar. Lett. 18, 195–202.
Koch, L., 1923. Preliminary report upon the geology of Peary Land, Arctic Greenland. Am. J. Sci. 5, 190–199.
Koenig, S., DeConto, R., Pollard, D., 2011. Late Pliocene to Pleistocene sensitivity of the Greenland Ice Sheet in response to external forcing and internal feedbacks. Clim. Dyn. 37, 1247–1268.

Kristoffersen, Y., Coakley, B., Jokat, W., Edwards, M., Brekke, H., Gjengedal, J., 2004. Seabed erosion on the Lomonosov Ridge, central Arctic Ocean: a tale of deep draft icebergs in the Eurasia Basin and the influence of Atlantic water inflow on iceberg motion? Paleoceanography 19, PA3006.
Kristoffersen, Y., Mikkelsen, N., 2006. On sediment deposition and nature of the plate boundary at the junction between the submarine Lomonosov Ridge, Arctic Ocean and the continental margin of Arctic Canada/North Greenland. Mar. Geol. 225, 265–278.
Laberg, J.S., Andreassen, K., Knies, J., Vorren, T.O., Winsborrow, M., 2010. Late Pliocene–Pleistocene development of the Barents Sea ice sheet. Geology 38, 107–110.
Laberg, J.S., Vorren, T.O., 1995. Late Weichselian submarine debris flow deposits on the Bear Island Trough Mouth Fan. Mar. Geol. 127, 45–72.
Lakeman, T.R., England, J.H., 2012. Paleoglaciological insights from the age and morphology of the Jesse moraine belt, western Canadian Arctic. Quat. Sci. Rev. 47, 82–100.
Lakeman, T.R., England, J.H., 2013. Late Wisconsinan glaciation and postglacial relative sea-level change on western Banks Island, Canadian Arctic Archipelago. Quat. Res. 80, 99–112.
Lambeck, K., 1995. Constraints on the Late Weichselian ice sheet over the Barents Sea from observations of raised shorelines. Quat. Sci. Rev. 14, 1–16.
Lambeck, K., 1996. Limits on the areal extent of the Barents Sea ice sheet in Late Weichselian time. Global Planet. Change 12, 41–51.
Lambeck, K., Esat, T.M., Potter, E.-K., 2002. Links between climate and sea levels for the past three million years. Nature 419, 199–206.
Lambeck, K., Purcell, A., Funder, S., Kjær, K., Larsen, E., Möller, P., 2006. Constraints on the Late Saalian to early Middle Weichselian ice sheet of Eurasia from field data and rebound modelling. Boreas 35, 539–575.
Lamoureux, S.F., England, J.H., 2000. Late Wisconsinan Glaciation of the Central Sector of the Canadian High Arctic. Quat. Res. 54, 182–188.
Landvik, J.Y., Alexanderson, H., Henriksen, M., Ingolfsson, O., 2013. Resolving glacial phases in a coastal ice sheet marginal area, western Svalbard. Quat. Sci. Rev. (in this volume).
Landvik, J.Y., Bondevik, S., Elverhøi, A., Fjeldskaar, W., Mangerud, J., Salvigsen, O., Siegert, M.J., Svendsen, J.I., Vorren, T.O., 1998. The last glacial maximum of Svalbard and the Barents Sea area: ice sheet extent and configuration. Quat. Sci. Rev. 17, 43–75.
Landvik, J.Y., Ingólfsson, Ó., Mienert, J., Lehman, S.J., Solheim, A., Elverhøi, A., Ottesen, D., 2005. Rethinking Late Weichselian ice-sheet dynamics in coastal NW Svalbard. Boreas 34, 7–24.
Larour, E.Y., Seroussi, H., Morlighem, M., Rignot, E., 2012. Continental scale, high order, high spatial resolution, ice sheet modeling using the Ice Sheet System Model (ISSM). J. Geophys. Res. (in press).
Larsen, E., Lysså, A., Demidov, I., Funder, S., Houmark-Nielsen, M., Kjær, K.H., Murray, A.S., 1999. Age and extent of the Scandinavian ice sheet in northwest Russia. Boreas 28, 115–132.
Larsen, N.K., Kjær, K.H., Funder, S., Möller, P., van der Meer, J.J.M., Schomacker, A., Linge, H., Darby, D.A., 2010. Late Quaternary glaciation history of northernmost Greenland – evidence of shelf-based ice. Quat. Sci. Rev. 29, 3399–3414.
Lemmen, D.S., England, J., 1992. Multiple glaciations and sea level changes, northern Ellesmere Island, high arctic Canada. Boreas 21, 137–152.
Levitan, M.A., Stein, R., 2008. History of sedimentation rates in the sea-ice sedimentation zone during the last 130 ka. Lithol. Miner. Resour. 43, 65–75.
Lisiecki, L.E., Raymo, M.E., 2005. A Pliocene–Pleistocene stack of 57 globally distributed benthic $d^{18}O$ records. Paleoceanography 20, PA1003.
Lohmann, G., Lorenz, S., 2000. On the hydrological cycle under paleoclimatic conditions as derived from AGCM simulations. J. Geophys. Res. 105, 17417–17436.
Lokrantz, H., Ingólfsson, Ó., Forman, S.L., 2003. Glaciotectonised Quaternary sediments at Cape Shpindler, Yugorski Peninsula, Arctic Russia: implications for glacial history, ice movements and Kara Sea Ice Sheet configuration. J. Quat. Sci. 18, 527–541.
Löwemark, L., O'Regan, M., Hanebuth, T.J.J., Jakobsson, M., 2012. Late Quaternary spatial and temporal variability in Arctic deep-sea bioturbation and its relation to Mn cycles. Palaeogeogr. Palaeoclimatol. Palaeoecol. 365–366, 192–208.
Lubinski, D.J., Korsun, S., Polyak, L., Forman, S.L., Lehman, S.J., Herlihy, F.A., Miller, G.H., 1996. The last deglaciation of the Franz Victoria Trough, northern Barents Sea. Boreas 25, 89–100.
Mackay, J.R., 1959. Glacier ice-thrust features of the Yukon Coast. Geogr. Bull. 13, 5–21.
MacLean, B., Blasco, S., Bennett, R., England, J., Rainey, W., Hughes-Clarke, J., Beaudoin, J., 2010. Ice keel seabed features in marine channels of the central Canadian Arctic Archipelago: evidence for former ice streams and iceberg scouring. Quat. Sci. Rev. 29, 2280–2301.
Mangerud, J., Dokken, T., Hebbeln, D., Heggen, B., Ingólfsson, O., Landvik, J.Y., Mejdahl, V., Svendsen, J.I., Vorren, T.O., 1998. Fluctuations of the Svalbard–Barents sea ice sheet during the last 150000 years. Quat. Sci. Rev. 17, 11–42.
März, C., Stratmann, A., Matthiessen, J., Meinhardt, A.K., Eckert, S., Schnetger, B., Vogt, C., Stein, R., Brumsack, H.J., 2011. Manganese-rich brown layers in Arctic Ocean sediments: composition, formation mechanisms, and diagenetic overprint. Geochim. Cosmochim. Acta 75, 7668–7687.
Mayer, L.A., Armstrong, A.A., Calder, B.R., Gardner, J.V., 2010. Seafloor mapping in the Arctic: support for a potential US Extended Continental Shelf. Int. Hydrogr. Rev. 3, 14–23.
Mercer, J.H., 1970. A former ice sheet in the Arctic Ocean? Palaeogeogr. Palaeoclimatol. Palaeoecol. 8, 19–27.
Milankovitch, M., 1920. Théorie mathématique des phénomènes thermique produits per la radiation solaire. Gautier-Villars, Paris.
Miller, G.H., 1982. Quaternary depositional episodes, western Spitsbergen, Norway: aminostratigraphy and glacial history. Arct. Alp. Res. 14, 321–340.
Minakov, A., Faleide, J.I., Glebovsky, V.Y., Mjelde, R., 2012. Structure and evolution of the northern Barents-Kara Sea continental margin from integrated analysis of potential fields, bathymetry and sparse seismic data. Geophys. J. Int. 188, 79–102.
Möller, P., Fedorov, G., Pavlov, M., Seidenkrantz, M.S., Sparrenbom, C., 2008. Glacial and palaeoenvironmental history of the Cape Chelyuskin area, Arctic Russia. Polar Res. 27, 222–248.
Möller, P., Hjort, C., Alexanderson, H., Sallaba, F., 2011. Glacial History of the Taymyr Peninsula and the Severnaya Zemlya Archipelago, Arctic Russia, pp. 373–384.
Möller, P., Larsen, N.K., Kjær, K.H., Funder, S., Schomacker, A., Linge, H., Fabel, D., 2010. Early to middle Holocene valley glaciations on northernmost Greenland. Quat. Sci. Rev. 29, 3379–3398.
Möller, P., Lubinski, D.J., Ingólfsson, O., Forman, S.L., Seidenkrantz, M.S., Bolshiyanov, D.Y., Lokrantz, H., Antonov, O., Pavlov, M., Ljung, K., Zeeberg, J., Andreev, A., 2006. Severnaya Zemlya, Arctic Russia: a nucleation area for Kara Sea ice sheets during the Middle to Late Quaternary. Quat. Sci. Rev. 25, 2894–2936.
Müller, J., Masse, G., Stein, R., Belt, S.T., 2009. Variability of sea-ice conditions in the Fram Strait over the past 30,000 years. Nat. Geosci. 2, 772–776.
Murton, J.B., Bateman, M.D., Dallimore, S.R., Teller, J.T., Yang, Z., 2010. Identification of Younger Dryas outburst flood path from Lake Agassiz to the Arctic Ocean. Nature 464, 740–743.
Murton, J.B., Frechen, M., Maddy, D., 2007. Luminescence dating of mid- to Late Wisconsinan aeolian sand as a constraint on the last advance of the Laurentide Ice Sheet across the Tuktoyaktuk Coastlands, western Arctic Canada. Can. J. Earth Sci. 44, 857–869.
Niessen, F., Hong, J.K., Hegewald, A., Matthiessen, J., Stein, R., Kim, H., Kim, S., Jensen, L., Jokat, W., Nam, S.-I., Kang, S.-H., 2013. Repeated Pleistocene glaciation of the East Siberian Continental Margin. Nat. Geosci. (online) (in press).
Niessen, F., Matthiessen, J., Stein, R., 2010. Sedimentary environment and glacial history of the Northwest Passage (Canadian Arctic Archipelago) reconstructed from high-resolution acoustic data. Polarforschung 79, 65–80.
Nilsson, J., Walin, G., 2010. Salinity-dominated thermohaline circulation in sill basins: can two stable equilibria exist? Tellus A 62, 123–133.
Noormets, R., Hogan, K., Austin, W., Chauhan, T., Roy, S., Rasmussen, T., Dowdeswell, J., 2012. Submarine glacial landform assemblages on the outer continental shelf north of Nordaustlandet, Svalbard. In: Immonen, N., Jakobsson, M., Lunkka, J.P., Strand, K. (Eds.), The 6th Arctic Paleoclimate and Its Extremes (APEX) Meeting. Oulu University, Oululanka Research Station, Finland, p. 70.
Nørgaard-Pedersen, N., Mikkelsen, N., Kristoffersen, Y., 2007. Arctic Ocean record of last two glacial–interglacial cycles off North Greenland/Ellesmere Island — implications for glacial history. Mar. Geol. 244, 93–108.
Nørgaard-Pedersen, N., Mikkelsen, N., Kristoffersen, Y., 2008. Late glacial and Holocene marine records from the Independence Fjord and Wandel Sea regions, North Greenland. Polar Res. 27, 209–221.
Nørgaard-Pedersen, N., Spielhagen, R.F., Erlenkeuser, H., Grootes, P.M., Heinemeier, J., Knies, J., 2003. Arctic Ocean during the Last Glacial Maximum: Atlantic and polar domains of surface water mass distribution and ice cover. Paleoceanography 18.
Nørgaard-Pedersen, N., Spielhagen, R.F., Thiede, J., Kassens, H., 1998. Central Arctic surface ocean environment during the past 80,000 years. Paleoceanography 13, 193–204.
Nøst, O.A., Isachsen, P.E., 2003. The large-scale time-mean ocean circulation in the Nordic Seas and the Arctic Ocean estimated from simplified dynamics. J. Mar. Res. 61, 175–210.
O'Regan, M., Jakobsson, M., Kirchner, N., 2010. Glacial geological implications of overconsolidated sediments on the Lomonosov Ridge and Yermak Plateau. Quat. Sci. Rev. 29, 3532–3544.
O'Regan, M., King, J.W., Backman, J., Jakobsson, M., Moran, K., Heil, C., Sakamoto, T., Cronin, T., Jordan, R., 2008. Constraints on the Pleistocene chronology of sediments from the Lomonosov Ridge. Paleoceanography 23, PA1S19.
Ó Cofaigh, C., England, J., Zreda, M., 2000. Late Wisconsinan glaciation of southern Eureka Sound: evidence for extensive Innuitian ice in the Canadian High Arctic during the Last Glacial Maximum. Quat. Sci. Rev. 19, 1319–1341.
Olausson, E., Jonasson, U.C., 1969. The Arctic Ocean during the Würm end Early Flandrian. Geol. Fören. Stockh. Förh. 91, 185–200.
Olsen, J., Kjær, K.H., Funder, S., Larsen, N.K., Ludikova, A., 2012. High-Arctic climate conditions for the last 7000 years inferred from multi-proxy analysis of the Bliss Lake record, North Greenland. J. Quat. Sci. 27, 318–327.
Ottesen, D., Dowdeswell, J.A., 2009. An inter-ice-stream glaciated margin: submarine landforms and a geomorphic model based on marine-geophysical data from Svalbard. Geol. Soc. Am. Bull. 121, 1647–1665.
Ottesen, D., Dowdeswell, J.A., Landvik, J.Y., Mienert, J., 2007. Dynamics of the Late Weichselian ice sheet on Svalbard inferred from high-resolution sea-floor morphology. Boreas 36, 286–306.
Ottesen, D., Dowdeswell, J.A., Rise, L., 2005. Submarine landforms and the reconstruction of fast-flowing ice streams within a large Quaternary ice sheet: the 2500-km-long Norwegian–Svalbard margin (57°–80°N). Geol. Soc. Am. Bull. 117, 1033–1050.
Otto-Bliesner, B.L., Hewitt, C.D., Marchitto, T.M., Brady, E., Abe-Ouchi, A., Crucifix, M., Murakami, S., Weber, S.L., 2007. Last Glacial Maximum ocean

thermohaline circulation: PMIP2 model intercomparisons and data constraints. Geophys. Res. Lett. 34 (n/a–n/a).
Pattyn, F., 2003. A new three-dimensional higher-order thermomechanical ice sheet model: basic sensitivity, ice stream development, and ice flow across subglacial lakes. J. Geophys. Res. Solid Earth 108 (n/a–n/a).
Pattyn, F., Perichon, L., Aschwanden, A., Breuer, B., De Smedt, B., Gagliardini, O., Gudmundsson, G.H., Hindmarsh, R.C.A., Hubbard, A., Johnson, J.V., Kleiner, T., Konovalov, Y., Martin, C., Payne, A.J., Pollard, D., Price, S., Rückamp, M., Saito, F., Souček, O., Sugiyama, S., Zwinger, T., 2008. Benchmark experiments for higher-order and full-Stokes ice sheet models (ISMIP-HOM). Cryosphere 2, 95–108.
Pattyn, F., Schoof, C., Perichon, L., Hindmarsh, R.C.A., Bueler, E., De Fleurian, B., Durand, G., Gagliardini, O., Gladstone, R., Goldberg, D., Gudmundsson, G.H., Huybrechts, P., Lee, V., Nick, F.M., Payne, A.J., Pollard, D., Rybak, O., Saito, F., Vieli, A., 2012. Results of the marine ice sheet model intercomparison project, MISMIP. Cryosphere 6, 573–588.
Peltier, W.R., 2004. Global glacial isostasy and the surface of the Ice-Age Earth: the ICE-5G (VM2) model and GRACE. Ann. Rev. Earth Planet. Sci. 32, 111–149.
Phillips, R.L., Grantz, A., 2001. Regional variations in provenance and abundance of ice-rafted clasts in Arctic Ocean sediments: implications for the configuration of late Quaternary oceanic and atmospheric circulation in the Arctic. Mar. Geol. 172.
Pieńkowski, A.J., England, J.H., Furze, M.F.A., Blasco, S., Mudie, P.J., MacLean, B., 2013. 11,000 yrs of environmental change in the Northwest Passage: a multiproxy core record from central Parry Channel, Canadian High Arctic. Mar. Geol. 341, 68–85.
Pieńkowski, A.J., England, J.H., Furze, M.F.A., Marret, F., Eynaud, F., Vilks, G., Maclean, B., Blasco, S., Scourse, J.D., 2012. The deglacial to postglacial marine environments of SEBarrow Strait, Canadian Arctic Archipelago. Boreas 41, 141–179.
Poirier, R.K., Cronin, T.M., Briggs Jr., W.M., Lockwood, R., 2012. Corrigendum to 'Central Arctic paleoceanography for the last 50 kyr based on ostracode faunal assemblages' [Mar. Micropaleon. 88–89C (May 2012) 65–76]. Mar. Micropaleontol.. http://dx.doi.org/10.1016/j.marmicro.2012.03.004.
Pollard, D., Deconto, R.M., 2012. Description of a hybrid ice sheet-shelf model, and application to Antarctica. Geosci. Model Dev. 5, 1273–1295.
Polyak, L., Bischof, J., Ortiz, J., Darby, D., Channell, J., Xuan, C., Kaufman, D., Lovlie, R., Schneider, D., Adler, R., 2009. Late Quaternary stratigraphy and sedimentation patterns in the western Arctic Ocean. Global Planet. Change 68, 5–17.
Polyak, L., Curry, W.B., Darby, D.A., Bischof, J., Cronin, T.M., 2004. Contrasting glacial/interglacial regimes in the western Arctic Ocean as exemplified by a sedimentary record from the Mendeleev Ridge. Palaeogeogr. Palaeoclimatol. Palaeoecol. 203, 73–93.
Polyak, L., Darby, D., Bischof, J., Jakobsson, M., 2007. Stratigraphic constraints on late Pleistocene glacial erosion and deglaciation of the Chukchi margin, Arctic Ocean. Quat. Res. 67, 234–245.
Polyak, L., Edwards, M.H., Coakley, B.J., Jakobsson, M., 2001. Ice shelves in the Pleistocene Arctic Ocean inferred from glaciogenic deep-sea bedforms. Nature 410, 453–459.
Polyak, L., Forman, S.L., Herlihy, F.A., Ivanov, G., Krinitsky, P., 1997. Late Weichselian deglacial history of the Svyataya (Saint) Anna Trough, northern Kara Sea, Arctic Russia. Mar. Geol. 143, 169–188.
Polyak, L., Jakobsson, M., 2011. Quaternary sedimentation in the Arctic Ocean: recent advances and further challenges. Oceanography 24, 52–64.
Polyak, L., Lehman, S.J., Gataullin, V., Jull, A.J.T., 1995. Two-step deglaciation of the southeastern Barents Sea. Geology 23, 567–571.
Polyak, L., Niessen, F., Gataullin, V., Gainanov, V., 2008. The eastern extent of the Barents-Kara ice sheet during the Last Glacial Maximum based on seismic-reflection data from the eastern Kara Sea. Polar Res. 27, 162–174.
Polyak, L., Solheim, A., 1994. Late- and postglacial environments in the northern Barents Sea west of Franz Josef Land. Polar Res. 13, 197–207.
Poore, R.Z., Osterman, L., Curry, W.B., Phillips, R.L., 1999. Late Pleistocene and Holocene meltwater events in the western Arctic Ocean. Geology 27, 759–762.
Raab, A., Melles, M., Berger, G.W., Hagedorn, B., Hubberten, H.W., 2003. Non-glacial paleoenvironments and the extent of Weichselian ice sheets on Severnaya Zemlya, Russian High Arctic. Quat. Sci. Rev. 22, 2267–2283.
Rampton, V.N., 1982. Quaternary Geology of the Yukon Coastal Plain. In: Bulletin 317. Geological Survey of Canada, p. 49.
Rasmussen, T.L., Thomsen, E., Ślubowska, M.A., Jessen, S., Solheim, A., Koç, N., 2007. Paleoceanographic evolution of the SW Svalbard margin (76°N) since 20,000 ^{14}C yr BP. Quat. Res. 67, 100–114.
Rokoengen, K., Bell, G., Bugge, T., Dekko, T., Gunleiksrud, T., Lien, R.L., Løfaldli, M., Vigran, J.O., 1977. Prøvetaking av fjellgrunn og løsmasser utenfor deler av Nord-Norge i 1976. Institutt for kontinentalsokkelundersøkelser, Norge, p. 65.
Rudels, B., Anderson, L., Eriksson, P., Fahrbach, E., Jakobsson, M., E., P.J., Melling, H., Prinsenberg, S., Schauer, U., Yao, T., 2012. Observations in the Ocean. In: Lemke, P. (Ed.), Arctic Climate Change: the ACSYS Decade and Beyond. Springer, pp. 117–198.
Rüther, D.C., Bjarnadóttir, L.R., Junttila, J., Husum, K., Rasmussen, T.L., Lucchi, R.G., Andreassen, K., 2012. Pattern and timing of the northwestern Barents Sea Ice Sheet deglaciation and indications of episodic Holocene deposition. Boreas 41, 494–512.
Salvigsen, O., 1981. Radiocarbon dated raised beaches in Kong Karls Land, Svalbard, and their consequences for the glacial history of the Barents Sea area. Geogr. Ann. Ser. A 63, 283–291.
Schirrmeister, L., Oezen, D., Geyh, M.A., 2002. ^{230}Th/U dating of frozen peat, Bol'shoyLyakhovsky Island (North Siberia). Quat. Res. 57, 253–258.
Schoof, C., 2007. Ice sheet grounding line dynamics: steady states, stability, and hysteresis. J. Geophys. Res. Earth Surf. 112 (n/a–n/a).
Seddik, H., Greve, R., Zwinger, T., Gillet-Chaulet, F., Gagliardini, O., 2012. Simulations of the Greenland ice sheet 100 years into the future with the full Stokes model Elmer/Ice. J. Glaciol. 58, 427–440.
Sejrup, H.P., Hjelstuen, B.O., Dahlgren, K.I.T., Haflidason, H., Kuijpers, A., Nygård, A., Praeg, D., Stoker, M.S., Vorren, T.O., 2005. Pleistocene glacial history of the NW European continental margin. Mar. Pet. Geol. 22, 1111–1129.
Sellén, E., O'Regan, M., Jakobsson, M., 2010. Spatial and temporal Arctic Ocean depositional regimes: a key to the evolution of ice drift and current patterns. Quat. Sci. Rev. 29, 3644–3664.
Shin, S.I., Liu, Z., Otto-Bliesner, B., Brady, E., Kutzbach, J., Harrison, S., 2003. A simulation of the Last Glacial Maximum climate using the NCAR-CCSM. Clim. Dyn. 20, 127–151.
Siegert, M.J., Dowdeswell, J.A., 2004. Numerical reconstructions of the Eurasian Ice Sheet and climate during the Late Weichselian. Quat. Sci. Rev. 23, 1273–1283.
Siegert, M.J., Dowdeswell, J.A., Melles, M., 1999. Late Weichselian glaciation of the Russian High Arctic. Quat. Res. 52, 273–285.
Solheim, A., Andersen, E.S., Elverhøi, A., Fiedler, A., 1996. Late Cenozoic depositional history of the western Svalbard continental shelf, controlled by subsidence and climate. Global Planet. Change 12, 135–148.
Solheim, A., Kristoffersen, Y., 1984. The Physical Environment in the Western Barents Sea, 1:5,000,000. In: Sediments Above the Upper Regional Unconformity: Thickness, Seismic Stratigraphy and Outline of the Glacial History, 179B. Norsk Polarinstitutt.
Solheim, A., Russwurm, L., Elverhøi, A., Nyland Berg, M., 1990. Glacial Geomorphic Features: Direct Evidence for Grounded Ice in the Northern Barents Sea and Implications for the Pattern of Deglaciation and Late Glacial Sedimentation. Geological Society of London, pp. 253–268. Special Publication 53.
Spall, M.A., 2012. Influences of precipitation on water mass transformation and deep convection. J. Phys. Oceanogr. 42, 1684–1700.
Spielhagen, R.F., Baumann, K.H., Erlenkeuser, H., Nowaczyk, N.R., Norgaard-Pedersen, N., Vogt, C., Weiel, D., 2004. Arctic Ocean deep-sea record of northern Eurasian ice sheet history. Quat. Sci. Rev. 23, 1455–1483.
Stärz, M., Gong, X., Stein, R., Darby, D.A., Kauker, F., Lohmann, G., 2012. Glacial shortcut of Arctic sea-ice transport. Earth Planet. Sci. Lett. 357–358, 257–267.
Stauch, G., Gualtieri, L., 2008. Late quaternary glaciations in northeastern Russia. J. Quat. Sci. 23, 545–558.
Stein, R., Fahl, K., 2013. Biomarker proxy shows potential for studying the entire Quaternary Arctic sea ice history. Org. Geochem. 55, 98–102.
Stein, R., Matthiessen, J., Niessen, F., Krylov, R., Nam, S., Bazhenova, E., 2010. Towards a better (Litho-) stratigraphy and reconstruction of Quaternary Paleoenvironment in the Amerasian Basin (Arctic Ocean). Polarforschung 79, 97–121.
Stein, R., Niessen, F., Dittmers, K., Levitan, M., Schoster, F., Simstich, J., Steinke, T., Stepanets, O.V., 2002. Siberian river run-off and Late Quaternary glaciation in the southern Kara Sea, Arctic Ocean: preliminary results. Polar Res. 21, 315–322.
Stigebrandt, A., 1984. The North Pacific: a global-scale estuary. J. Phys. Oceanogr. 14, 464–470.
Stigebrandt, A., 1985. On the hydrographic and ice conditions in the northern North Atlantic during different phases of a glaciation cycle. Palaeogeogr. Palaeoclimatol. Palaeoecol. 50, 303–321.
Stokes, C., Clark, C., Darby, D., Hodgson, D., 2005. Late Pleistocene ice export events into the Arctic Ocean from the M'Clure Strait Ice Stream, Canadian Arctic Archipelago. Global Planet. Change 49, 139–162.
Stokes, C.R., Clark, C.D., Storrar, R., 2009. Major changes in ice stream dynamics during deglaciation of the north-western margin of the Laurentide Ice Shee. Quat. Sci. Rev. 28, 721–738.
Stokes, C.R., Clark, C.D., Winsborrow, M.C.M., 2006. Subglacial bedform evidence for a major paleo-ice stream and its retreat phases in Amundsen Gulf, Canadian Arctic Archipelago. J. Quat. Sci. 21, 399–412.
Stokes, C.R., Tarasov, L., 2010. Ice streaming in the Laurentide Ice Sheet: a first comparison between data-calibrated numerical model output and geological evidence. Geophys. Res. Lett. 37.
Svendsen, J.I., Alexanderson, H., Astakhov, V.I., Demidov, I., Dowdeswell, J.A., Henriksen, M., Hjort, C., Houmark-Nielsen, M., Hubberten, H.W., Ingólfson, O., Jakobsson, M., Kjær, K., Larsen, E., Lokrantz, H., Lunkka, J.P., Lysså, A., Mangerud, J., Maslenikova, O., Matioushkov, A., Murray, A., Möller, P., Niessen, F., Saarnisto, M., Siegert, C., Stein, R., Siegert, M.J., Spielhagen, R., 2004a. Late Quaternary ice sheet history of northern Eurasia. Quat. Sci. Rev. 23, 1229–1271.
Svendsen, J.I., Gataullin, V., Mangerud, J., Polyak, L., 2004b. The glacial history of the Barents and Kara Sea Region. In: Ehlers, J., Gibbard, P.L. (Eds.), Developments in Quaternary Sciences. Elsevier, pp. 369–378.
Svendsen, J.I., Mangerud, J., Miller, G.H., 1989. Denudation rates in the Arctic estimated from lake sediments on Spitsbergen, Svalbard. Palaeogeogr. Palaeoclimatol. Palaeoecol. 76, 153–168.
Svindland, K.T., Vorren, T.O., 2002. Late Cenozoic sedimenatry environments in the Amundsen Basin, Arctic Ocean. Mar. Geol. 186, 541–555.
Tarasov, L., Peltier, W.R., 2004. A geophysically constrained large ensemble analysis of the deglacial history of the North American ice-sheet complex. Quat. Sci. Rev. 23, 359–388.
Thiede, J., Astakhov, V., Bauch, H., Bolshiyanov, D.Y., Dowdeswell, J.A., Funder, S., Hjort, C., Kotlyakov, V.M., Mangerud, J., Pyramikov, S.M., Saarnisto, M., Schluechter, C., 2004. What was QUEEN? Its history and international framework – an introduction to its final synthesis issue. Quat. Sci. Rev. 23, 1225–1227.

Thomas, R.H., 1979. Ice shelves: a review. J. Glaciol. 24, 273–286.
Thomas, R.H., Bentley, C.R., 1978. A model for Holocene retreat of the West Antarctic Ice Sheet. Quat. Res. 10, 150–170.
Vanneste, M., Mienert, J., Bünz, S., 2006. The Hinlopen Slide: a giant, submarine slope failure on the northern Svalbard margin, Arctic Ocean. Earth Planet. Sci. Lett. 245, 373–388.
Vincent, J.-S., 1982. The Quaternary History of Banks Island, N.W.T., Canada. Géogr. phys. Quat. 36, 209–232.
Vincent, J.-S., 1983. La geologie du quaternaire et la géomorphologie de Lıle Banks, arctique Canadien. In: Geological Survey of Canada Memoir. Geological Survey of Canada, p. 118.
Vincent, J.-S., Prest, V.K., 1987. The Early Wisconsinan history of the Laurentide Ice Sheet. Géogr. phys. Quat. 41, 199–213.
Vogt, P.R., Crane, K., Sundvor, E., 1994. Deep Pleistocene iceberg plowmarks on the Yermak Plateau: sidescan and 3.5 kHz evidence for thick calving ice fronts and a possible marine ice sheet in the Arctic Ocean. Geology 22, 403–406.
Vogt, P.R., Crane, K., Sundvor, E., 1995. Deep Pleistocene iceberg plowmarks on the Yermak Plateau: sidescan and 3.5 kHz evidence for thick calving ice fronts and a possible marine ice sheet in the Arctic Ocean: reply. Geology 23, 477–478.
Vorren, T.O., Hald, M., Thomsen, E., 1984. Quaternary sediments and environments on the continental shelf off northern Norway. Mar. Geol. 57, 229–257.
Vorren, T.O., Kristoffersen, Y., Andreassen, K., 1986. Geology of the inner shelf west of North Cape, Norway. Nor. Geol. Tidsskr. 66, 99–105.
Vorren, T.O., Laberg, J.S., 1996. Late Glacial Air Temperature, Oceanographic and Ice Sheet Interactions in the Southern Barents Sea Region. In: Late Quaternary Palaeoceanography of the North Atlantic Margins, pp. 303–321.
Vorren, T.O., Laberg, J.S., 1997. Trough mouth fans – palaeoclimate and ice-sheet monitors. Quat. Sci. Rev. 16, 865–881.
Vorren, T.O., Laberg, J.S., Blaume, F., Dowdeswell, J.A., Kenyon, N.H., Mienert, J., Rumohr, J., Werner, F., 1998. The Norwegian–Greenland Sea continental margins: morphology and late quaternary sedimentary processes and environment. Quat. Sci. Rev. 17, 273–302.
Vorren, T.O., Landvik, J.Y., Andreassen, K., Laberg, J.S., 2011. Glacial History of the Barents Sea Region, pp. 361–372.
Vorren, T.O., Richardsen, G., Knutsen, S.M., Henriksen, E., 1991. Cenozoic erosion and sedimentation in the western Barents Sea. Mar. Pet. Geol. 8, 317–340.
Vorren, T.O., Strass, I.F., Lind-Hansen, O.W., 1978. Late Quaternary sediments and stratigraphy on the continental shelf off Troms and west Finnmark, northern Norway. Quat. Res. 10, 340–365.
Weertman, J., 1974. Stability of the junction between an ice sheet and an ice shelf. J. Glaciol. 13, 3–11.
Wetterich, S., Rudaya, N., Tumskoy, V., Andreev, A.A., Opel, T., Schirrmeister, L., Meyer, H., 2011. Last Glacial Maximum records in permafrost of the East Siberian Arctic. Quat. Sci. Rev. 30, 3139–3151.
Weyl, P.K., 1968. The role of the oceans in climatic change: a theory of the ice ages. Meteorol. Monogr. 8, 37–62.
Winkelmann, D., Schäfer, C., Stein, R., MacKensen, A., 2008. Terrigenous events and climate history of the Sophia Basin, Arctic Ocean. Geochem. Geophys. Geosyst. 9.
Winkelmann, D., Stein, R., 2007. Triggering of the Hinlopen/Yermak Megaslide in relation to paleoceanography and climate history of the continental margin north of Spitsbergen. Geochem. Geophys. Geosyst. 8.
Winsborrow, M.C.M., Andreassen, K., Corner, G.D., Laberg, J.S., 2010. Deglaciation of a marine-based ice sheet: Late Weichselian palaeo-ice dynamics and retreat in the southern Barents Sea reconstructed from onshore and offshore glacial geomorphology. Quat. Sci. Rev. 29, 424–442.
Winsborrow, M.C.M., Stokes, C.R., Andreassen, K., 2012. Ice-stream flow switching during deglaciation of the southwestern Barents Sea. Bull. Geol. Soc. Am. 124, 275–290.
Wollenburg, J.E., Knies, J., Mackensen, A., 2004. High-resolution paleoproductivity fluctuations during the past 24 kyr as indicated by benthic foraminifera in the marginal Arctic Ocean. Palaeogeogr. Palaeoclimatol. Palaeoecol. 204, 209–238.
Zazula, G.D., Duk-Rodkin, A., Schweger, C.E., Morlan, R.E., 2004. Late pleistocene chronology of glacial lake old crow and the north-west margin of the Laurentide Ice Sheet. In: Ehlers, J., Gibbard, P.L. (Eds.), Developments in Quaternary Sciences. Elsevier, pp. 347–362.